

Interscience Research Network

Interscience Research Network

Conference Proceedings - Full Volumes

IRNet Conference Proceedings

3-18-2012

Proceedings of International Conference on Computational Vision & Robotics

Prof.Srikanta Patnaik Mentor

Follow this and additional works at: https://www.interscience.in/conf_proc_volumes



Part of the [Computational Engineering Commons](#), and the [Robotics Commons](#)

Recommended Citation

Patnaik, Prof.Srikanta Mentor, "Proceedings of International Conference on Computational Vision & Robotics" (2012). *Conference Proceedings - Full Volumes*. 49.

https://www.interscience.in/conf_proc_volumes/49

This Book is brought to you for free and open access by the IRNet Conference Proceedings at Interscience Research Network. It has been accepted for inclusion in Conference Proceedings - Full Volumes by an authorized administrator of Interscience Research Network. For more information, please contact sritampatnaik@gmail.com.

Proceedings of International Conference on
COMPUTATIONAL VISION & ROBOTICS



(ICCV-2012)
18th March, 2012
CHANDIGARH, India

Interscience Research Network (IRNet)
Bhubaneswar, India

Editorial

With an emerging and exponential growth of computational solutions to multifarious socio-technical problems, the field of computer science is celebrated with radical innovations and advancements. The standing philosophy of such an enduring discipline is to duplicate the abilities of human vision by electronically perceiving and understanding an image. This image understanding can be seen as the disentangling of symbolic information from image data using models constructed with the aid of geometry, physics, statistics, and learning theory. As a technological discipline, computer vision seeks to apply its theories and models to the construction of computer vision systems. Examples of applications of computer vision include systems for, Controlling processes (e.g., an industrial robot), navigation (e.g. by an autonomous vehicle or mobile robot), detecting events (e.g., for visual surveillance or people counting), organizing information (e.g., for indexing databases of images and image sequences), modeling objects or environments (e.g., medical image analysis or topographical modeling), interaction (e.g., as the input to a device for computer-human interaction), automatic inspection, e.g. in manufacturing applications.

The field is embodied with diversified with many application areas such as: medical computer vision or medical image processing. This area is characterized by the extraction of information from image data for the purpose of making a medical diagnosis of a patient. Generally, image data is in the form of [microscopy images](#), [X-ray images](#), [angiography images](#), [ultrasonic images](#), and [tomography images](#). A second application area in computer vision is in industry, sometimes called [machine vision](#), where information is extracted for the purpose of supporting a manufacturing process. Military applications are probably one of the largest areas for computer vision. The obvious examples are detection of enemy soldiers or vehicles and [missile guidance](#). One of the newer application areas is autonomous vehicles, which include [submersibles](#), land-based vehicles (small robots with wheels, cars or trucks), aerial vehicles, and unmanned aerial vehicles ([UAV](#)).

The organization of a computer vision system is highly application dependent. Some systems are stand-alone applications which solve a specific measurement or detection problem, while others constitute a sub-system of a larger design which, for example, also contains sub-systems for control of mechanical actuators, planning, information databases, man-machine interfaces, etc. The specific implementation of a computer vision system also depends on if its functionality is pre-specified or if some part of it can be learned or modified during operation.

The concept and creation of machines that could operate autonomously dates back to [classical times](#), but research into the functionality and potential uses of robots did not grow substantially until the 20th century. Today, robotics is a rapidly growing field, as we continue to research, design, and build new robots that serve various practical purposes, whether [domestically](#), [commercially](#), or [militarily](#). Many robots do jobs that are hazardous to people such as defusing bombs, exploring shipwrecks, and mines.

The field of Robotics has surpassed a long journey since third century before Christ by Yan Shi and still it continues. The [mechanical](#) structure of a robot must be controlled to perform tasks. The control of a robot involves three distinct phases - perception, processing, and action ([robotic paradigms](#)). [Sensors](#) give information about the environment or the robot itself (e.g. the position of its joints or its end effector). This information is then processed to calculate the appropriate signals to the actuators ([motors](#)) which move the mechanical.

A first particular new innovation in robot design is the open sourcing of robot-projects. To describe the level of advancement of a robot, the term "Generation Robots" can be used. This term is coined by Professor [Hans Moravec](#), Principal Research Scientist at the [Carnegie Mellon University Robotics Institute](#) in describing the near future evolution of robot technology. *First generation* robots, Moravec predicted in 1997, should have an intellectual capacity comparable to perhaps a lizard and should become available by 2010. Because the *first generation* robot would be incapable of [learning](#), however, Moravec predicts that the *second generation* robot would be an improvement over the *first* and become available by 2020, with the intelligence maybe comparable to that of a [mouse](#). The *third generation* robot should have the intelligence comparable to that of a [monkey](#). Though *fourth generation* robots, robots with [human](#) intelligence, professor Moravec predicts, would become possible, he does not predict this happening before around 2040 or 2050.

The second is [Evolutionary Robots](#). This is a [methodology](#) that uses [evolutionary computation](#) to help design robots, especially the body form, or motion and behavior [controllers](#). In a similar way to [natural evolution](#), a large population of robots is allowed to compete in some way, or their ability to perform a task is measured using a [fitness function](#). Those that perform worst are removed from the population, and replaced by a new set, which have new behaviors based on those of the winners. Over time the population improves, and eventually a satisfactory robot may appear. This happens without any direct programming of the robots by the researchers. Researchers use this method both to create better robots, and to explore the nature of evolution. Because the process often requires many generations of robots to be simulated, this technique may be run entirely or mostly in [simulation](#), then tested on real robots once the evolved algorithms are good enough. Currently, there are about 1 million industrial robots toiling around the world, and Japan is the top country having high density of utilizing robots in its manufacturing industry.

As the area is broad and requires cross functionally expert reviewers for technical scrutiny of the papers, we have tried to impart justice to all the paper in its publication in the proceeding. In all sense we have been transcendental in this field in developing the fauna of the conference. In meeting the professional commitments we maintained the sanctity by adhering to ethics, ontology and semiotics. I beg apology for any inconveniency caused to the participants and delegates in the journey of this conference. I have regards for the IRNet family members, reviewers, and support staffs for their generous gifts of time, energy and effort. Specifically I owe indebtedness to the authors for their intellectual contributions in this conference.

The conference is designed to stimulate the young minds including Research Scholars, Academicians, and Practitioners to contribute their ideas, thoughts and nobility in these two integrated disciplines. I must acknowledge your response to this conference. I ought to convey that this conference is only a little step towards knowledge, network and relationship

I express best wishes to all the paper presenters. I extend my heart full thanks to the reviewers, editorial board members, programme committee members of the conference. If situations prevail in favor we will take the glory of organizing the second conference of this kind during this period next year.

Editor-in-Chief

Prof. Srikanta Patnaik, Professor,
Computer Science and Engineering,
ITER, SOA University, Bhubaneswar
Dist. Khurda 752 024, Orissa, INDIA

Mini-Bot : Autonomous Charging Robot with Swap Algorithm

Arul. V. H & A. L.Vallikannu

Hindustan Institute of Technology and Science, Hindustan University, Chennai, India

Abstract - The main contribution of this paper is an improved method for charging the patrol robot, without human machine interaction. The robot retains their charging position as per the commands stored in the memory. The other feature in this patrol robot is design of a track wheel, which helps to move in the rough terrain surface with high precision. For the large storage of data we are implementing an external SD card to the controller. A single folded mechanical joint is set up with the base for the site surveillance and which is rotated 360 degree. For the real time visuals a camera is mounted on the top of the mechanical joint. All the control commands are exchanged between the base station and robot through zig bee module. A battery monitoring mechanism is also attached with the system. As the battery charge reaches the threshold level, drive the robot to the charging panel with the proper command which is stored in the memory of the microcontroller.

Keywords - robotics, locomotion, arm, charging, memory.

I. INTRODUCTION

Robot is a machine to execute different task repeatedly with high precision. Thereby many functions like collecting information and studies about the hazardous sites which is too risky to send human inside. Robots are used to reduce the human interference nearly 50 percent. Robots are mainly in different types like fire fighting robot, metal detecting robot, rescue robots, patrol robots other humanoid robots etc. Mostly used in industrial purpose, military, defense, research and development etc. The focus for the patrol robot applications are on difficult surfaces and simple smooth platforms. Some patrol robots use their small size model, for the easy site assessment. However the small size robots will have a problem while climbing over the steps higher than their height and want to move fast. There are some jumping patrol robots which try to move over the high obstacles by using a pneumatic cylinder, which also having the problem of gravity and stability. For the better surveillance of the vital environment visual sensor must be placed at certain height. Hence a camera is fixed on the tip of the joint. such as the mini bot will equipped with the track wheeled method along with the charging option to overcome this problem.

This paper focuses on the systems of hardware and software which control robot locomotion and mechanical arm movement. It gives the details to the hardware and battery monitoring system as well. Section two and three gives literature survey and limitations and idea of new methodology. In section four, the robot mechanical design and hardware parts are explained. Section five gives the methodological design. And

section six gives basic software aspects. Section seven shows the result and discussion last section gives the conclusion and the future work of the robot.

II. HARDWARE CONCEPT

The main design concept is using the simple method but highly effective and reliable. The block diagram of the patrol robot system is shown in fig 1 and fig 1.1. All of controlling commands are sent from the base station computer to robot via zig bee. The controlling commands compose of the locomotion control, robot's navigation path and multi-joint mechanical arm control. In order to monitor video in real time, a wireless surveillance camera is mounted on the mechanical joint. The controlling commands are generated from the base station. The codes are transmitted with the help of terminal window. On the receiver side zig bee is configured as receiving purpose. A separate power station is setup for the independent power delivery to the motors and to the on board. A secondary back up power source is also arranged. All the control commands are received and compared with the help of pre determined program which is loaded in the microcontroller. A battery monitoring mechanism is setup along with the board for the awareness of the current charge level. Whenever the voltage level reaches the threshold value, the driving motors will get the power to drive the robot to the charging station. The movement of the robot is based on the commands stored in the memory during the real time. Commands are executed in last in first out, will be executed by swap algorithm.

A stepper motor is fixed at the base of the mechanical joint. This will help to rotate the arm up to 360 degree. This takes 8 steps to complete one rotation. Thus the surveillance became easier. DC gear motors are also attached to other mechanical joints for several purposes like stretching the arm, tilting the camera and one at the charging terminal for rotating the flap to make the contact with the charging station.

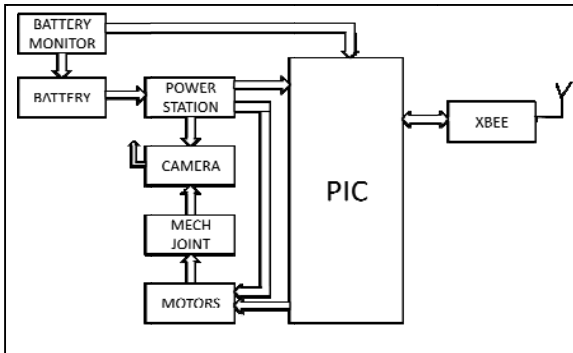


Fig. 1 : Receiver side

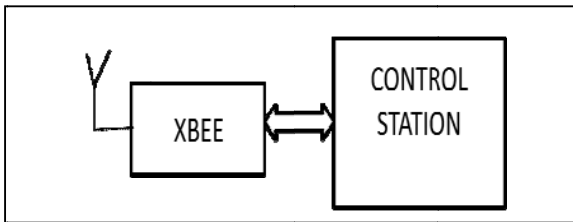


Fig. 1.1 : Base station

III. LITERATURE REVIEW AND LIMITATION

The major criteria for the patrol robots are the navigation path. Several methods are implemented for the path following purposes like developing a sensor packages and algorithms [14]. Such a robots designed on these aspects should lack on the simplicity of the hardware. This will also increment the software complexity. Other approaches like stereo vision based obstacle avoidance and visual servings, both follows algorithms and image recognition methods [15]. Hence high end processors and modules are needed to compute the path. In order to overcome this difficulty some map creation as well as artificial route mapping approaches are used [18][20][21][23]. But the mathematical computation becomes much more complex. Especially by locating the position of the robot using the markov localization method, bayes approach. This will take large amount of time to fix the position of the robot and also the next goal positions. All of these executions will drain too much power and it will affect the system performance.

IV. NEW METHODOLOGY

In order to reduce the complexity in both the hardware and software, we are introducing a robot with a swap algorithm along with track wheel. By this we can reduce the power consumption and it will lead to minimize the software as well as hardware complexity. Thereby the cost of the robot should be an economical one. With the usage of swap algorithm the robot can easily driven to the charging panel without any other human machine interactions. Mostly we can reduce the computational time.

V. MECHANICAL DESIGN

Robots are several types wheeled, tracked, and legged, multi robots, vibration types. The simplest are wheeled robots, while tracked wheels are used because of their ability to move in rough terrain surface and their greater stability. The mini bot is tracked wheel vehicle. They are relatively lightweight about 10 kg. They are quite active and fast in unstructured environments and they also perform well on uneven terrain. The whole robot structure is constructed in mild steel and the mechanical joints are effectively works with gears.

1. Body and Driving System

Thick aluminum sheet is folded to be the base frame. The locomotion driving system, all motors and mechanical joint sets and the batteries are placed in this frame in order to have the low level centre of gravity. Two 12V DC motors are used for driving base wheels separately. Both are controlled bi-directionally. Mechanical joint is fitted at the centre of the robot. With suitable commands from the operator the joint moves.

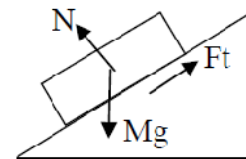


Fig. 2 : Free body diagram

When a solid body slides over a rough or smooth stationary surface, a force is exerted at the surface of contact by the moving body. This force is frictional force and is always acting in the opposite direction [25]. Consider a simplified model of the system as shown in Fig. 3. The minimum torque required for climbing a surface with slope of 20° is calculated by second law of Newton. The mini bot can be covers the steps up to 20° , because the height of the wheel is 8cm.

$$F=Ma$$

Assume the linear acceleration and thus the rotational acceleration of the wheels to be zero.

$$a=0$$

$$F_t = mg \sin$$

$$F_t = mg \sin ; \text{ let } m=10\text{kg}$$

$$F_t = 33.5\text{N}$$

The torque becomes,

$$T = F_t * r \approx 10\text{Nm}$$

The locomotion system consists of two separate sides connected to the main body while a motor independently drives the track at each side. So the desired torque is obtained by dividing the T/2 [3].

$$T = 5\text{Nm}$$

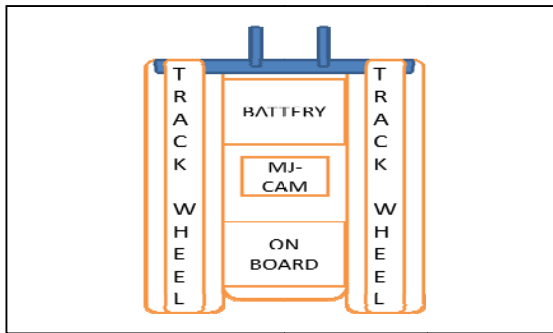


Fig. 3 : Hardware model

2. Flipper and Driving System

The flippers (dark color flap) are created in order to raise the charging terminal up for better connectivity, which is shown in the fig 3. Another 12V DC motors and transmission chains are required for flipper driving. Separate commands are generated for this action.

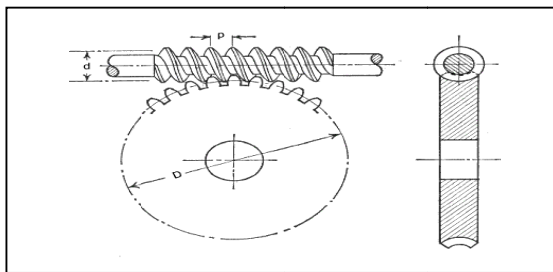


Fig. 4 : Worm Gear

For a large speed reduction worm gear is used as shown in fig.4. It consists of a large diameter worm wheel with a worm screw meshing with teeth on the periphery of the worm wheel. The worm is similar to a screw and worm wheel is similar to a screw and worm wheel is similar to a section of a nut. As the screw wheel rotates leads to rotate the wheel also.

$$\text{Reduction ratio, } R = z_2/z_1$$

3. Mechanical joint

The mechanical arm does credit to the mini –bot. This enables the robot to expand its tracks whenever it needs to close vision on the obstacles. It helps the robot to explore in many ways such as, from high level and able to get vital signs of victims [12][15][4][17][16]. In Fig. 5 shows the drawing of mechanical arm. Because the pay load at the tip of arm is small and the arm structure weight is not much, DC motor with gear set still can regulate the joint angle quite well. Arm motor is coupled to the planetary gear set with 20:1 worm gear set, which results a maximum speed of 4rpm. Let ‘h’ be the height from base to the joint. The angle of rotation is determined by θ_1 and θ_2 . If two rotational angles could change between 0 and 360 degrees, the work-space should be between a spherical surface and a cylinder. Therefore, the work-space is between a semi-spherical surface and a cylinder. A stepper motor is fixed at the bottom of the mechanical joint for the full surveillance. It takes 8 steps instead of 4 to complete one complete rotation.

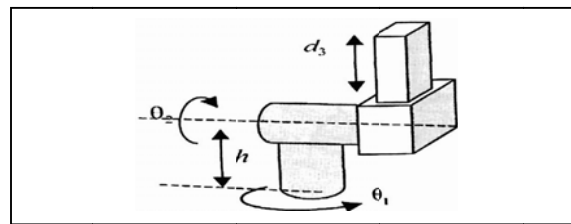


Fig. 5 : Mechanical joint

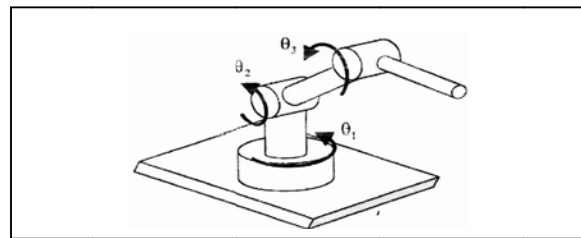


Fig. 6 : Mechanical arm

4. Visual sensor

This part is the place to install sensors which are used for searching vital sign of the victims like camera [23]. The second and the third rotary joints cannot freely rotate between 0 and 360 degree in practice. Therefore, the work-space cannot be a complete spherical volume, as shown in Fig.6. A camera is mounted in the top of the mechanical joint, which is used for getting the real time visuals, to have the site study. The data collected by the camera is transmitted to the receiver which is attached to the PC and the data is displayed on the suitable window.

5. SD card

This is the most challenging factor in robotics. Every general purpose robots, especially patrolling robots, rescue robots, navigation robots etc does not having the large storage capacity. Even though the robot uses external peripherals like hard disk, personal computers for data storage, the system should look bulky. The usage of SD card will overcome this difficulty. SD cards are available with applications from 4MB to 2TB. The data transfer speed is 15-20MB/s. SD card is connected to PORTC of the controller. CS, CLK, DO, DI, these pins are mainly used to connect with respect to controller. Thereby large amount of data can be stored. Thus the hardware space can be saved with this implementation.

Data can be read by single block, issuing the command READ_SINGLE_BLOCK to the card. For writing the data, after the valid write command card sends a response token and wait for the data block response. Whenever it receives the block it responds with a response token and write operation takes place.

VI. METHODOLOGICAL DESIGN

Here we are implementing the mini bot with two new methodologies like battery monitoring system and is followed by a swap algorithm. Charging the battery is a challenging task in robotics [5]. Robots like automatic charging, solar charging robots having some complexity in the coding. But automatic charging robots will move to the area where the electric field is present. For this high end processors are used. A monolithic integrated circuit LM3914 is used to monitor the battery charge level. This senses the voltage levels of the battery and drives the 10 light emitting diodes based on the voltage level. This IC works in two modes DOT/BAR mode. In BAR mode the current consumption is much more. In order to avoid this we are using the DOT mode, which blinks only the respective LED. When the battery charge reaches the threshold level, this will interrupt the microcontroller. There by the driving wheels get the power and remaining motors are disabled. The movement of the robot depends up on the commands stored on the memory during the running process. These commands are then executed by a swap algorithm. The robot is then driven to the charging panel. This will executed in last in first out manner. The charging of the robot can be held at the charging panel.

For the patrol robot navigation several methods are used like sensing the paths, graphical user interface, map following algorithms and compass, other Kalman filtering methods[1][2][3][14][20]. All these approaches are somehow complex. This can be overcome by using the EEPROM of the microcontroller. PIC16F877A has 256 bytes of EEPROM inside it. So memory can use it

to store data that need on a permanent basis and we can read it back from it. There are two functions to accomplish the task. Eeprom_Read and Eeprom_Write. Eeprom_Read function returns an integer and takes a parameter of the address from which the data has to be fetched. Eeprom_Write takes two parameters the first one is the address and the second one is the data.

```
unsigned short Eeprom_Read(unsigned int address);
```

```
void Eeprom_Write(unsigned int address, unsigned short data);
```

Most of the robot will navigate with different algorithm.[22][24][18][19]. The robot will navigate with respect to the commands from the user. All the running commands are stored in the memory and also a timer is set to determine how long the commands are executed. Now the current position of the robot is at B after starting from A. Whenever it needs to return, the last stored command will execute first (LIFO). If the last executed command is forward, that swaps it into backward command at the same time the timer starts decrements the value. If the path having the deviation as shown in fig.7, halts and proceeds to the left and move forward. At the time of returning, initially the command is fetched and checked which command is executed lastly. Let the last executed command is forward. Then it swaps it in to backward command by calling the forward function in the program. Similarly,

Backward \approx Forward

Left \approx Left

Right \approx Right

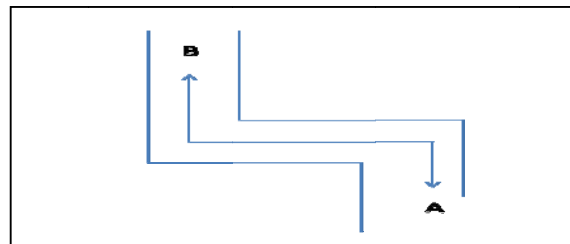


Fig. 7 : Navigation path

VII.SOFTWARE ASPECT

Onboard software is mainly developed with micro C. This software interfaces between the operator station software and the robot by receiving operator's command to control all robot functions. Simulations have been executed both in Mat lab and PIC simulator. In Mat lab the approaches were implemented under ideal hypothesis, more realistic settings. The commands are sends through serial communication with the help of terminal window to zig bee module. Zig bee module is configured as a transparent mode for the normal

transmission. On recharging and navigation of the robot swap algorithm is executed. Real time visuals can be captured and displayed on the window with the help of surveillance camera. A tunable receiver is connected to the base station for proper reception.

VIII. RESULT AND DISCUSSION

The proposed robot was successfully designed and implemented. With the help of swap algorithm the navigation operation was also effective. Thereby the power consumption is reduced. Battery monitoring system is also worked well. The limitation of this robot is obstacle detection, far objects cannot be detected. Instead of IR we can use ultrasonic sensors.

IX. CONCLUSION AND FUTURE WORK

The mini bot robot was designed and implemented. The patrol robotic system with track wheel type and gearing, driving method has been briefly described. Its performances were observed to be excellent in unstructured environments. The development of this mini-bot robot can be adapted to fit many other applications easily by changing the top part of the robot. Single stretched mechanical arm is designed and implemented. It cannot stretch not much longer. This can solve with the design and implementation of robot with more degree of freedoms mechanical arm which can stretch to 150 cm or more. For better the access of the robot instead of zig bee we can choose WIFI/internet. Instead of using the internal memory, external EEPROM can be implemented. Hence large amount of information can be stored.

X. ACKNOWLEDGMENT

The research in this paper was carried out at Hindustan Institute of Technology and science, Chennai. This work was supported by the e-MEN Robotic Research centre, palakkad.

REFERENCES

- [1] Fen Xu, Zheng Xi Li, Kui Yuan "The design and implementation of an autonomous campus patrol robot" Proceedings of the 2008 IEEE International Conference on Robotics and Biomimetics.
- [2] Mbaïtiga Zacharie "Intelligent okikosen PBXI security patrol robot via network and map based route planning" journal of computer science 5(1):79-85,2009.
- [3] S. Ali A. Moosavian, Hesam Semsarilar, Arash Kalantari "Design and manufacturing of a mobile rescue robot" international conference on intelligent robots and system oct 9-15-2006 IEEE.
- [4] Amon Tunwannarux, and Supanunt Tunwannarux "Design of a 5-Joint Mechanical Arm with User-Friendly Control Program" World Academy of Science, Engineering and Technology 27 2007.
- [5] Ying Zhang, Kimon D. Roufas and Mark Yim "Software Architecture for Modular Self-Reconfigurable Robots" Xerox Palo Alto Research Center
- [6] Ying Zhang, Markus P.J. Fromherz, Lara S. Crawford and Yi Shang" A General Constraint Based Control Framework with Examples in Modular Self-Reconfigurable Robots"
- [7] Andreas Kolling Stefano Carpin"multirobot surveillance: an improved algorithm for the GRAPH CLEAR problem"
- [8] Andreas Kolling and Stefano Carpin" Multi-Robot Pursuit-Evasion without Maps"
- [9] Andreas Kolling and Stefano Carpin" Extracting Surveillance Graphs from Robot Maps"
- [10] Stefano Carpin, Gorkem Erinc "A genetic algorithm for nonholonomic motion planning"
- [11] Stefano Carpin "RANDOMIZED MOTION PLANNING – A TUTORIAL" International University Bremen, Germany
- [12] Principles of Robotics page 24-38, pg54-57
- [13] Fung Po TSO, Lizhuo Zhang, Weijia Jia "Video Surveillance Patrol Robot System in 3G, Internet and Sensor Networks" SenSys'07, November 6–9, 2007, Sydney, Australia
- [14] Robert W. Hogg, Arturo L. Rankin, Stergios I. Roumeliotis "Algorithms and Sensors for Small Robot Path Following"
- [15] C. Won, T. Frost "A Portable, Autonomous, Urban Reconnaissance Robot" IS Robotics, Somerville MA, 02143
- [16] Redwan Alqasemi and Rajiv Dubey "Control of a 9-DoF Wheelchair-Mounted Robotic Arm System" 2007 Florida Conference on Recent Advances in Robotics, FCRAR 2007
- [17] Jegede Olawale, Awodele Oludele, Ajayi Ayodele and Ndong Miko Alejandro "Development of a Microcontroller Based Robotic Arm" Proceedings of the 2007 Computer Science and IT Education Conference.

- [18] Yongxing Hao, Benjamin Laxton, Sunil K. Agrawal, Edward Lee, Eric Benson "Planning and Control of UGV Formations in a Dynamic Environment: A Practical Framework with Experiments" Proceedings of the 2003 IEEE International Conference on Robotics & Automation Taipei, Taiwan, September 14-19, 2003
- [19] Johann Borenstein+ and Yoram Koren "MOTION CONTROL ANALYSIS OF A MOBILE ROBOT" Transactions of ASME, Journal of Dynamics, Measurement and Control, Vol. 109, No. 2, pp. 73-79. [20]
- [20] Sebastian Thrun¹, Maren Bennewitz², Wolfram Burgard²"MINERVA: A Second Generation Museum Tour-Guide Robot" Carnegie Mellon University
- [21] Stephen J. Tobias, A. Antonio Arroyo "Autonomous Path finding" 2000 Florida Conference on Recent Advances in Robotics May 4-5, 2000, Florida Atlantic University
- [22] Namal A. Senanayake, Khoo B. How, and Quah W. Wai "Tele-Operated Anthropomorphic Arm and Hand Design" World Academy of Science, Engineering and Technology 39 2008
- [23] Ali Sekmen, Sheldon Greene "Vision-based Mobile Robot Learning and Navigation" 2005 IEEE International Workshop on Robots and Human Interactive Communication
- [24] Brandi House, Jonathan Malkin, Jeff Bilmes "The VoiceBot: A Voice Controlled Robot Arm" CHI 2009, April 4-9, 2009, Boston, Massachusetts, USA.
- [25] Dr.R.K.Bansal "a textbook of engineering mechanics" page no 195-199, page no 205-209



Design and Implementation of a Simplified Humanoid Robot with 8 DOF

Hari Krishnan R & Vallikannu A. L

Department of Electronics and Communication Engineering, Hindustan Institute of Technology and Science, Hindustan University, Chennai, India

Abstract - This paper discusses a simplified design of Humanoid Robot with 8 DOF. The main objective is to analyze the theoretical and practical challenges involved in making it. The paper emphasis on bringing down the control complexity by reducing the number of actuators used . This in turn simplifies the entire design processes and reduces the production cost. It also describes the stability issues and different walking phases in detail. The proposed robot finds the place in between simple, miniaturized humanoids and the most advanced, sophisticated humanoids.

Keywords - Humanoid Robot, Degrees Of Freedom (DOF), Dead Weight, Centre Of Gravity, Joint Structure, Center Of Mass (COM).

I. INTRODUCTION

Humanoid Robots basically resembles human physical structure. Humanoid Robotics is an attempt to design a tool that works with human and is specifically not an attempt to recreate human being. Humanoids are expected to co-exist and work together with humans in environments which are meant for human beings. Such Robots has to interact with humans, who lives a social life. Simulation of human body gives a better idea about Humanoids.

A minimalistic approach for designing Humanoids is achieved by utilizing springs and the oscillatory motion of pendulums [1]. The robots designed with such an approach has simple control mechanisms, minimal actuation , minimal energy usage and minimal cost of production. Though robot locomotion by walking could be accomplished with these robots, it lacks areas of application due to its insane structure and design. On the other hand researches are being carried out for developing complex humanoid robots, which is similar to human beings. This could be called the complex approach. The ASMO humanoid manufactured by Honda, the WABIAN series of humanoids of Waseda University, Bonten-Maru II[2] , KHR-2 [3] , HRP2 [5] are well known for human like design. Researchers has also developed designs for humanoid robot from the perspective of DOFs and joint angles to attain Flexibility in human-like motion [2]. To achieve this they closely monitored physical structure flexibility of human and correlated it to their design.

The objective of this research is to develop a humanoid robot that could find a place in between, the robots developed using the 2 approaches. The proposed robot design emphasis on minimal computational and mechanical skill, minimal

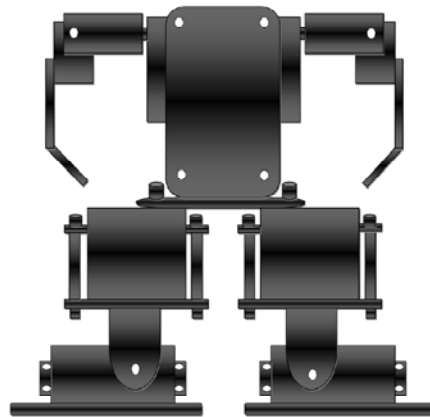


Fig. 1 : Model of Proposed Robot

actuators, simple control algorithms and electronics and most importantly it reduces production cost. The Robot has 8 DOFs, with 4 DOFs on upper body and 4 DOFs on lower body. The upper body has 2 arms with shoulder and elbow (2 DOFs each .) Lower body has 2 legs with Hip and Ankle (2 DOFs each). Design model of the proposed humanoid robot is shown in Figure 1.

II. MECHANICAL DESIGN

A. Design Considerations

The Design considerations are as follows[4].

- 1) Height of the Humanoid
- 2) Angle of body in frontal plane
- 3) Angle of body in lateral plane
- 4) Position of feet with respect to body
- 5) Position of feet with respect to floor
- 6) Speed of robot movement

B. Configuration of Links and Joints

Figure 2 shows configuration of links and joints of the proposed robot with respect to yaw, pitch and roll rotation axes. The shoulders of left and right arm of the robot has 1 DOF each with pitch rotation axis. Rotation axis of elbows are roll. At the lower limbs, the hips exhibits yaw and the ankles exhibits roll rotation axes. Figure 3 gives a detailed idea on joint structure of leg and arm of the humanoid robot. Table 1 shows a comparison of joints of proposed robot with that of

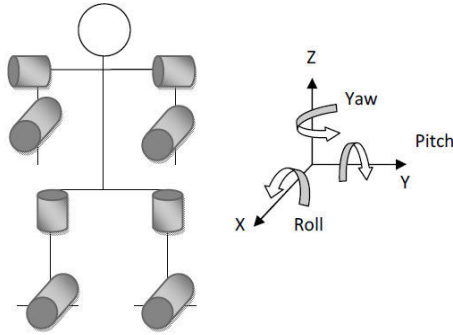


Fig. 2 : Configuration of Links and Joints

main joints of human and with that of Bonten-Maru II humanoid robot[2].

C. Lower body design

Compared to upper body, legs of Human are of less weight. This allows them to lift a foot without adjusting the upper body position. The situation of a Humanoid Robot is entirely different. The actuators on the legs of the robot makes them heavier than the upper body. So for successful locomotion, when one foot is moved, the entire upper body is leaned towards the opposite side. A biped walker undergoes 2 basic support phases. In single support phase, only one feet of the robot is on ground and in Double support phase, both the feet are on ground [4].

1) An Overview on Kinematic Model of 4 DoF Biped

Kinematic Model is the mapping of Cartesian space from Joint space. This mapping is necessary, as it determines the orientation of the foot and to calculates the positions of Centre of Mass of the links. Generalized position vector (q), generalized velocity vector (\dot{q}) and generalized acceleration vector (\ddot{q}) are the net result of the kinematic model .

The Joint angles and Link parameters of a 4 DOF biped robot is shown in Figure 4. It is a 5 links, 4 joints structure. For the sake of simplicity foot links, a_4 and a_5 are considered to be virtual links with zero mass, zero length and hence zero inertia [8]. Thus the structure under consideration becomes, a biped with 3 links and 4 joints. From figure 4, every joint i , has a unique reference name, j_i and are actuated revolute joints. a_i is the link vector connecting the joints j_{i-1} to j_i . A COM vector is a vector, b_i , specifying the COM of link i relative to j_{i-1} . Mass of link i is called m_i . Θ_i represents angle of rotation of each joints.

TABLE 1 : COMPARISON OF JOINT DISTRIBUTION

Joint	DOF at right/left (rotation axis)		
	Human	Bonten-Maru II	Proposed Robot
Neck	3(Yaw.Pitch.Roll)	2 (Yaw.Pitch)	0
Right/Left Shoulder	3/3 (Yaw.Pitch.Roll)	2/2 (Pitch.Roll)	1/1 (pitch)
Right/Left Elbow	1/1 (Roll)	1/1 (Roll)	1/1 (Roll)
Right/Left wrist	3/3 (Yaw.Pitch.Roll)	0/0	0/0
Waist	3(Yaw.Pitch.Roll)	1 (Yaw)	0/0
Right/Left Hip	3/3 (Yaw.Pitch.Roll)	3/3 (Yaw.Pitch.Roll)	1/1 (Yaw)
Right/Left Knee	1/1 (Pitch)	1/1 (Pitch)	0/0
Right/Left Ankle	3/3 (Yaw.Pitch.Roll)	2/2 (Pitch.Roll)	1/1(Roll)

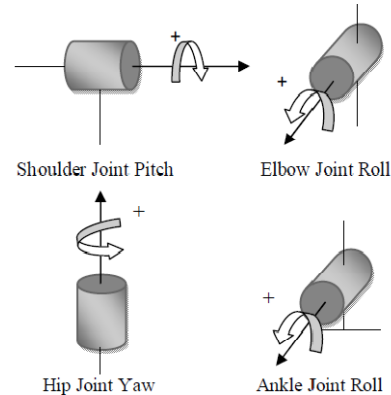


Fig. 3 : Leg and Arm Joint Structure

The orientation of the third link frame of the biped structure shown in Figure 4, can be found using

$${}^0R(\Theta_1, \Theta_2, \Theta_3) = {}^0R(\Theta_1) {}^1R(\Theta_2) {}^2R(\Theta_3) \quad (1)$$

The orientation of first link frame is

$${}^0R(\Theta_1) = \begin{bmatrix} 1 & 0 & 0 \\ 0 & C_1 & -S_1 \\ 0 & S_1 & C_1 \end{bmatrix} \quad (2)$$

Where $C_1 = \cos(\Theta_1)$ and $S_1 = \sin(\Theta_1)$

The orientation of second link frame is

$${}^1R(\Theta_2, \Theta_3) = \begin{bmatrix} C_2 & -S_2 & 0 \\ C_1 S_2 & C_1 C_2 & -S_1 \\ S_1 S_2 & S_1 C_2 & C_1 \end{bmatrix} \quad (3)$$

and orientation of third link frame is

$${}^2R(\Theta_1, \Theta_2, \Theta_3) = \begin{bmatrix} C_2 C_3 - S_2 S_3 & -C_2 S_3 - S_2 C_3 & 0 \\ C_1 S_2 C_3 + C_1 C_2 S_3 & -C_1 S_2 S_3 + C_1 C_2 C_3 & -S_1 \\ S_1 S_2 C_3 + S_1 C_2 S_3 & -S_1 S_2 S_3 + S_1 C_2 C_3 & C_1 \end{bmatrix} \quad (4)$$

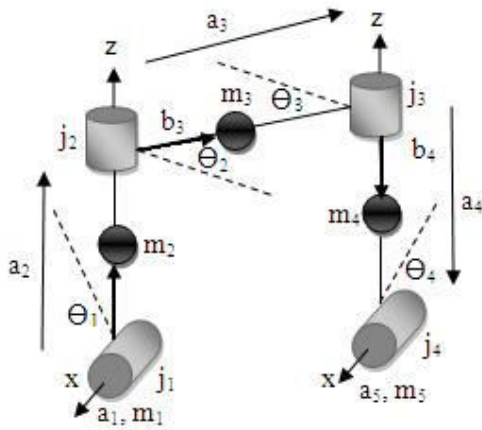


Fig. 4 : Joint angles and link parameters

The iterative equation for position of COM of link $i+1$ is

$$P_{i+1} = \begin{bmatrix} x_{i+1} \\ y_{i+1} \\ z_{i+1} \end{bmatrix} = {}^0R D_i + P_i \quad (5)$$

where

P_{j_i} is the position of joint i defined as

$$P_{i+1} = \begin{bmatrix} x_{i+1} \\ y_{i+1} \\ z_{i+1} \end{bmatrix} = {}^0R D_i + P_i \quad (6)$$

The Generalized position vector is

$$q = \begin{bmatrix} x \\ y \\ z \\ \Theta \end{bmatrix} \quad (7)$$

where

$$x = [x_1 \ x_2 \ x_3]^T$$

$$y = [y_1 \ y_2 \ y_3]^T$$

$$z = [z_1 \ z_2 \ z_3]^T$$

which contains x, y, z co-ordinates of all COM's

$$\Theta = [\Theta_1 \ \Theta_2 \ \Theta_3 \ \Theta_4]^T$$

contains all joints

Generalized velocity vector

$$\dot{q} = \frac{\partial q}{\partial t} \quad (8)$$

and generalized acceleration vector

$$\ddot{q} = \frac{\partial^2 q}{\partial t^2} \quad (9)$$

2) Stability Issue and Biped Logic gait phases

Extreme care should be taken while designing the lower body of a humanoid robot. Stability is the major problem that arises during robot walking. For a biped robot to walk, it stands on single leg and swings, the other leg forward. When both the legs comes to footing, in other words, if it is in double support phase, then the robot is said to be in a stable condition. To provide stability in single support phase, the concept of a moving 'Dead Weight' is utilized. According to this concept, the upper body weight is moved, so as to bring the centre of gravity on the axis of the footing leg. By this the momentum during single support phase is balanced[4].

Various phases of forward walking of the proposed humanoid robot is illustrated in Figure 5. From the Figure 5, W_M is the Weight of the upper body, Θ_R and Θ_L are angles around the axis of Left and Right legs respectively. Biped logic gait phases are divided into six

. While walking, these phases are continuously repeated. The phases are selected in such a way that, the robot is statically stable at the end of each phase. Each phases are described as follows:

- Phase 1- Initially the robot will be in neutral condition. The Weight will be shared among the two legs. When considering Centre of Gravity, it is maintained between the two legs. The robot is now said to be in Double support phase.

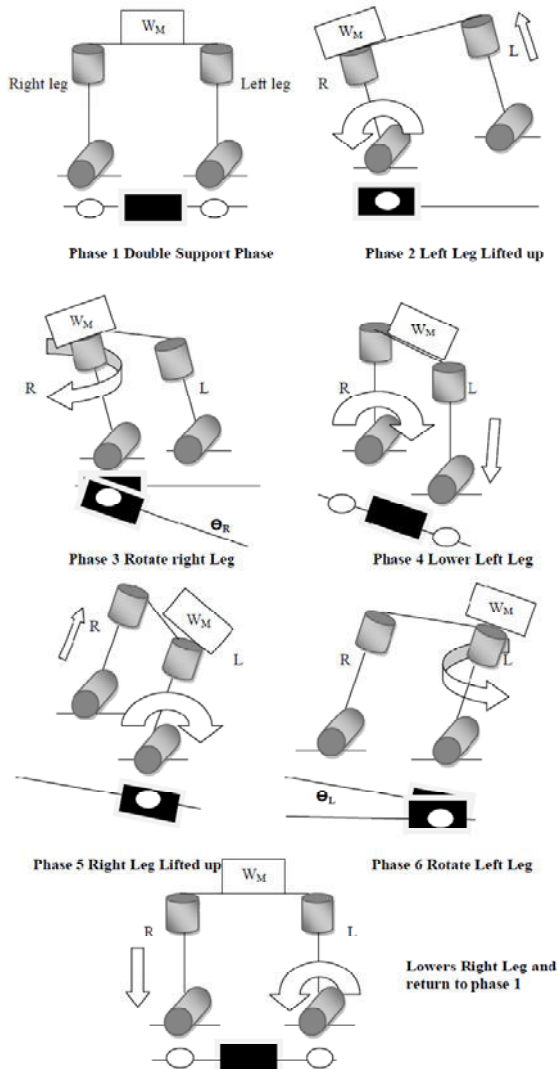


Fig. 5 : Step by step illustration of forward walking

- Phase 2 - In this phase the robot leans from left to right. The roll orientation at the ankle shifts the Weight towards right leg. As the weight is shifted towards the right leg, the centre of gravity is now

concentrated on right foot region. This phase is called Pre-swing single support phase.

- Phase 3- In this phase, the lifted left leg is made to swing in air, keeping the right feet left under the upper body. This phase is known as Swing Single support phase. This movement is achieved by Yaw orientation of the hip.
- Phase 4- As left feet reaches highest point of its trajectory, the feet is lowered back to the ground. Now the robot is said to be in Post swing double support phase. The centre of gravity is now between the two legs.
- Phase 5- The robot leans from right to left. The Weight is shifted towards right.
- Phase 6- right leg swings in air.

After Phase 6, motion continues with a transition to phase 1 and the walking continues[3,4,6,7].

3) Structural Design

The lower limbs of the robot has 4 angular motions. I.e. 1 Yaw orientation at hip and 1 roll orientation at the ankle of each legs. In biped robots, movable range of the legs and capacity of the actuators also plays an important role[3]. So high quality motors which exhibits high torque has to be selected for practical design. Servo motors with double ball bearing and metal gears having stall Torque of 14 Kg/cm are used in the proposed design. Large foot pads of 9x6.5 cm, makes the robot more stable in one foot phase. The ankle motors are fixed on to the foot pads. The bracket that joints the hip motor and ankle motor is made of plastic. The servomotors at the hips that provide yaw orientation is designed to hang on shaft to the plastic link, that connects the two legs. While walking, to ensure that the legs doesn't hit each other, an optimal distance has been maintained.

D. Upper body Design

The upper body of the proposed robot consists of arms and torso that include 4 DOFs in total. In upper body, space for installing the controller board and electronics has been considered. The size of the torso is 9x5 cm and is made of plastic. To provide pitch orientation at the shoulders, servo motors with double ball bearing and plastic gears, having stall torque of 5.5 Kg/cm are used. Micro Servos of lesser size and stall Torque of about 1.8 Kg/cm are employed for attaining roll orientation at the elbows. Aluminum brackets are used to connect shoulder servo and elbow servo. The elbow motor is designed to hang on to the bracket, which is connected to the shoulder motor. The arm part of the robot is also made of Aluminum. No space has

been reserved for battery, as in the proposed robot external power source is used .

Figure 6 shows, the fabricated model of the robot and Figure 7 illustrates, the implemented result of various phases of robot gait

III. ELECTRICAL DESIGN

Every Robot has a number of motors to provide actuation and sensors which are controlled using a processing element. There are varieties of actuators, sensors and processing elements. In this project, two separate PIC 18F452, microcontrollers are employed as processing elements. The circuit is designed in such a way that, only one microcontroller will be active at a particular time. Controller selection switch is provided to select the microcontroller to be used The idea of implementing the design using two microcontrollers is to

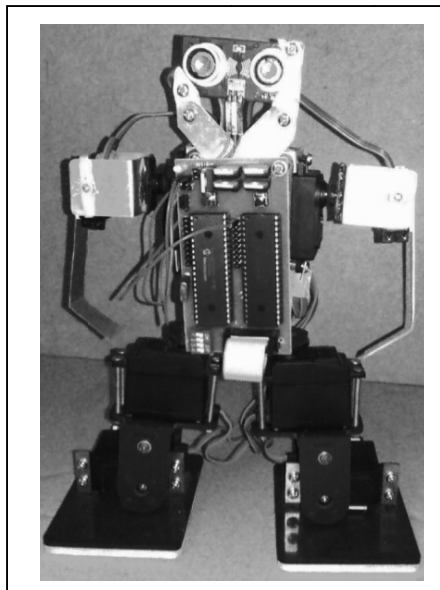


Fig. 6 : Fabricated model of the robot

increase the number of applications, that can be performed by the robot in future. By this the entire load of applications could be divided on to two microcontrollers, thus making the control part easier and simple. A 4 pin DIP switch is provided to select a particular application embedded in each controller. Due to space limitations in Main Controller Board, a Servo Extension board is provided. This board provides power and signals for the servo motors. Servo Extension Board is connected to Main controller board via FRC. An Ultrasonic Sensor Module is included for obstacle detection. This sensor module is mounted on top of the

torso so that it represents the head of the robot. The various modules used are showed in Figure 8.

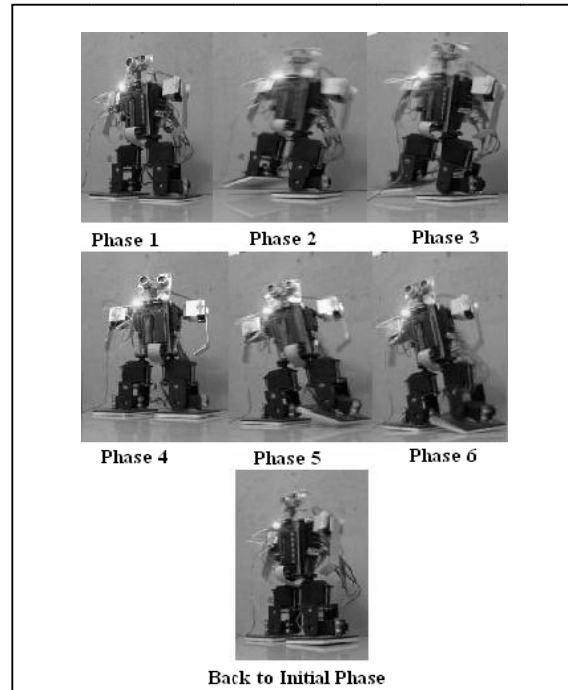


Fig. 7 : Implemented results of phases of robot gait

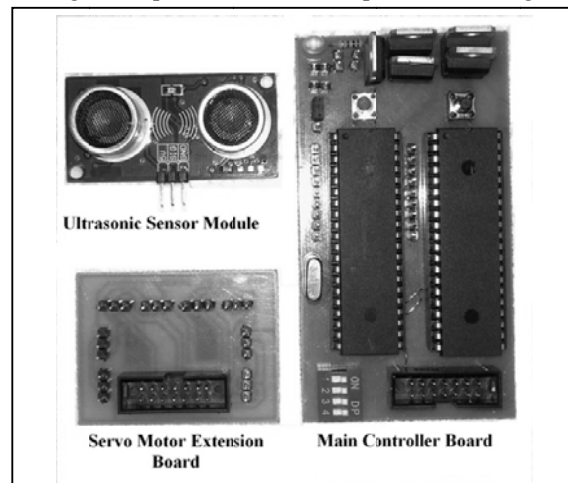


Fig. 8 : Various Modules Used

IV. FIRMWARE DEVELOPMENT

In this paper, the firmware developed to make the robot walk is discussed. All the 4 motors on the lower limbs are controlled and actuated simultaneously. Servo Motors are actuated using Pulse Width Modulation. So major aim is to program to generate PWM signal for each motors. Initially, all the motors are brought to ideal position. Now the robot is in attention posture. The first

motor which initiates the movement is serviced with on-time pulse period. During the off-time pulse period of this motor, the next motor is serviced with on-time pulse period. Likewise all the remaining motors are serviced. No special algorithms or sensors for feedback are used for balancing. So while continuous walking, after every five steps, all the motors are brought to ideal position. Figure 9 shows the flowchart for forward walking based on phases illustrated in Figure 5.

V. CONCLUSION

The reduction in number of DOF of the robot, reduces the robot development cost as well as increases robustness. The biped gait discussed is simple and could be implemented easily. As the number of DOFs increases, the complexity of mechanical design and design of control electronics becomes more complex. Making a humanoid to walk with lesser number of DOFs is a choice of interest, as it leads to energy efficient design. This paper proposes some foundations for further research and development of humanoid robots with minimum number of DOFs.

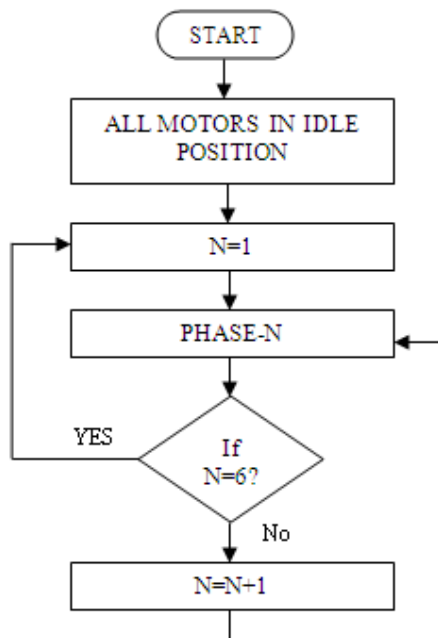


Fig. 9 : Flow Chart for forward walking

REFERENCES

- [1] Leonid Paramonov, Henrik Hautop Lund, "A Minimalistic Approach to Humanoids," in Proc. IEEE-RAS Int. Conf. on Humanoid Robots, 2001
- [2] Hanafiah Yussof, Mitsuhiro Yamano, Yasuo Nasu, Masahiro Ohka, "Design of a 21-DOF Humanoid Robot to Attain Flexibility in Human – Like Motion," in Proc 15th IEEE Int. Conf on Robot and Human Interactive Communication (RO-MAN06), 2006, pp.202-207.
- [3] Jung-Yup Kim, Ill-Woo Park, Jungho Lee, Min-Su Kim, Baek-kyu Cho, Jun-Ho Oh, "System Design and Dynamic Walking of Humanoid Robot KHR-2," in Proc IEEE Int. Conf. on Robotics and Automation, 2005, pp.1443-1448.
- [4] Appuu Kuttan K.K, Robotics, I.K International Publishing House Pvt. Ltd, India, 2007.
- [5] Kenji KANEKO1, Fumio KANEHIRO, Shuuji KAJITA, Kazuhiko YOKOYAMA, Kazuhiko AKACHI, Toshikazu KAWASAKI, Shigehiko OTA, Takakatsu ISOZUMI, "Design of Prototype Humanoid Robotics Platform for HRP," in Proc. IEEE/RSJ Int. Conf. on Intelligent Robots and Systems, 2002, pp. 2431-2436.
- [6] Andre Senior, Sabri Tosunoglu, "Robust Bipedal Walking: The Clyn Project," The 18th Florida Conf. on Recent Advances in Robotics, 2005.
- [7] Jacky Baltes, Sara McGrath, John Anderson, "Active Balancing Using Gyroscopes for a Small Humanoid Robot," in Proc. 2nd Int. Conf. on Autonomous Robots and Agents, 2004, pp. 470-475.
- [8] Jens Christensen, Jesper Lundgaard Nielsen, Mads Solver Svendsen, Peter Flakesgaard Orts, "Development, Modelling and Control of a Humanoid Robot," Technical report, Aalborg University, 2007

□□□

Design of a Simple Maze Solving Robot Using Sensor Fusion Unit

Shyam. R. Nair

Hindustan Institute of Technology and Science, Hindustan University, Chennai, India

Abstract - Robots are now a day's used in all leading companies, defense purpose, research and development etc. Robots are also used for amusement purpose. This paper focuses on designing a robot that solves simple maze using a sensor fusion unit. The robot can identify and differentiate destination and trap. Hence it can come out of the trap automatically.

Keywords - robotics, sensor fusion, maze, eeprom.

I. INTRODUCTION

Robot is a machine to execute different task repeatedly with high precision. Thereby many functions like collecting information and studies about the hazardous sites which is too risky to send human inside. Robots are used to reduce the human interference nearly 50 percent. Robots are mainly in different types like fire fighting robot, metal detecting robot, rescue robots, patrol robots other humanoid robots etc. Mostly used in industrial purpose, military, defense, research and development etc. Security robots are used in all major areas of industries, defense units and other places which require high security. Certain robots are used for amusement purpose like robot race, maze solving etc.

This paper focus on developing a hardware and software scheme for a simple maze solving robot using a sensor fusion unit. The hardware and software is schemed in such a manner that the robot takes logical decisions according to the data obtained from the sensor fusion unit and can come out of a trap by itself using the same intelligence.

II. HARDWARE CONCEPT

The robot has a platform with four wheels for free motion. The wheels are coupled to DC geared motors with an appropriate rpm. The platform is designed to fit a microcontroller board, three IR sensors, motor driving circuits and a battery.

When the robot is turned on, it checks the sensor fusion unit and starts motion accordingly. When the robot identifies an ideal or non-ideal junction it takes deviation and proceeds in the path. An ideal junction is the one where the robot can take only one deviation to proceed. Whereas, non-ideal junction is the one where the robot can take more than one deviation. If the robot finds a dead end, it checks whether the last junction was

ideal or non ideal. If it was ideal, then the robot has reached the destination otherwise it is a trap. If a trap is identified, the robot goes back to the previous non-ideal junction and takes the other deviation.

IR1	IR2	IR3	Action	Comment
0	0	0	Forward; Left; Right	Non-ideal
0	0	1	Forward; Left	Non-ideal
0	1	0	Left; Right	Non-ideal
0	1	1	Left	Ideal
1	0	0	Forward; Right	Non-ideal
1	0	1	Forward	Ideal
1	1	0	Right	Ideal
1	1	1	Destiny; Trap	Finished; Go back to previous non-ideal

Fig. 1

	IR1 IR2 00	01	11	10
IR3 0	X	X	Y	X
1	X	Y		Y

Fig. 2

III. MOVEMENT OF ROBOT USING THE DATA FROM SENSOR FUSION UNIT

The robot moves and takes deviations according to the logic defined in the table in fig.1. IR1, IR2 and IR3 are infrared sensor at the left side, right side and front side of the robot. A 0 in the output of the sensor

indicates availability of a free path and 1 indicates presence of wall. The robot uses this data and moves in the free path. If the robot identifies only one free path, then it is known as ideal junction and if the robot identifies more than one free path, then it is a non-ideal junction.

- *Ideal junction*

The robot is said to have reached an ideal junction if the sensor fusion data is 011, 101 and 110. That is, the robot can take a deviation in only one path. The “Y” in the fig.2 indicates ideal junctions.

- *Non-ideal junction*

The robot is said to have reached a non-ideal junction if the sensor fusion data is 000, 001, 010 and 100. That is, the robot can take a deviation in more than one path. The “X” in fig.2 indicates non-ideal junction. There is priority given to the robot when it identifies a non-ideal junction as shown in the fig.2 separated by semicolon. In such situations, the robot stores all the movement data and time delay of the movement in the eeprom of the pic microcontroller. The robot continues the navigation and if it identifies a dead end, 111, the robot returns back to the previous non-ideal junction by using the data in eeprom and takes the next possible deviation. The robot continues navigation in similar manner for all possible deviations and if the robot identifies a dead end and if it has no more deviations to take, then the robot identifies that the maze cannot be completed. If the robot reaches the destination, then the sensor at the top is activated as there is an upper wall at the destination.

IV. RETURNING OF ROBOT TO JUNCTION USING THE DATA IN EEPROM

When the robot identifies a dead end, it uses the data in eeprom to return back to the previous non-ideal junction. For the patrol robot navigation several methods are used like sensing the paths, graphical user interface, map following algorithms and compass, other Kalman filtering methods[1][2][3][4][7]. All these approaches are somehow complex. This can be overcome by using the EEPROM of the microcontroller. PIC16F877A has 256 bytes of EEPROM inside it. So memory can use it to store data that need on a permanent basis and we can read it back from it. There are two functions to accomplish the task. Eeprom_Read and Eeprom_Write.

Eeprom_Read function returns an integer and takes a parameter of the address from which the data has to be fetched. Eeprom_Write takes two parameters the first one is the address and the second one is the data.

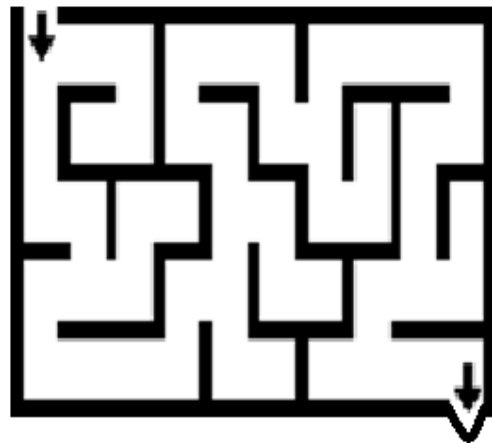
unsigned short Eeprom_Read(**unsigned int** address);

void Eeprom_Write(**unsigned int** address, **unsigned short** data);

Most of the robot will navigate with different algorithm.[8][9][5][6] All the running commands are stored in the memory and also a counter is set to determine how long the commands are executed. Whenever it needs to return, the last stored command will execute first (LIFO). If the last executed command is forward, that swaps it into backward command. Similarly,

Backward \approx Forward

SAMPLE MAZE



MECHANICAL PART

Robots are several types wheeled, tracked, and legged, multi robots, vibration types. The simplest are wheeled robots, while tracked wheels are used because of their ability to move in rough terrain surface and their greater stability. The mini bot is tracked wheel vehicle. They are relatively lightweight about 10 kg. They are quite active and fast in unstructured environments and they also perform well on uneven terrain. The whole robot structure is constructed in mild steel and the mechanical joints are effectively works with gears.

- *Body and Driving System*

Thick aluminium sheet is folded to be the base frame. The locomotion driving system, all motors and mechanical joint sets and the batteries are placed in this frame in order to have the low level centre of gravity. Two 12V DC motors are used for driving base wheels separately. Both are controlled bi-directionally. Mechanical joint is fitted at the centre of the robot. With suitable commands from the operator the joint moves.

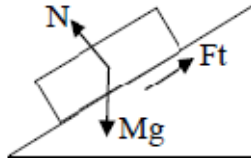


Fig. 3 : Free body diagram

When a solid body slides over a rough or smooth stationary surface, a force is exerted at the surface of contact by the moving body. This force is frictional force and is always acting in the opposite direction [10]. Consider a simplified model of the system as shown in Fig. 3. The minimum torque required for climbing a surface with slope of 20° is calculated by second law of Newton. The mini bot can be covers the steps up to 20° , because the height of the wheel is 8cm.

$$F=Ma$$

Assume the linear acceleration and thus the rotational acceleration of the wheels to be zero.

$$a=0$$

$$F_t - mg \sin\theta$$

$$F_t = mg \sin\theta; \text{ let } m=10\text{kg}$$

$$F_t = 33.5\text{N}$$

The torque becomes,

$$T = F_t * r \approx 10\text{Nm}$$

The locomotion system consists of two separate sides connected to the main body while a motor independently drives the track at each side. So the desired torque is obtained by dividing the $T/2$ [3].

$$T = 5\text{Nm}$$

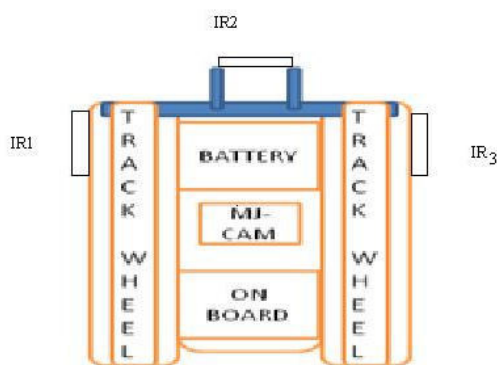


Fig. 4

SOFTWARE ASPECT

Onboard software is mainly developed with micro C. The program is flashed to the PIC microcontroller using a pic burner. Simulations have been executed both in Mat lab and PIC simulator. In Mat lab the approaches were implemented under ideal hypothesis, more realistic settings.

V. CONCLUSION AND FUTURE WORK

The maze solving robot moves identifies and moves through free paths by using the sensor fusion unit. The robot also has the advantage of identifying the trap and destination. The hardware and software scheme assures that the robot comes out of trap and reaches destination without any human involvement.

In future, more sensors can be added to the sensor fusion unit to solve complicated mazes.

ACKNOWLEDGMENT

The research in this paper was carried out at Hindustan Institute of Technology and science, Chennai. This work was supported by the e-MEN Robotic Research Centre Palakkad.

REFERENCES

- [1] Fen Xu, Zheng Xi Li, Kui Yuan "The design and implementation of an autonomous campus patrol robot" Proceedings of the 2008 IEEE International Conference on Robotics and Biomimetics.
- [2] Mbaïtiga Zacharie "Intelligent okikosen PBXI security patrol robot via network and map based route planning" journal of computer science 5(1):79-85,2009.
- [3] S. Ali A. Moosavian, Hesam Semsarilar, Arash Kalantari "Design and manufacturing of a mobile rescue robot" international conference on intelligent robots and system oct 9-15-2006 IEEE
- [4] Robert W. Hogg, Arturo L. Rankin, Stergios I. Roumeliotis "Algorithms and Sensors for Small Robot Path Following"
- [5] Yongxing Hao, Benjamin Laxton, Sunil K. Agrawal, Edward Lee, Eric Benson "Planning and Control of UGV Formations in a Dynamic Environment: A Practical Framework with Experiments" Proceedings of the 2003 IEEE International Conference on Robotics & Automation Taipei, Taiwan, September 14-19, 2003

- [6] Johann Borenstein+ and Yoram Koren "MOTION CONTROL ANALYSIS OF A MOBILE ROBOT" Transactions of ASME, Journal of Dynamics, Measurement and Control, Vol. 109, No. 2, pp. 73-79. [20]
- [7] Sebastian Thrun¹, Maren Bennewitz², Wolfram Burgard²"MINERVA: A Second Generation Museum Tour-Guide Robot" Carnegie Mellon University.
- [8] Stephen J. Tobias, A. Antonio Arroyo "Autonomous Path finding" 2000 Florida Conference on Recent Advances in Robotics May 4-5, 2000, Florida Atlantic University.
- [9] Ali Sekmen, Sheldon Greene "Vision-based Mobile Robot Learning and Navigation"2005 IEEE International Workshop on Robots and Human Interactive Communication
- [10] Dr. R. K. Bansal "a textbook of engineering mechanics" page no 195-199,page no 205-209



Energy Efficient Protocol for Data Gathering in Wireless Sensor Network using Multi-Sensor

Soni Chaurasia & Meenakshi Dhull

Computer Science & Engineering Deptt., Lingaya's University, Faridabad, (H. R.), India

Abstract - A sensor in wireless sensor networks (WSNs) periodically produces data as it detects its locality. The basic operation in such a network is the systematic accumulation and transmitting of sensed data to the sink node for further processing. A key challenging question in WSNs is to choose best routing protocol to amass data from various sensing devices and send it to the sink node. Routing protocols are used in various networks like: homogeneous sensor and heterogeneous network. The proposed routing algorithm is based on heterogeneous sensors environment. The information will be sensed and transmitted by the trans-receiver units. Two different radios, low power radio used for detection of the event and high power radio used for data transmission. Routing protocol which consumes less energy and produces minimum traffic is used in that particular network. The proposed protocol is based on a network which uses hybrid heterogeneous sensors and it will depend upon the range of sensors to detect the locality. The protocol work focuses on minimizing traffic in the sensor node and energy consumption by sensor nodes.

Keywords - WSN, wireless heterogeneous network, cluster, radio, routing.

I. INTRODUCTION

Wireless sensor networks consist of sensors deployed over a given area. Sensors monitor physical or various environmental conditions and then pass their data to the base station. Wireless sensor networks (WSNs) periodically produce data as it monitors its locality. Sensor node consists of multiple sensing devices. The collection of different sensor node called as heterogeneous wireless sensor network. In heterogeneous sensing network there are various sensing devices which sense different parameter or attributes like:-Temperature field unit, Pressure field unit, humidity field unit etc. The basic operation of wireless sensing network is the systematic accumulation and transmitting of sensed data to the sink node for further processing. Scheduling of nodes' activities is done in such a way that uses minimum energy consumption.

The development of wireless sensor networks was motivated by military applications such as battlefield surveillance; today such networks are used in many industrial and consumer applications, such as industrial process monitoring and control, machine health monitoring, and so on. Wireless sensor network consists of several sensor nodes. In many applications, sensor nodes are usually powered by battery and keep on working for several months to one year without recharging. Such densely (up to 20 nodes/m³), with severe problems such as scalability, redundancy and radio channel contention expectation cannot be achieved

without scheduling the energy utilization, especially when sensors are deployed [1].

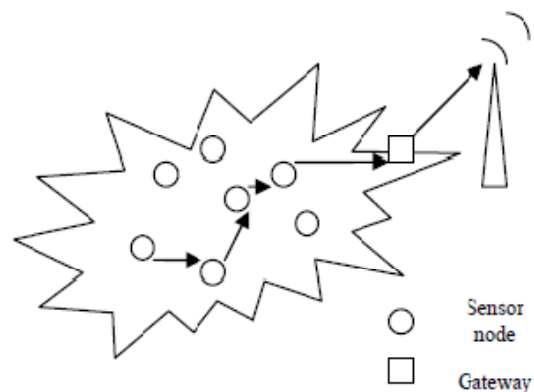


Fig. 1 : Wireless Sensor Network

As shown in figure 1, based on wireless sensor network, each sensor node consists of sensing unit, processing unit (micro-controller), a transceiver unit and power unit. In wireless sensor network, the resources of sensor node are limited in terms of the processing capability, wireless bandwidth, battery power and storage capacity, which distinguishes wireless sensor network from traditional networks. Various sensor nodes are MICA, TinyOS and so on.

II. RELATED WORK

The main task of data accumulation is to forward the sensed data gathered by sensors node to the sink node (base station). Routing protocols for Wireless Sensor Networks (WSNs) are chiefly classified into two categories: Network Structure Based protocols and Protocol Operation Based protocols. The network structure based protocols depends upon the system architecture of the network. These protocols are classified as: Data centric or flat routing protocols, Hierarchical routing protocols, and Location based routing protocols. Protocol operation based protocols are classified into five categories as: Negotiation based routing protocol; Multi-path based routing protocol, Query-based routing protocol, QoS-based routing protocol, and Coherent-based routing protocol.

Data-centric or Flat Routing protocols [2]: In this protocol every node in the network has been assigned the same role i.e. whenever source node requires the data it fires a query in the whole network, then all the sensors nodes cater the information whatever they have related to that query. However this introduces complexity to query data from a specific set of nodes. Therefore the data is collected from the deployed region. Since the collected data is correlated and mostly redundant; collected data is aggregated in some nodes resulting decrease in the amount of transmitted data and so transmission power.

Hierarchical or Cluster-Based Routing Protocols [3, 4, 5] are based on energy efficiency and scalability of the WSNs. The main issue is forming sub network clusters, encouraging multi hop transmission and enabling data fusion.

Localization Routing Protocol [6] is divided into two parts based on the measuring system used: GPS based and GPS free localization algorithm. In this technique, few nodes commonly known as anchors, use GPS to determine their location using GPS system and, broadcast its position's information in the network. In GPS free localization algorithm, it is free of GPS system to know the position of the node.

“Energy-efficient scheduling for multiple access in wireless sensor networks: A job scheduling method” [7] is to minimize transmission energy cost, the energy-efficient scheduling problem is considered in a single hop multi-access data gathering network. It proved by theoretical induction that transmitting with reduced powers decreases the energy budget, optimal rate control can be achieved by controlling the successive decoding order of the transmitting sensor nodes.

“LEACH, Low Energy Adaptive Clustering Hierarchy” [8] is based on clustering. Clusters of sensor nodes are formed according to the received signal rate of

the nodes. Local cluster heads act as a router to the sink. The number of the cluster heads is limited, approximately 5% of the all nodes. The cluster head selection is performed randomly, in order to balance the energy of the network. LEACH is completely distributed; no global knowledge is applied.

“Energy-efficient forwarding in wireless sensor networks” [9] for maximizing the energy efficiency in a wireless network, two forwarding schemes termed single-link and multi-link energy-efficient forwarding are proposed that tradeoff delivery ratios against energy costs. It is derived how the energy efficiency of a forwarding path can be computed and how a forwarding tree is established.

“An energy-efficient protocol for data gathering and aggregation in wireless sensor networks” proposed a DEEG [10] protocol based on cluster, which assume that heterogeneous sensor network. All sensing node maintain a neighborhood table to store the information about its neighbors. It save energy signal collision and interference in the wireless channel is ignored. There is using a multi sensor node but in our proposed protocol is based on multi sensor in one sensing node and how it saves its energy in form of transmission and removes replication.

III. PROPOSED WORK

Wireless sensor networks (WSNs) periodically produce data as it monitors its surroundings. Sensor node consisting of multiple sensing devices. The collection of different sensor node called as heterogeneous wireless sensor network. In heterogeneous sensing network there are various sensors which sense different parameter or attributes like:- Temperature field unit, Pressure field unit, humidity field unit, Analog input field unit etc. The propose protocol is based on a network which uses hybrid sensors and it will depend upon the range of sensors to detect the vicinity. The protocol focused on minimizing traffic in the sensor node and energy consumption by sensors. The information will be transmitted as trans-receiver. There are using a two different radio, low power radio is use for detect to the event and high power radio is used for data transmission. The basic operation of wireless sensing network is the systematic gathering and transmitting of sensed data to a base station for further processing. Scheduling of nodes' activities is done in a way that reduces minimum energy consumption

A. Node architecture

The proposed work involve multi-sensor which have many sensing units in a single sensor node. The various sensing devices sense different field units like:

temperature field unit, pressure field unit, humidity field unit etc. In multi-sensor node we lower energy consumption of sensing unit. Also only relevant data is send to the base station. The Sensor devices sense various field units at the same time. The data is being processed by the processing unit like CPU (Central

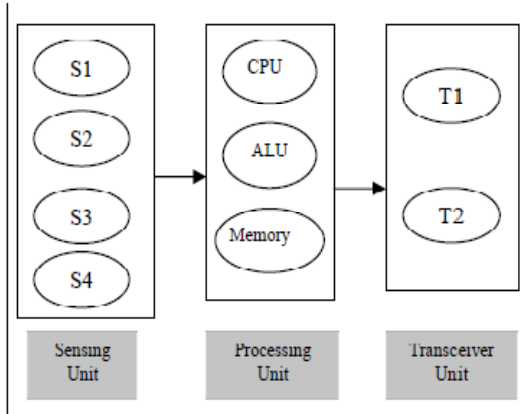


Fig. 2 : Sensor Node

Processing unit), ALU (Arithmetic field unit) and memory. The transceiver is used to send and receive the data from the sensing unit and cluster head. The transceiver used in sensing unit is radio channel. In fig 2. sensor node represented as

S1, S2, S3, S4 - Sensing devices

T1, T2- Radios

CPU- Central Processing Unit

ALU- Arithmetic Logic Unit

T1- low power signal-> detect event

T2- high power signal-> send the data to base station

B. Proposed algorithm

In the proposed algorithm is based on cluster formation and node scheduling.

1) event sensing:

Sensor S1 and S2 sense the event and send to the cluster head(CH) and base station (BS) in data packet format as shown in figure 3.



Fig. 3 : Data packet

Flag bit = 0, temperature

= 1, humidity

2) Data transmission:

Consider two sensing devices S1, S2 in a sensor node sense the event through T1 such as low power radio. When sensing device S1 detects any event in its vicinity then it wakes up and sends the accurate data to the base station via high power radio T2. When S1 is in wake mode then sensing device S2 is in sleep mode. When sensing device S1 detects no change in its vicinity then it goes to sleep mode and then S2 wakes up and senses the neighbors. No two sensing devices can be in same mode at the same time. In figure 4 (a). sensor S1 is in wake mode and detect if there is any change in its vicinity. At that time S2 is in sleep mode.

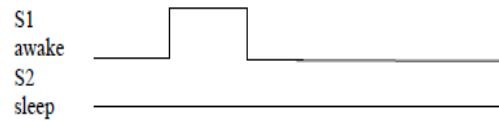


Fig. 4(a) : Sensor device scheduling

When S1 detects changes it goes to sleep mode and S2 awakes and observe its neighbor, if there occurs any change as figure 4(b).

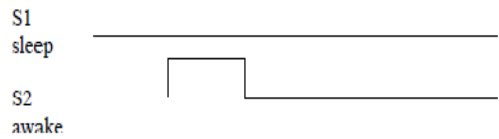


Fig. 4(b) : Sensor device scheduling

3) Algorithm:

a) Cluster formation:

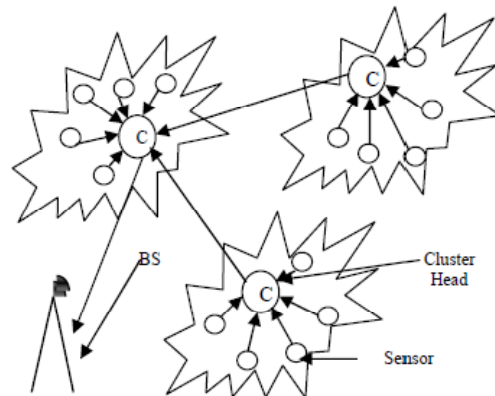


Fig. 5 : Cluster in WSN

As shown in the figure 5, initially "HELLO" message is broadcasted by a sensor node to all other sensor nodes in the network. The broadcast message consists of the information regarding to the energy of

the sensor nodes. The node with highest energy level is considered to be as Cluster Head (CH). The CH then collects the data from various member nodes and sends to the base station for further processing.

Table 1.

Cluster Head Selection Algorithm:

1. $N \leftarrow$ set of nodes present in the network.
2. If ($|N|=1$) then
3. Consider it as Cluster Head (CH).
4. Else if ($|N|>1$) then
5. $N' \leftarrow$ subset of N nodes that provides the shortest paths.
6. If ($|N'| \geq 1$) then
7. Randomly selects a node from N' as the CH.

In table 1. consider all the nodes in the network. N is the set of nodes under consideration in the given area. If the node is single, it is considered as the CH. Else subset of the nodes is chosen, which includes the shortest path from one node to other. If there are many subsets of the subset chosen then randomly chooses the CH. The CH, after elected, sends the selection messages to all its member nodes. The member nodes further deliver the selection message to its neighbors. In this way, all the member nodes come to know about their new Cluster Head. When member nodes get any information from the surroundings, it observe the changes and then send the collected data to the CH and CH further sends the data to the Base Station (BS).

Table 2.

Message Sending by Cluster:- Algorithm: Cluster (CH):

1. If $CH = 0$ (free) then
2. Message is send directly to the CH.
3. Else $CH = 1$ (busy in receiving packet data from other node) then
4. CH is checked after regular intervals by member node, want to send the data to the CH, for sending its aggregated data.
5. When CH becomes free then
6. Data is send to the cluster head (CH).
7. The CH further sends the data to the Base Station.

In table 2 show the message is send from the member nodes to the cluster head. The member nodes notice the changes in the surroundings and then send the aggregated data to the CH.

b) *Node Scheduler:*

Table 3.

Node Scheduler:

```

Sensing devices S1, S2.
Base station BS,
Radio T1 & T2
Event E
Sense the data; (dataS1 and dataS2) through T1; E
if (T1=E detected)
{
    If (E = DataS1) then
        Sensor S1 detect the data and send
        through T2 to the BS or CH; DataS1
        RRD( E ):
        S2-sleep mode;
    Else
        E=DataS2
        S2 = wake up mode
        Sensor S1 = sleep mode
        RRD( E ):
        transmit the dataS2 through T2
}
else T2 = sleep mode.

```

In WHSN a sensor node having multiple sensing devices, which sense the different attribute in environment. As shown in table 3, a proposed protocol used node scheduling algorithm for different devices. Therefore taking two sensing devices S1 and S2 of a sensor node are sense the event through low power radio T1 and send the data to the high power radio T2. The transceiver units send the sense data to the Base Station (BS) and Cluster Head (CH). In the proposed algorithm the event is detected by T1, if the detected data is S1 attribute then S2 is in sleep mode and aggregated data is send by T2. Otherwise S2 is sent the aggregated data through T2 to the CH and BS. In table 4. shown the Replicated data remove (RRD) algorithm. The data send by the member node to its adjacent node or to the CH is checked regularly with its previous data sent. If the data

is send earlier then repeated data is dropped there else data is accepted and send to the destination.

Table 4.

RRD(E)

n = current data

p = previous data

Data = T (when no repetition)

If data = T then

$$Data_p \leftarrow Data_n$$

Else ($Data_p = Data_n$)

Packet is rejected.

Aggregated data send to CH (Cluster Head) or BS.

In figure 6 shown the flow chart of the our proposed protocol (EEDRP protocol).

IV. RESULT AND ANALYSIS

Omnnet++ an open source simulator was used for simulation of EEDRP protocols. The simulation model used for simulating these proposed protocols is as presented here. The graph is plotted between Total energy consumed by the nodes vs. Number of nodes for EEDRP protocol (our proposed) as shown in figure 7. The energy consume in the proposed protocol is less compare to DEEG & LEACH protocols. There the proposed protocol is more energy efficient as compared to the other two protocols.

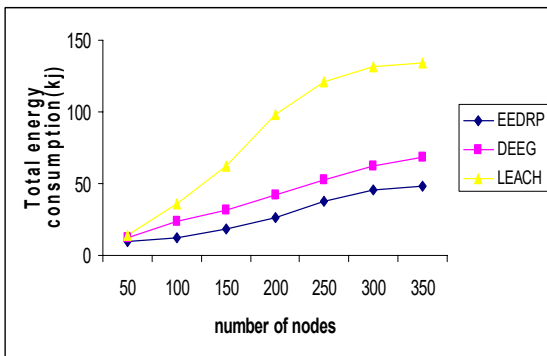


Fig. 7 : Total energy consumption Vs. Number of nodes

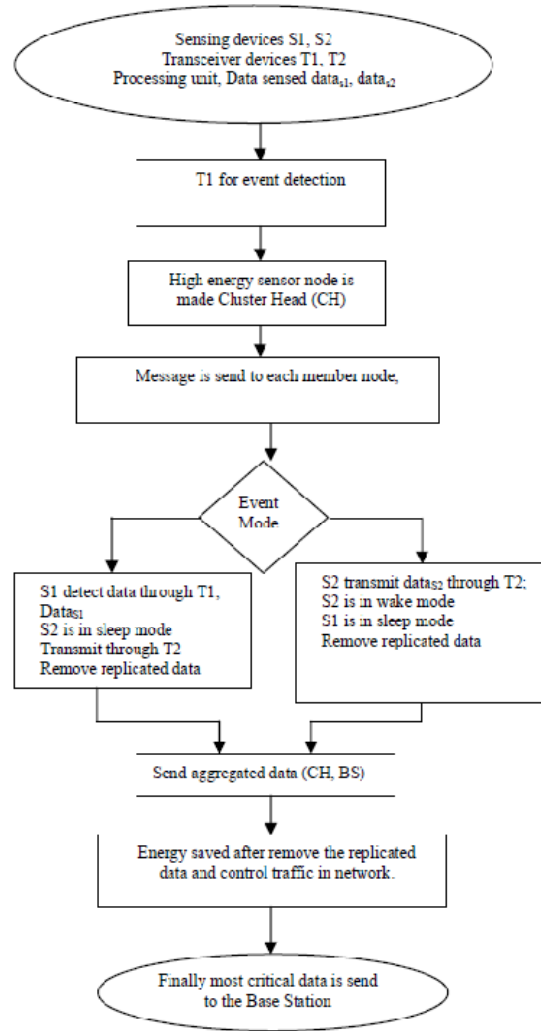


Fig. 6: Flow Chart of Proposed Algorithm (EEDRP)

V. CONCLUSION

In this paper, we try to minimize the energy used by the hybrid heterogeneous networks. Also traffic is minimized. In this paper, we take two attributes for a sensing device to improve the working and other attributes (e.g. energy used, traffic etc) of a sensor node. Initially all the sensing devices send the “hello” message to other sensor nodes. The message also consists of the energy of the sensor node. The message is broadcasted to all other member nodes and the sensing node with higher energy is selected as the Cluster Head (CH). Then all other member nodes sense the locality for any change in the event. If there is any change then the changed data is send to the cluster head through transceiver. Then the cluster head send the sensed data

to the BS. In previous papers a single node is used for a single attribute but we have taken two attributes in a sensor node. This improves energy efficiency, less data lost and it is real time based. In proposed algorithm the number of attributes can increase as to improve energy efficiency, data traffic and avoid replicated data. The replicated data causes traffic and energy loss in the routing protocol.

REFERENCES

- [1] I. Akyildiz, W. Su, Y. Sankarasubramaniam, and E. Cayirci, "A survey on sensor networks," *IEEE Communications Magazine*, Volume: 40 Issue: 8, August 2002, pp.102-114.
- [2] S. Hedetniemi and A. Liestman, "A Survey of Gossiping and Broadcasting in Communication Networks", *IEEE Network*, vol. 18, no. 4, 1988, pp. 319-349.
- [3] M. Younis, M. Youssef and K. Arisha, "Energy-Aware Routing in Cluster-Based Sensor Networks", in the Proceedings of the 10th IEEE/ACM International Symposium on Modeling, Analysis and Simulation of Computer and Telecommunication Systems (MASCOTS2002), Fort Worth, TX, October 2002.
- [4] A. Manjeshwar and D. P. Agarwal, "TEEN: a routing protocol for enhanced efficiency in wireless sensor networks," In 1st International Workshop on Parallel and Distributed Computing Issues in Wireless Networks and Mobile Computing, April 2001.
- [5] A. Manjeshwar and D. P. Agarwal, "APTEEN: A hybrid protocol for efficient routing and comprehensive information retrieval in wireless sensor networks," *Parallel and Distributed Processing Symposium*, Proceedings International, IPDPS 2002, pp. 195-202.
- [6] A Research paper on "localization routing protocol in Wireless Sensor Network" yuan zinag 2009
- [7] Xiaomao Mao, Huifang Chen, Peiliang Qiu, Zhaoyang Zhang, "Energy-efficient scheduling for multiple access in wireless sensor networks: A job scheduling method", Institute of Information and Communication Engineering, Zhejiang University, Yuquan Campus, Hangzhou, Zhejiang 310027, China
- [8] W.R. Heinzelman, A. Chandrakasan, H. Balakrishnan, "Energy-efficient communication protocol for wireless microsensor networks", *Proceedings of the 33rd IEEE Hawaii International Conference on System Sciences, HICSS*, IEEE Computer Society, Maui, HI, USA (2000).
- [9] Marcel Busse, Thomas Haenselmann, Wolfgang Effelsberg, "Energy-efficient forwarding in wireless sensor networks", *University of Mannheim, Computer Science IV, Seminargebäude A5, D-68159 Mannheim, Germany* volume 4, issue 1.
- [10] Ming Liu, Jiannong Cao, Yuan Zheng, Haigang Gong, Xiaomin Wang, "An energy-efficient protocol for data gathering and aggregation in wireless sensor networks", 2008, 43:107-125, DOI 10.1007/s11227-007-0122-8, Springer science.



Self Securable Security Robot using High Speed Internet for Communication with the Human Master

Shyam. R. Nair¹ & Manjula Promod²

Hindustan Institute of Technology and Science, Hindustan University, Chennai

Abstract - This paper focuses on developing a new technique for robots for protecting itself from exploitation by unauthorized access. The Paper also emphasize on the advantage of using high speed network for communication between the robot and the human master. The robot continuously verifies whether there is an unauthorized access or whether the communication link is hacked. If it identifies one, then it blocks all communication channels and other features and comes back to the source point by using the data stored in eeprom.

Keywords - robotics, high speed network, communication security.

I. INTRODUCTION

Robot is a machine to execute different task repeatedly with high precision. Thereby many functions like collecting information and studies about the hazardous sites which is too risky to send human inside. Robots are used to reduce the human interference nearly 50 percent. Robots are mainly in different types like fire fighting robot, metal detecting robot, rescue robots, patrol robots other humanoid robots etc. Mostly used in industrial purpose, military, defense, research and development etc. Security robots are used in all major areas of industries, defense units and other places which require high security. Of these certain security robots are supposed to do survey and provide security in a fixed area or a continuous closed path.

This paper focus on developing a hardware and software scheme for a security robot to execute the tasks given by a human master using a high speed network. The software scheme is designed in such a manner that the robot verifies the environmental conditions before executing a task given by the human master. The software scheme also ensures to check the communication link security. If the robot identifies any security issue, it comes back to the source point by using the data stored in eeprom.

II. HARDWARE CONCEPT

The robot has a platform with four wheels for free motion. The wheels are coupled to high torque DC geared motors with an appropriate rpm. The platform is

designed to fit a laptop, three arms, and four 12V 7aH lead acid batteries. One arm is used for mounting a camera, second for mounting a gun. The third arm is used as a trigger for the gun. The platform also contains the electronics hardware including a relay based circuit for driving the dc geared motors, a pic microcontroller circuits, and ultrasonic sensors.

The task to be executed is given as voice commands[25] by the human master at the client pc. A serial code is generated for each word and is transmitted to the laptop on the robot platform. For generating, transmitting and receiving the code software's known as Roboclient and Roboserver is used. Both these software's are developed in Microsoft Visual Studio. The client pc and the server laptop is connected to internet using high speed 3G network. The serial code is transmitted from the laptop to the microcontroller circuit by a RS-232 cable. When the microcontroller receives this signal, it checks for the environmental conditions using the ultrasonic sensors. The environmental condition, here, refers to any obstacle for the task execution. Now if there are no obstacles, then, the robot executes the task. But if there is any obstacle, it sends the human master a serial code indicating its problem and waits for further instruction from human master. The human master can view the area under survey with the help of the camera mounted on the robot platform. This is made possible by using the Gmail video chat or the Skype software.

The robot platform also contains a battery monitoring circuit. If this circuit identifies a power

crisis, then, the circuit switches to the next power source. The number of power sources can be fixed according to the need and availability. If the last battery is switched, then, the robot closes all its applications and comes back to the source point by using the data in the eeprom. The robot also returns to the source point if it identifies a security issue in the communication link.

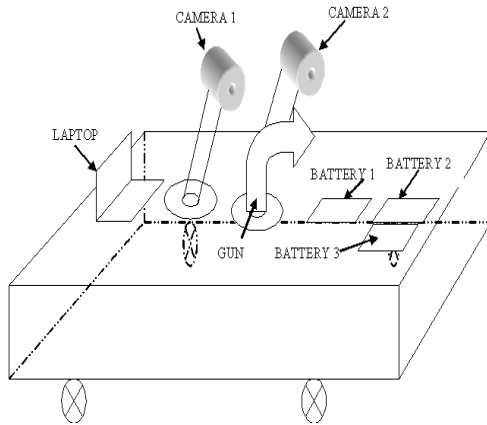


Fig. 1 : Schematic

- IDENTIFICATION OF A SECURITY ISSUE IN COMMUNICATION LINK

The client pc and the server laptop continuously exchange a serial code. If the pic microcontroller does not receive this code in a specified delay, it comes to a conclusion that the communication link is lost or hacked. In that case, the robot closes all its communication links and other activities and returns back to the source point. By using the data stored in eeprom.

- RETURNING OF ROBOT TO SOURCE POINT USING THE DATA IN EEPROM

The robot stores all the movement codes in the internal eeprom of the pic microcontroller. The first location contains the movement code and the next location contains the time delay for the code. This continues for all the movement codes. When the robot faces a security or power problem, the robot executes the data in eeprom in last in first out method. The controller swaps the forward and backward instructions. That is if there is a forward movement in the eeprom location, the robot moves backward and vice versa. The rest of the instructions remain the same. This helps robot from protecting itself from exploitation from unauthorized access.

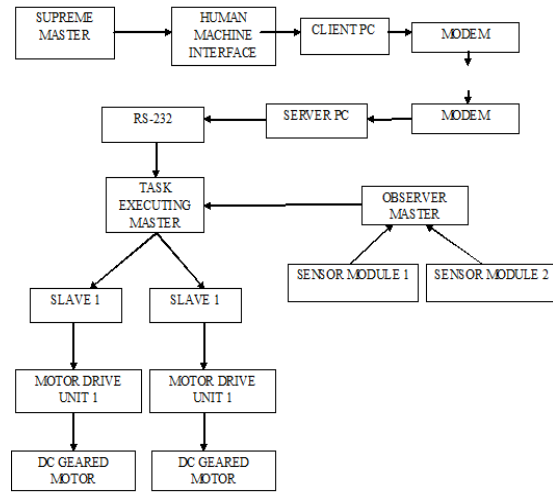


Fig. 2 : Block Diagram

III. MECHANICAL PART

Robots are several types wheeled, tracked, and legged, multi robots, vibration types. The simplest are wheeled robots, while tracked wheels are used because of their ability to move in rough terrain surface and their greater stability. The mini bot is tracked wheel vehicle. They are relatively lightweight about 10 kg. They are quite active and fast in unstructured environments and they also perform well on uneven terrain. The whole robot structure is constructed in mild steel and the mechanical joints are effectively works with gears.

1. Body and Driving System

Thick aluminium sheet is folded to be the base frame. The locomotion driving system, all motors and mechanical joint sets and the batteries are placed in this frame in order to have the low level centre of gravity. Two 12V DC motors are used for driving base wheels separately. Both are controlled bi-directionally. Mechanical joint is fitted at the centre of the robot. With suitable commands from the operator the joint moves.

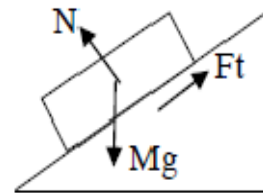


Fig. 3 : Free body diagram

When a solid body slides over a rough or smooth stationary surface, a force is exerted at the surface of

contact by the moving body. This force is frictional force and is always acting in the opposite direction [26]. Consider a simplified model of the system as shown in Fig. 3. The minimum torque required for climbing a surface with slope of 20° is calculated by second law of Newton. The mini bot can be covers the steps up to 20° , because the height of the wheel is 8cm.

$$F=Ma$$

Assume the linear acceleration and thus the rotational acceleration of the wheels to be zero.

$$a=0$$

$$Ft=mg \sin$$

$$Ft= mg \sin ; \text{ let } m=10\text{kg}$$

$$Ft=33.5\text{N}$$

The torque becomes,

$$T=Ft*r \approx 10\text{Nm}$$

The locomotion system consists of two separate sides connected to the main body while a motor independently drives the track at each side. So the desired torque is obtained by dividing the T/2 [3].

$$T=5\text{Nm}$$

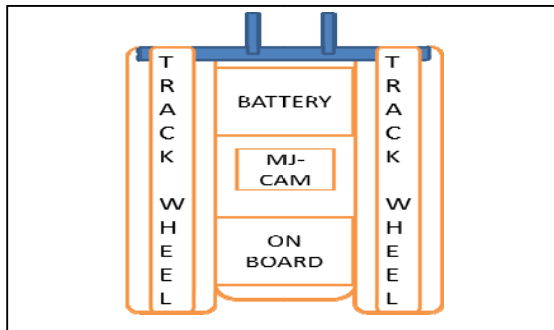


Fig. 4 : Hardware model

2. Mechanical joint

The mechanical arm does credit to the mini –bot. This enables the robot to expand its tracks whenever it needs to close vision on the obstacles. It helps the robot to explore in many ways such as, from high level and able to get vital signs of victims [12][15][4][17][16]. In Fig. 5 shows the drawing of mechanical arm. Because the pay load at the tip of arm is small and the arm structure weight is not much, DC motor with gear set still can regulate the joint angle quite well. Arm motor is coupled to the planetary gear set with 20:1 worm gear set, which results a maximum speed of 4rpm. Let 'h' be the height from base to the joint. The angle of rotation is determined by θ_1 and θ_2 . If two rotational angles could change between 0 and 360 degrees, the work-space

should be between a spherical surface and a cylinder. Therefore, the work-space is between a semi-spherical surface and a cylinder. A stepper motor is fixed at the bottom of the mechanical joint for the full surveillance. It takes 8 steps instead of 4 to complete one complete rotation.

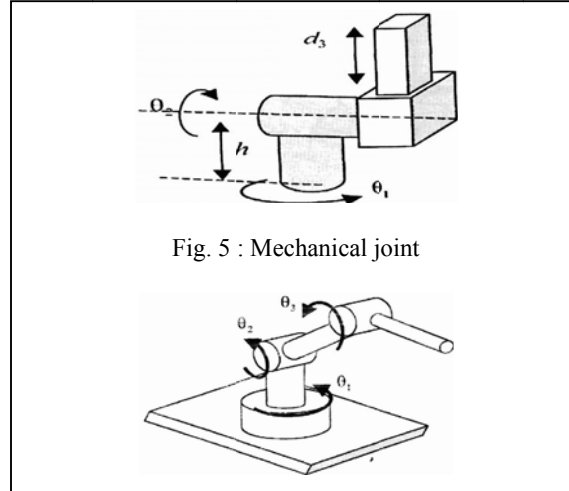


Fig. 5 : Mechanical joint

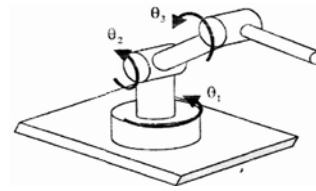


Fig. 6 : Mechanical arm

3. Visual sensor and gun

This part is the place to install sensors which are used for searching vital sign of the victims like camera [24]. The camera can be made to continuously rotate as per the command from human master. The gun also can be rotated as the human master wish. The camera mounted on the gun is used to aim the target. The visuals obtained by the camera are transmitted through the Gmail video chat or the skype software.

4. Monitoring and Navigation of robot

The robot is monitored using the camera in the robot platform. The robot uses ultrasonic sensors for identifying any obstacle in the path of its motion. The sensors are connected to the controller circuit for making appropriate decision. When the robot navigates automatically, it uses the data in eeprom. For the patrol robot navigation several methods are used like sensing the paths, graphical user interface, map following algorithms and compass, other Kalman filtering methods[1][2][3][14][21]. All these approaches are somehow complex. This can be overcome by using the EEPROM of the microcontroller. PIC16F877A has 256 bytes of EEPROM inside it. So memory can use it to store data that need on a permanent basis and we can read it back from it. There are two functions to accomplish the task. Eeprom_Read and Eeprom_Write.

Eeprom_Read function returns an integer and takes a parameter of the address from which the data has to be

- [11] Stefano Carpin “RANDOMIZED MOTION PLANNING – A TUTORIAL” International University Bremen, Germany
- [12] Principles of Robotics page 24-38, pg54-57
- [13] Fung Po TSO, Lizhuo Zhang, Weijia Jia “Video Surveillance Patrol Robot System in 3G, Internet and Sensor Networks” SenSys’07, November 6–9, 2007, Sydney, Australia
- [14] Robert W. Hogg, Arturo L. Rankin, Stergios I. Roumeliotis “Algorithms and Sensors for Small Robot Path Following”
- [15] C. Won, T. Frost “A Portable, Autonomous, Urban Reconnaissance Robot” IS Robotics, Somerville MA, 02143
- [16] Redwan Alqasemi and Rajiv Dubey “Control of a 9-DoF Wheelchair-Mounted Robotic Arm System” 2007 Florida Conference on Recent Advances in Robotics, FCRAR 2007
- [17] Jegede Olawale, Awodele Oludele, Ajayi Ayodele and Ndong Miko Alejandro “Development of a Microcontroller Based Robotic Arm” Proceedings of the 2007 Computer Science and IT Education Conference.
- [18] Yongxing Hao, Benjamin Laxton ,Sunil K. Agrawal, Edward Lee , Eric Benson “Planning and Control of UGV Formations in a Dynamic Environment: A Practical Framework with Experiments” Proceedings of the 2003 IEEE International Conference on Robotics & Automation Taipei, Taiwan, September 14-19, 2003
- [19] Johann Borenstein+ and Yoram Koren “MOTION CONTROL ANALYSIS OF A MOBILE ROBOT” Transactions of ASME, Journal of Dynamics, Measurement and Control, Vol. 109, No. 2, pp. 73-79. [20]
- [21] Sebastian Thrun1, Maren Bennewitz2, Wolfram Burgard2”MINERVA: A Second Generation Museum Tour-Guide Robot” Carnegie Mellon University.
- [22] Stephen J. Tobias, A. Antonio Arroyo “Autonomous Path finding” 2000 Florida Conference on Recent Advances in Robotics May 4-5, 2000, Florida Atlantic University.
- [23] Namal A. Senanayake, Khoo B. How, and Quah W. Wai “Tele-Operated Anthropomorphic Arm and Hand Design” World Academy of Science, Engineering and Technology 39 2008
- [24] Ali Sekmen, Sheldon Greene “Vision-based Mobile Robot Learning and Navigation”2005 IEEE International Workshop on Robots and Human Interactive Communication.
- [25] Brandi House, Jonathan Malkin, Jeff Bilmes “The VoiceBot: A Voice Controlled Robot Arm” CHI 2009, April 4-9, 2009, Boston, Massachusetts, USA.
- [26] Dr.R.K.Bansal ”a textbook of engineering mechanics” page no 195-199,page no 205-209



Humanoid Locomotion Manipulated Using Dynamic Finger Gestures

Hari Krishnan R & Vallikannu A. L

Department of Electronics and Communication Engineering, Hindustan Institute of Technology and Science,
Hindustan University, Chennai, India

Abstract - The fundamental technologies for Human-Computer Interaction are Hand motion tracking and Gesture Identification. The same technology has been adapted for Human-Robot Interaction. This paper discusses a natural methodology for Human-Robot Interaction. In the proposed system, the accelerometers at the fingers, tracks specific gestures. These gestures are identified by the controller, which in turn controls the actuators that results in Humanoid walking. The Humanoid under consideration has 8 Degrees of Freedom.

Keywords - Human-Computer Interaction; Human-Robot Interaction (HRI); Degrees Of Freedom (DOF); Humanoid; Hand Motion Tracking; Gestures; Accelerometer;

I. INTRODUCTION

According to Webster dictionary, a Gesture is defined as, “a movement usually of the body or limbs that expresses or emphasis an idea.” Earlier, conventional input devices like Keyboard and Mouse were used for Human-Computer Interaction. These type of interaction lacks naturality. Thus interaction using gestures became a subject of study. The same interaction method can be utilized for Human-Robot Interaction (HRI). HRI is the study of interaction dynamics between Humans and Robots. Many researches are under way to develop an efficient system for Human-Robot Interaction using Gesture Identification. This type of interaction schemes are difficult to design for robots due to complex processes involved in it. Difficulty to recognize gestures and to interpret their meaning, complex backgrounds, person-independent recognition, processing speed, computational costs etc are the challenging factors involved in the design of such a system[1]. There had been several research works on telemanipulation of Robotic arm using finger gestures [4]. This paper emphasis on developing a simple system for HRI using finger gesture Identification to make a Humanoid Robot walk successfully.

II. OVERVIEW ON GESTURES AND GESTURE RECOGNITION

A. Gestures

Gestures are broadly classified into two types.

1) Static Gestures

Static Gestures are also known as Postures. If the finger position does not change for an amount of time, known as the gesturing period, then those gestures are known as static finger gestures or finger postures. Static gestures, deals with information on bend, turn or fold parameters of the fingers[1].

2) Dynamic Gestures

Dynamic Gestures could be simply called Gestures. In Dynamic finger gestures, the position of the finger is temporary and it changes, with respect to time. It could be interpreted as a sequence of static gestures[1].

B. Gesture Recognition

There are different methods for Gesture Recognition. The most widely used are-

1) Sensor Based Systems

In this type of system, finger joint angles and spatial positions which reflects finger Gestures are measured using different sensors. Parameters like acceleration from accelerometer, angular velocity from gyroscopes etc are used to detect and determine the motion of a particular human limb. Advantages of sensor based systems are that, they are independent of surroundings, not affected by environment and are always attached to the user. Thus these types of systems are said to be reliable ones. Constraints in execution of natural gestures is major limitation factor of such a system[1,2,3].

2) Vision Based Systems

Vision Based systems, makes use of images captured by a video camera for gesture recognition. Advantage of such a system is that, they produce extremely excellent results in indoor conditions. But in such a system, the user has to stay in restricted camera field. Variations in light levels and various environmental interferences, makes the system more complex[1,2,3].

The present paper deals with recognition of Dynamic finger gestures using Sensor based systems.

III. PROPOSED SYSTEM

The block diagram of the proposed system is shown in Figure 1. The whole system is classified into two parts- Human End and Robot End. The gestures are picked up using 2 accelerometers attached on to the fingers. Accelerometer converts, finger movements into various voltage levels. These voltages are fed to the Analog to Digital Converter of the microcontroller within the Monitoring circuitry. The microcontroller is programmed in

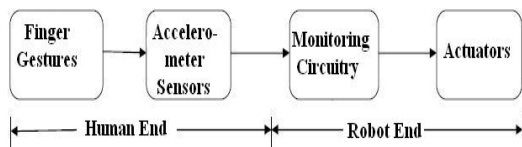


Fig. 1 : Block Diagram

such a way that, each voltage level is assigned to a particular actuator movement, which results in Humanoid walking.

The Human End is composed of Finger Gestures and picking up of these Gestures using Accelerometer sensors. The accelerometers are attached on to middle finger and index finger. Human walking like Gesture is mimicked using these two fingers as shown in figure 2. Consider that, accelerometers are connected on to middle finger and index finger of right hand. The main aim is to make the robot walk in such a way that, when middle finger is moved forward, by keeping index finger positioned at a point, the robot lifts its left leg and moves it forward. Now when, index finger is moved forward by keeping middle finger idle, the robot lifts the right leg and moves it forward.

The Humanoid robot under consideration is specially designed for this particular application. It is an 8 DOF humanoid robot with PIC 18F452 microcontroller as its heart. The upper body has two arms with shoulder and elbow (2 DOFs each). The

lower body has 2 legs with hip and ankle (2 DOFs each). Design Model and configurations of links and joints of the proposed robot is shown in Figure 3. The elbows and the ankles are of roll orientation. The shoulders exhibits pitch orientation and hips are of Yaw orientation[8].

IV. STAGES OF GESTURING AND BIPED LOGIC GAIT PHASES

Consider that there are three stages while imitating walking like gesture using fingers. Biped logic gait phases are broadly classified into seven, including the initial phase. Each stages of gesturing is assigned to attain certain biped gait phases for successful walking. Stability is the major problem that arises during robot walking. For a Humanoid robot to walk, it stands on single leg and swings the other leg forward. To provide stability when only one leg is on ground, a 'Dead Weight' is utilized. By this, the weight of the upper body of the robot is moved, so as to bring the centre of gravity on the axis of footing leg[5].

Various gesturing stages and biped logic phases assigned are explained as follows.

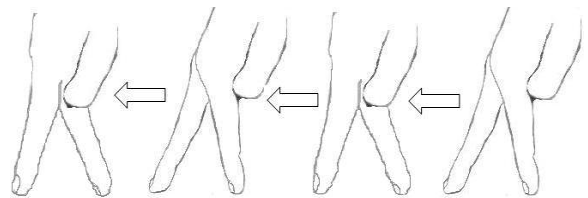


Fig. 2 : Finger Gestures Under Consideration

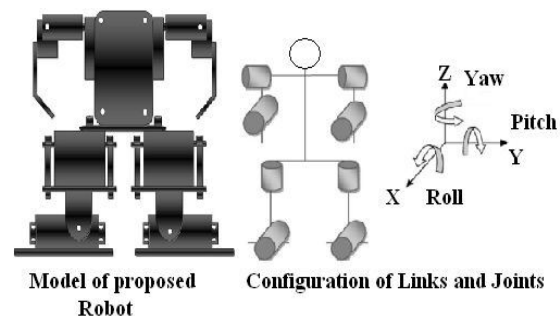


Fig. 3 : Design Model and Configuration of Links and Joints

- Stage 1- Both Middle finger and Index finger are aligned in same line. Now the robot should execute phase 1 of Biped logic gait. In phase 1, the dead weight will be shared among the two legs. Dead Weight is denoted by W_M . This is the neutral condition, in which Centre of Gravity is maintained between the two legs. This is shown in Figure 4.
- Stage 2- Stage 2 is illustrated in Figure 5. The middle finger is moved forward, while keeping index finger positioned at a point. This executes phase 2, phase 3 and phase 4 of biped gait phases. During phase 2, the robot leans from left to right. The dead weight is moved towards right leg, by the roll orientation at the right leg. The centre of gravity is now concentrated on right foot region. Once the left leg is lifted, it is made to swing in air at an angle Θ_R , keeping right feet under the upper body using the yaw orientation of the hip. This is the phase 3 of biped gait logic. In phase 4, as left feet reaches the highest point of trajectory, the feet is lowered back to the ground. The centre of gravity is now again between the two legs.
- Stage 3- The Index finger is moved forward, while keeping the middle finger positioned at a point. Phase 5, Phase 6 and Phase 7 are executed now. During Phase 5, the robot leans from right to left. Dead weight moves towards left leg. Centre of Gravity is concentrated on to left foot region. In phase 6, right leg is made to swing in air at an angle Θ_L , keeping left feet under the upper body. As right feet reaches the highest point of trajectory, the feet is lowered back to ground. This is phase 7. Stage 3 is illustrated in Figure 6 [5,6,7].

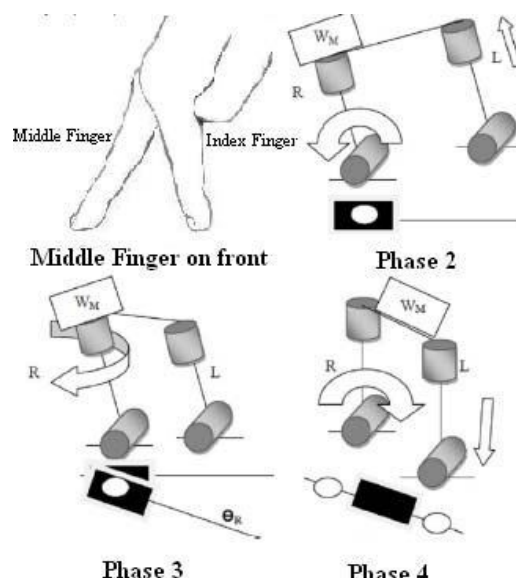


Fig. 5 : Stage 2

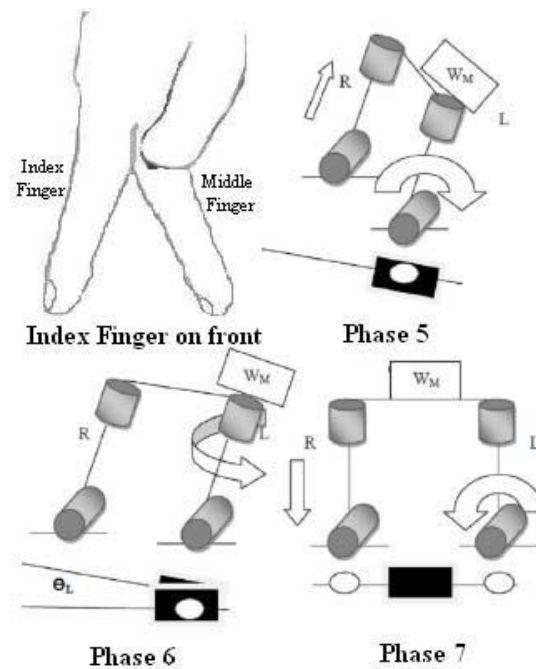


Fig. 6 : Stage 3

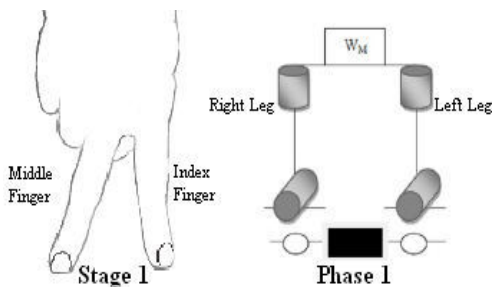


Fig. 4 : Stage 1

V. ELECTRICAL DESIGN

A. Monitoring Circuitry

Monitoring Circuitry is within the main control board of the Robot. There are two PIC 18F452 microcontrollers which acts as, processing elements in the main control board. The circuit is designed in such a way that only one microcontroller will be active at a particular time. With the help of controller selection switch, microcontroller to be used, could be selected. A servo extension board is provided, due to space limitations in the main control board. This board provides power and signals for the servomotors. The servo extension board is connected to main control board via FRC. Main Control Board and Servo extension is shown in Figure 7.

B. Accelerometer

An Accelerometer is an electromechanical device that will measure, acceleration forces. Different types of Accelerometers are available. The module used in this project is capacitive micro machined and is based on Freescale's MMA7361L . It is shown in Figure 8. It is a simple, 3 Axis accelerometer which provides analog output at each axis. The module operates at a voltage range of 5 v and is highly sensitive. Accelerometer is connected to analog pins of any one of the microcontroller in the main control board, after selecting the required controller.

VI. FIRMWARE DEVELOPMENT

A 3 axis Accelerometer has 3 outputs, i.e. X, Y and Z. For each gesturing stages, a range of voltages are assigned. So during a legitimate gesturing, a particular voltage range will be fed into the analog input pins of the microcontroller, from accelerometer. The microcontroller is programmed in such a way that, the voltage ranges fed are compared with a set of predetermined, voltage ranges within the controller. Each predetermined voltage ranges are assigned with programs to generate PWM signals for servo motors, to achieve various walking phases associated with each gesturing stages. It should be noted that, once middle finger is kept forward, next the index finger should be kept forward and not the former. In other words, same voltage levels shouldn't come consecutively. This leads to execution of same phases one after the other causing the robot to fall.

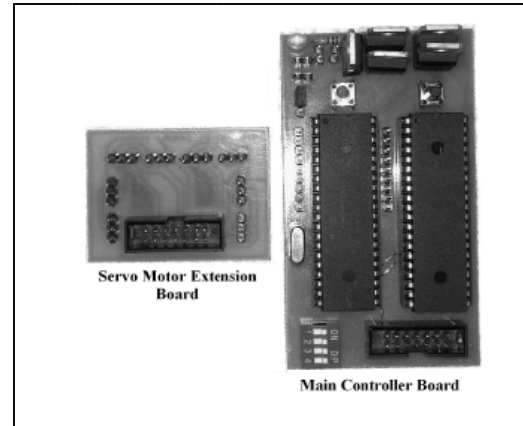


Fig. 7 : Main Control Board and Servo Extension

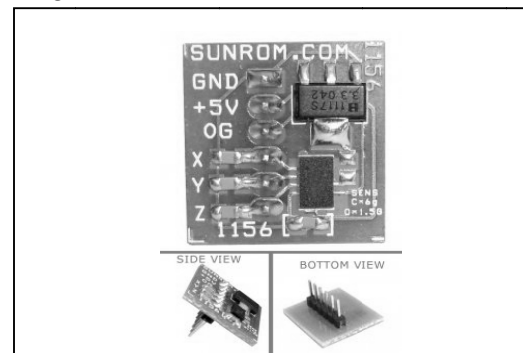


Fig. 8 : Accelerometer module used

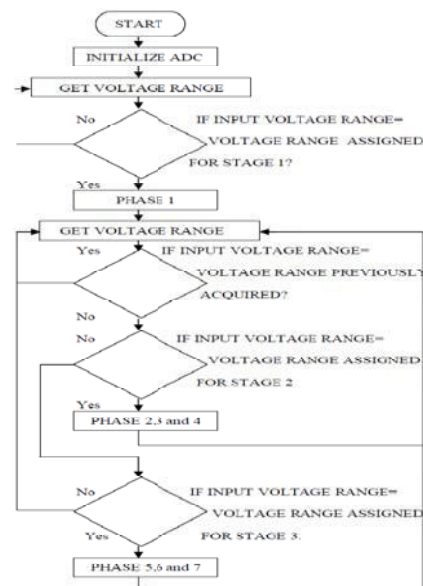


Fig. 8 : Flow Chart

The flow chart of firmware logic is shown in Figure 8, with respect to each stages and phases, illustrated in Figures 4,5 and 6 .

VII.CONCLUSION

This paper presents the design of a low cost and natural way of Human Robot Interaction, to make a Humanoid robot walk successfully. The system is simple and easily understandable. The calibration of accelerometers to acquire correct voltage ranges for each stages of gesturing is the complex action involved in the design phase. Only Robot locomotion is discussed in this paper. Same methodology can be used to make the robot to do an application like pick and place. More useful and advance applications can be incorporated by future research in this area.

REFERENCES

- [1] P. Pramod Kumar, Prahlad Vadakkepat, Loh Ai Poh, "Hand Posture and face Recognition using Fuzzy-Rough Approach," in Int. Journal of Humanoid Robotics, vol 7, No.3, 2010, pp. 331-356
- [2] Ji-Hwan Kim, Nguyen Duc Thang, Tae-Seong Kim, "3-D Hand Motion Tracking and Gesture Recognition Using a Data Glove," in Proc. IEEE Int. Symposium on Industrial Electronics (ISIE2009), 2009, pp. 1013-1018.
- [3] Thomas Allevard, Eric Benoit, Laurent Foulloy, "Fuzzy Glove For Gesture Recognition," in Proc. XVII World Congress on Metrology in 3rd Millennium, 2003, pp. 2026-2031.
- [4] Marcelo Romero Huetas, J. Raymundo Marcial Romero, Hector A. Montes Venegas, "A Robotic Arm Telemanipulated through a Digital Glove," in Proc.of IEEE 4th Congress of Electronics, Robotics and Automotive Mechanics, 2007, pp. 470-475.
- [5] Appuu Kuttan K.K, Robotics, I.K International Publishing House Pvt. Ltd, India, 2007.
- [6] Andre Senior, Sabri Tosunoglu, "Robust Bipedal Walking: The Clyon Project," The 18th Florida Conf. on Recent Advances in Robotics, 2005.
- [7] Jacky Baltes, Sara McGrath , John Anderson, "Active Balancing Using Gyroscopes for a Small Humanoid Robot," in Proc. 2nd Int. Conf. on Autonomous Robots and Agents, 2004, pp. 470-475.
- [8] Hari Krishnan R, Vallikannu A.L, "Design and Implementation of Simplified Humanoid Robot with 8 DoF,"accepted for ICCVR 2012, Chandigarh



Cascaded Computational Intelligence for Robotics

Multiple Master Control

Shyam. R. Nair

Hindustan Institute of Technology and Science, Hindustan University, Chennai

Abstract - This paper focuses on developing a new technique for robot communication. The technique involves three modes of operations namely manual, automatic and cascaded control. Of these, in cascaded control, the commands are given by human master. And once these commands are received, the robot controller unit verifies the environmental conditions using a sensor fusion unit and then executes the commands if and only if the conditions are ideal for executing the commands. This mode also involves a continuous check on communication system security and if identifies a hack or corruption, the system goes to isolated mode by disconnecting all communication channels and then returns back to source point. This mode also continuously checks the battery level and switches to the secondary power source accordingly.

Keywords - Robotics, computational intelligence, communication security, hack.

I. INTRODUCTION

Robot is a machine to execute different task repeatedly with high precision. Thereby many functions like collecting information and studies about the hazardous sites which is too risky to send human inside are done by robots these days. Robots are used to reduce the human interference nearly 50 percent. Robots are used in different types like fire fighting robot, metal detecting robot, etc. Humanoids are robots which resembles human joints. Humanoids are nowadays used in industrial purpose, military, research etc.

This paper focuses on developing a new communication technique for robotics which involves combination of manual and automated mode of operation. The paper also proposes a method of self securing technique for robots so as to save them from unauthorized access and to overcome power problems.

II. HARDWARE CONCEPT

A. Electronics

There are two nodes in this technique. One is client node and the other is server node. The client node requires a human, a human machine interface, a PC or laptop, high speed internet. The server node requires a laptop, a RS232 cable, two microcontroller circuits, a sensor fusion unit, a web camera and high speed internet.

III. MODES OF OPERATION

There are three modes of operations namely manual, automated and cascaded.

A. Manual

In manual mode, the robot is controlled by the human master. The task that is to be executed is instructed by the human master as voice, finger gesture, eye ball movement, brain cap etc.

The instruction is fed to the client PC as characters using appropriate human machine interface. These characters are fed serially to the server laptop using high speed internet. The server laptop receives these instructions through high speed internet and feeds it to the master PIC microcontroller. The visuals are obtained through the camera in the robot by using the Gmail video chat or Skype software. This also introduces a dual channel communication, ie, the instructions are given through one channel and the visuals are obtained through other channel. So if one of the channels is hacked we get access to the robot using the other channel.

Suppose we lose the video signals, we can command the robot to come back to the source point. Otherwise if we lose the instruction channel, the video chat helps us to locate the robot.

In this mode, the sensor fusion unit is not activated. This mode is usually used for training purpose.

B. Automated

In this mode, the robot does not get the instructions from the human master. Instead, it will use the data in

eprom to execute task or it will use neural scheme for executing task.

In this mode, the sensor fusion unit is activated and it is used to analyze the environmental conditions.

C. Cascaded

In certain places, we cannot expect the robot to execute task by itself and neither can we expect human commands enough to execute the task like surveying of an unknown area or in warfare. In such area, we use both human intelligence and sensors for executing a task. In such situations the cascaded mode will be of great use.

In this mode the instructions from master is received in the client node as explained in manual mode. Once the instruction is received at the master controller it verifies the environmental conditions. This master controller is connected to sensor fusion unit which is used to observe the environmental conditions. The sensor fusion unit consists of ultra sonic sensors for identifying and locating obstacles, temperature sensor for analyzing the surrounding temperature, etc. The master controller verifies the environmental conditions and executes the task if and only if the conditions are ideal to be executed.

In this mode the robot continuously verifies the communication system security. This is done by transmitting and receiving a peculiar code in a definite interval of time. If the code is not received in either of the ends at proper time then the robot disconnects all the communication channels and returns back to the source point by using the data stored in eeprom of the controller.

In this mode the robot also verifies the battery level using a battery monitoring circuit. If the robot identifies a drain in battery charge, it automatically switches to the secondary power source. Once the robot switches to the last battery, it will stop all the task and returns back to the source point using the data in eeprom.

IV. DATA IN EEPROM AS ARTIFICIAL INTELLIGENCE

For the patrol robot navigation several methods are used like sensing the paths, graphical user interface, map following algorithms and compass, other Kalman filtering methods[6][5][7][8][9]. All these approaches are somehow complex. This can be overcome by using the EEPROM of the microcontroller.

The data can be stored in eeprom which could be used in two ways. If the robot is supposed to do repetitive task, eeprom can be fed with serial instructions one by one and can be executed in LIFO or FIFO mode. But if the robot is used to do the survey in

same track but action according to the situation, then the eeprom need to be fed only with movement instructions. And if the sensor unit finds a undesirable condition, then the signal can be taken as interrupt and required task may be executed using the program of the controller. For example, if the robot finds a obstacle, it can move away from it or if it finds a high temperature and presence of flame, then it can use the fire extinguisher and give an alarm.

PIC16F877A has 256 bytes of EEPROM inside it. So memory can use it to store data that need on a permanent basis and we can read it back from it. There are two functions to accomplish the task. Eeprom_Read and Eeprom_Write.

Eeprom_Read function returns an integer and takes a parameter of the address from which the data has to be fetched. Eeprom_Write takes two parameters the first one is the address and the second one is the data.

```
unsigned short Eeprom_Read(unsigned int address);
```

```
void Eeprom_Write(unsigned int address, unsigned short data);
```

The eeprom can also be used to store movement data while the robot is in normal mode and use it in LIFO mode if the robot identifies a hack or power problem.

Most of the robot will navigate with different algorithm.[1][2][3][4] The robot will navigate with respect to the commands from the user (initially from A to B) as shown in fig.7. All the running commands are stored in the memory and also a counter is set to determine how long the commands are executed. Now the current position of the robot is at B. Whenever it needs to return, the last stored command will execute first (LIFO). If the last executed command is forward, that swaps it into backward command.

Similarly,

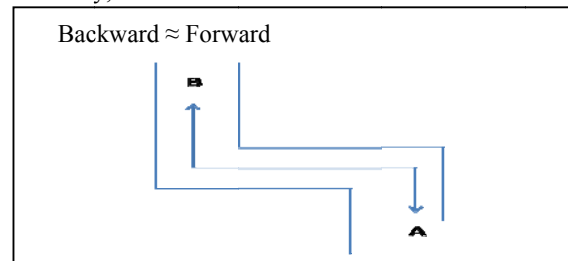


Fig. 1

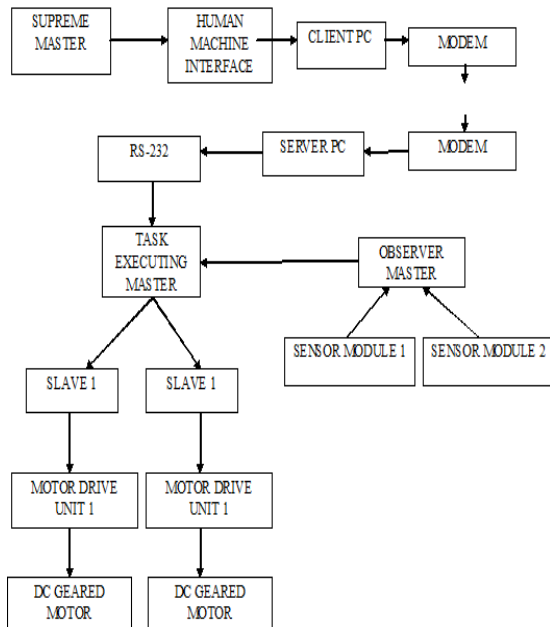


Fig. 2

V. SOFTWARE

Onboard software is mainly developed with micro C. This software interfaces between the operator station software and the robot by receiving operator's command to control all robot functions. Simulations have been executed both in Mat lab and PIC simulator. In Mat lab the approaches were implemented under ideal hypothesis, more realistic settings. The commands are send through serial communication with the help the software Roboclient developed in Microsoft Visual studio. The data is received using the software Roboserver developed in Microsoft Visual studio. Real time visuals can be captured and displayed on the window with the help of Gmail video chat or Skype software.

VI. CONCLUSION AND FUTURE EXPANSION

The cascaded computational intelligence for robotics seems to be a very useful communication technique. The technique has the advantages of high speed internet which allows unbounded communication and the dual channel allows more security to the communication system. The use of eeprom for data storage and the security check and battery monitoring makes the robot more secured from unauthorized access and power problems.

In future this method can be used in military applications for warfare and unknown area surveying.

ACKNOWLEDGMENT

The research in this paper was carried out at Hindustan Institute of Technology and science, Chennai. This work was supported by the e-MEN Robotic Research Centre Palakkad.

REFERENCES

- [1] Stephen J. Tobias, A. Antonio Arroyo "Autonomous Path finding" 2000 Florida Conference on Recent Advances in Robotics May 4-5, 2000, Florida Atlantic University.
- [2] Ali Sekmen, Sheldon Greene "Vision-based Mobile Robot Learning and Navigation" 2005 IEEE International Workshop on Robots and Human Interactive Communication
- [3] Yongxing Hao, Benjamin Laxton, Sunil K. Agrawal, Edward Lee, Eric Benson "Planning and Control of UGV Formations in a Dynamic Environment: A Practical Framework with Experiments" Proceedings of the 2003 IEEE International Conference on Robotics & Automation Taipei, Taiwan, September 14-19, 2003
- [4] Johann Borenstein+ and Yoram Koren "MOTION CONTROL ANALYSIS OF A MOBILE ROBOT" Transactions of ASME, Journal of Dynamics, Measurement and Control, Vol. 109, No. 2, pp. 73-79. [20]
- [5] Mbaitiga Zacharie "Intelligent OkiKOSenPBX Security Patrol Robot via Network and Map-Based Route Planning", Journal of Computer Science 5(1);79-85,2009.
- [6] Fen Xu, Zheng Xi Li, Kui Yuan "The design and implementation of an autonomous campus patrol robot" Proceedings of the 2008 IEEE International Conference on Robotics and Biomimetics. M. Young, The Technical Writer's Handbook. Mill Valley, CA: University Science, 1989.
- [7] S. Ali A. Moosavian, Hesam Semsarilar, Arash Kalantari "Design and manufacturing of a mobile rescue robot" international conference on intelligent robots and system oct 9-15-2006 IEEE
- [8] Robert W. Hogg, Arturo L. Rankin, Stergios I. Roumeliotis "Algorithms and Sensors for Small Robot Path Following"
- [9] Sebastian Thrun¹, Maren Bennewitz², Wolfram Burgard² "MINERVA: A Second Generation Museum Tour-Guide Robot" Carnegie Mellon University.

Applied Computer-assisted Programs in Language Assessment

Akram Hashemi

Islamic Azad University, Roudehen Branch, Iran
Persian Literature and Foreign Languages

Abstract - This paper explores the complexity of researching networked learning and tutoring on two levels. Firstly, on the theoretical level, the researcher argues that the nature of networked environments (that is, learning and tutoring) is so complex that no single theoretical model, among those currently available, is a sufficiently powerful, descriptively, rhetorically, inferentially or in its application to real contexts, to provide a framework for a research agenda that takes into account the key aspects of human agency. Furthermore, the researcher argues that this complexity of networked learning requires a multi-method approach to empirical investigation, in order that theory may converse, with both being enriched by these investigations. Secondly, on an empirical level, and as an example that draws upon our theoretical argument about complexity, the researcher presents the findings of a multi-method analysis of the learning and tutoring processes occurring in English classes engaged in a Bachelors' Programme in E-Learning. This investigation is informed by two mainstream theoretical perspectives on learning, and employs computer-assisted content analysis and critical event recall as complementary methodologies. This study reveals the differentiated nature of participants' learning, even within a highly structured collaborative learning environment, identifies some of the key functions and roles of participants, and provides an indication of the value of such multi-method studies. Future prospects for this approach to research in the field are considered.

Keywords - E-learning, networked learning, Assessment tasks

I. INTRODUCTION

This study yielded two major sets of data including the scores of the subjects at the pretest and post-test stages. The data collected through administration of formative tests were not of particular interest, since they were regarded as feedback providing tools at the service of the students' deep learning and ultimately better performance on the final achievement test in all four groups (email summary, computer word type summary, group-net-work summary and control group).

II. PRETEST STAGE

To get assured that the four involved groups were homogeneous at the outset of the study, they were pre-tested of which the descriptive statistics is presented in table 1. Then, their mean scores were compared through a one-way ANOVA at the .05 level of significance. The results of this comparison are in Table 2.

Table 1 : Mean scores of the groups on the pretest

Variable	X	SD
group-net-work	23.93	3.09
computer word type email summary	22.54	3.05
Control group	23.32	3.59
	22.52	3.99

Table 2 : ANOVA for comparing the performance of the four groups on the pretest.

Sources of variation	SS	d.f.	MS	F
Between groups	31.50	3	9.86	
Within groups	974.92	82	11.77	.85
Total	997.43	85		

P<.05

F-critical = 2.73

The results reported in Table 1 indicate no significant difference in terms of the four groups' performance on the pretest at the beginning of the study, since the value of F-observed, .85, was lower than that of F-critical, 2.73. Thus, it could be concluded that the four groups met the condition of homogeneity before undergoing the treatments.

III. POST-TEST STAGE

After one month _ 12 sessions – of treatment, an achievement post-test was administered at the end of the course. As mentioned before, this study was conducted on the basis of the null hypothesis that group-net-work and email summary through formative tests has no significant effect on EFL learners' achievement'. In

order to test the null hypothesis, the mean scores of the groups on the post-test stage (Table 3) were compared through one-way ANOVA at the .05 level of significance. The results are presented in table 4.

Table 4. Mean scores of the groups on the post-test

Variable	X	SD
group-net-work	28.24	2.52
computer word type email summary	25.28	3.20
Control group	26.75	4.06
	21.66	4.79

Table 4. ANOVA for comparing the performance of the four groups on the post-test.

Sources of variation	SS	d.f.	MS	F
Between groups	321.56	3	107.18	
Within groups	1043.82	82	12.72	8.44
Total	1365.39	85		

P<.05

F-critical = 2.73

As shown in the Table 4, the value of F-observed, 8.44, exceeds that of F-critical, 2.73. Therefore, the null hypothesis was rejected due to a significant difference observed among the groups which can be attributed to the effectiveness of the treatments.

To pinpoint the independent variable(s) – (email summary, computer word type summary, group-net-work summary and control group).

Through formative tests – that influenced the subjects' performance on the dependent variable – i.e. achievement scores- and caused the difference, the statistical technique of Scheffé test was utilized the results of which are shown in Table 5.

The results of the Scheffé test show that the significant difference lies between just two of the groups i.e. control group (Group 4) and group-net-work (Group 1). It was also implied that other treatment did not cause any significant difference and the subjects receiving them performed equally on the final achievement test.

Meanwhile, an insignificant overmarking is observed in the net-work group which has outperformed the other groups on the post-test. Brown et al. (1997), too, report such overmarkings in some of the studies .

IV. DISCUSSION

After 12 sessions of treatment, the effects of different techniques through formative tests on Iranian elementary EFL learners were investigated. The obtained data indicated that the group in which students' performances on formative tests were assessed by the net-work-group outperformed the other ones. The results of this study correspond with the findings of Berger (1990) and Zhang (1995), who found peer-assessment as having more favorable effects than self- and teacher-assessment. However, they are not consistent with the findings of Chaudran (1984).

The out-performance of the net-work group in the final achievement test indicates the significance of leaving the students' performance on formative tests to their peers. This can be justified by resorting to Vygotsky (1986)'s zone of proximal development (ZPD). ZPD is a psychological space where latent abilities are vulnerable to maturation with the aid of others for instance net-work-group working.

net-work group can also be due to the reciprocal process of giving and receiving feedback. This process was at work while the students were engaged in correcting and scoring their peers' papers in net and received their own peers' feedback . To make sure that their peers had assessed their performances on the tests correctly, they exerted much more effort to challenge the assessment and this challenge may have contributed to their better learning of the points, and consequently better performance on the achievement test through net.

On the whole, it is generally concluded that net work group as a form of collaborative learning is beneficial because of the nature of interactions as well as inspection that occur through giving and receiving peer feedback. The conclusion of this study supports the contention that Internet and computer can improve the effectiveness of instruction.

Furthermore, since providing the opportunity for the learners to assess their peers' performances proved effective, teachers are recommended to increase students' interaction through creating a cooperative atmosphere in their classes and allowing the students to take active roles in the assessment of the formative tests they take. As also recommended by Brown et al., (1997), teachers should encourage students' engagement in giving and receiving feedback through providing the appropriate opportunities which make the students reflect upon the processes of their learning, and ultimately improve their achievement.

A good process oriented Net work based syllabus should meet the following criteria:

- provide opportunities for language practice

- provide opportunities for meta-communication and meta-cognition
- promote learning training for problem-solving and problem-sensing and problem-solving
- promote sharing of information and expertise
- provide monitoring and feedback
- heighten learners' consciousness of the process and encourage reflection
- allow for co-evaluation by the learner and the teacher

The findings of this study call the material developers to include net work group – developed and validated by language testers – in the textbooks developed for classroom use.

Thus, it can be concluded that those in and around ELT should be aware of the fluctuating viewpoints held by applied net work toward language, researchers toward language learning, teaching, and testing, along with the principles and beliefs currently held in education.

REFERENCES

- [1] Alexander, R. , Rose, J. and Woodhead, C. (1992) Curriculum Organization and Classroom Practice in Pirmary Schools, London, DES.
- [2] Allwright, R. (1988) Autonomy and individuation in whole class instruction.' In Brooks, A. and Grundu, P., (eds) Individuation and Autonomy in Language Learning , pp. 35-44. British Council.
- [3] Beavon, B., Soars, L., and Soars, J. (1995) Headstart, London: Oxford University Press.
- [4] Berger, V. (1990) 'The effects of peer and self-feedback', The CATESOL Journal, November: 21-35
- [5] Biggs, J. (1996) 'Assessing learning quality: reconciling institutional, staff and educational demands', Assessment and Evaluation in Higher Education, 21/1, pp.5-15.
- [6] Black, E. (1995). Behaviorism as a learning theory.[On-line]. Available: <http://129.7.160.115/inst5931/Behaviorism.html>
- [7] Standards Through Classroom Assessment. London: Kappan Home.
- [8] Boud, D. and Brew, A. (1995) Enhancing Learning through Self-Assessment, London: Kogan Page.
- [9] Brew, A.(1995) 'What is the scope of self-assessment?' in D.Boud and A. Brew (1995) Enhancing Learning through Self-Assessment, London: Kogan Page.



Automated Blocking of Malicious Code with NDIS Intermediate Driver at Kernel Mode

Madhusmita Mohanty & Ranjana P

Hindustan Institute of Technology and Science, Department of computer Science and Engineering

Abstract - Malware often hide its malicious behaviour in various methods. One of the popular manners is to conceal the network communication. Firewall is the core technology of today's network security and the first line of defence against external network attacks and threats, most personal firewall deals with the packets under the user model, there are a lots of limits, in order to protect our privates better some operations need to be done under the kernel model. The NDIS by which we can easy do something under the kernel model is introduced in the windows operating system that is the mostly used system in personal computer. Modern. This concealment technique poses obstacles to security mechanisms, which detecting the malicious behaviours. This paper clearly describes the architecture of the NDIS, on the base of the NDIS intermediate drivers presents a personal firewall model which operations under the kernel model. We propose a technique for the Network Driver Interface Specification (NDIS) integrate together with a unified malicious software analysis platform. The NDIS model supports hybrid network transport NDIS drivers, called NDIS intermediate drivers. This driver lies between transport driver and NDIS driver. The advantage of using NDIS intermediate drivers is, it can see the entire network traffic taking place on a system as the drivers lie between protocol drivers and network drivers. In this paper, we give an overview of the automated blocking malicious code project, a new approach to computer security via malicious software analysis and automatic blocking software.

Keywords - Network Driver Interface Specification, NDIS Intermediate Driver, Interception, Malicious Traffic, Malware Analysis

I. INTRODUCTION

Malware, short for malicious software, is software designed to disrupt computer operation, gather sensitive information, or gain unauthorized access to computer systems. Malware includes computer viruses, worms, trojan horses, spyware, dishonest adware, most rootkits, and other malicious program. The evolution of modern malware now a day is not only attack inside computer system, but through the convenience of the Internet, spreading from one victim computer to another. There are also some malicious codes, conceal the communication pathway, and avoid the detections from security protection mechanisms such as firewall, sniffer, antivirus, IDS system etc. In general, security mechanisms on Windows such as firewall, Intrusion Detection System (IDS), etc rely on native TCP/IP for network traffic related functions. However Microsoft has imposed restrictions on raw socket as below:

- CP data cannot be sent over a raw socket.
- UDP datagram cannot spoof their source address over a raw socket
- Raw sockets cannot make calls to the bind() function.

A raw socket is a socket that allows direct access to the headers of a network frame. on between NDIS interface with WSK and Winsock Interface. In this paper we address a design system for intercepting and automating blocking of malicious network traffic by using NDIS Intermediate driver. The reason that we choose NDIS intermediate driver as our automated project is NDIS can capture all the packets passing through the system, including packets such as rootkit that can bypass local firewall. Our approach is to capture the entire network traffic packet and control it in a real time manner. An output of the network traffic log file will export into a user readable file, and can display any field in any headers protocol as user want.

II. BACKGROUND AND RELATED WORK

The Network Driver Interface Specification (NDIS) is a standardized interface for OS/2 network platforms. One of the biggest challenge is host based network security software relying on the underlying Operating System's support for data gathering and monitoring. However, the evolutions of malware programs have proof that they are capable to exploit the weakness. The capability to bypassing virtually all commodity, host-based firewall and intrusion detection system

software on the market today has force security researchers seeking new method on detecting and blocking the malicious activities, and there is security organizations decided to use NDIS Intermediate Driver as the solution.

Kaspersky Anti-Virus is one of the security products on the market which implemented the technology of NDIS Intermediate Driver. The current firewall technology on defending against external network attacks and threats which deals with the packets under user mode has a lot of limitation. NDIS provides access to the network services at the datalink layer and is especially useful if the access must be shared. It has proposed that the protection can be done better by using NDIS intermediate driver.

III. NDIS_PACKET REPRESENTATION

The main function of NDIS packets (represented by NDIS_PACKET structure) is to ensure all network data can be sent to or from the network in a system. NDIS_PACKET can be used to encapsulate packet data. The NDIS_PACKET has one chained NDIS_BUFFER.

The NDIS_BUFFER describes 74-bytes range of virtual memory that contains the complete packet data. Prior sending data on the network, a protocol driver allocates NDIS packets, (represented by a NDIS_PACKET), filled with data, and passed to the next lower NDIS driver. The first NDIS_BUFFER describes the range of virtual memory that contains the Ethernet header while the second NDIS_BUFFER describe the range of virtual memory that contains the Ethernet payload.

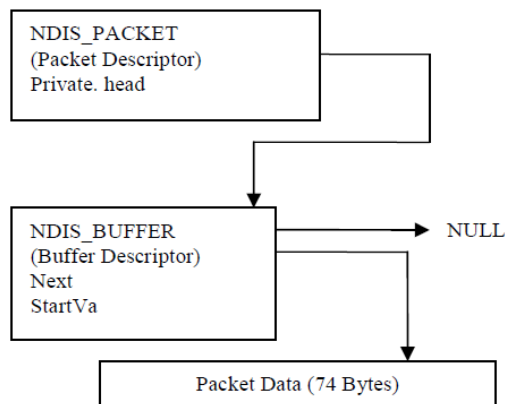


Fig. 1 : Simple NDIS_Packet Illustration

The number of chained for NDIS_BUFFER is depending on the size of the NDIS packet. If the packet size is small, there will be only one chained for NDIS_BUFFER and this buffer enough to

describe the range of virtual memory that contains the complete packet data.

A protocol driver allocates an NDIS packet, fills it with data, and passes it to the next lower NDIS driver so that the data can be sent on the network. A protocol driver allocates a packet and passes it to a NIC driver with a request that the NIC driver copy received data into the provided packet. NDIS provides functions allocating and manipulating the substructures that constitute a packet.

A packet contains packet descriptors and buffer descriptors, each of which contains other elements.

The following list shows the contents of a typical packet descriptor:

- Private areas for the miniport NIC driver and a protocol driver
- Flags associated with the packet, defined by a cooperating miniport(s) and protocol driver(s)
- Number of physical pages that contain the packet
- Total length of the packet
- Pointer to the first buffer descriptor that maps the first buffer in the packet

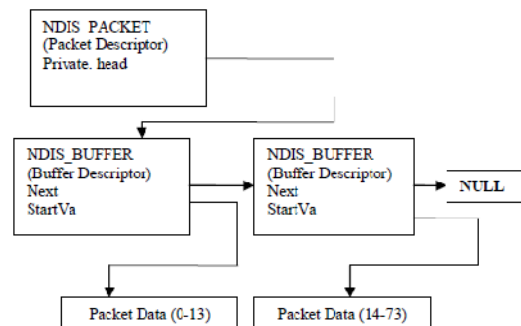


Fig. 2 : Multi-Buffer NDIS_PACKET Illustration

The following list shows the contents of a typical buffer descriptor:

- Starting virtual address of each buffer
- Buffer's byte offset into the page pointed to by the virtual address
- Total number of bytes in the buffer
- Pointer to the next buffer descriptor, if any
- Virtual range, possibly spanning more than one page that makes up the buffer described by the

buffer descriptor. These virtual pages map to physical memory.

A driver that allocates shared memory, such as a bus master NIC driver for receiving incoming packets or a protocol driver that allocates memory for sending packet, must ensure that any buffer used to contain incoming or outgoing data is cache aligned. This is necessary so that the minport can flush the buffer to assure coherency before sending a packet and to flush a received buffer before indicating the data to an upper layer.

IV. INTERCEPTION AND BLOCKING ARCHITECTURE

The NDIS model supports hybrid network transport NDIS drivers, called NDIS intermediate driver. The driver is lie between transport drivers and NDIS drivers. To an NDIS driver, an NDIS intermediate driver looks like a transport driver; to a transport driver, an NDIS intermediate driver looks like an NDIS driver. In this section, we give an overview of the interception and blocking architecture using NDIS intermediate driver. As shown in Figure 3, all network traffics are first intercepted by the interception mechanism.

In the process of interception, the entire network packets will dump into a log file in hexadecimal format. The purpose of creating a log file is to see what activities is taking place.

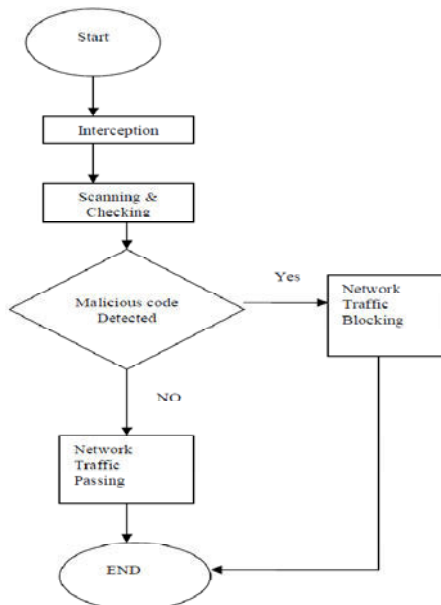


Fig. 3 : Interception and Blocking Architecture

The purpose of creating a log file is to see what activities is taking place. The scanning and checking

mechanism will execute pattern matching function. This function will compare the intercepted network traffic with pre-defined unique signature strings where each unique string represents malicious portion code signatures.

Knuth- Morris-Pratt (KMP) algorithm was used to observe when a mismatch occurs. The KMP algorithm looks for the malicious code signature pattern in a left-to-right order. It looks like the brute force algorithm but it shifts the pattern more intelligently than the brute force algorithm.

Figure 3 illustrates the fragment code of this function. If the pattern matching occurs, NDIS intermediate driver will immediately drop the interception network traffic. STATUS_DROP function can be used to drop the network packet as shown in Figure 4. If none of the pattern is match, network traffic will allow pass through on the system.

```

TT[0]= -1;
TT[1]=0;
l=2;
K=0;
While(T[l]!='\0'){
If(T[l-1]==T[k]){
TT[l]=k+1;
K++;
l++;}
Else if(k>0){
K==TT[k];}
Else{
TT[l]=0;
l++;
K=0;}}
If(pPacketContent[34]==0 && pPacketContent[35]==80)
{
Ddbgprint("Receive Http port 80");
For(i=54;i<=Dataoffset;i++)
{
While(pPacketContent[i+j]!='\0' && T[j]!='\0')
{

```

```

If(pPacketContent[i+j]==T[j])
{
Dbgprint("Signature match success");
{
++j;
If(T[j]=='\0')
Dbgprint("myndis blocking -malicious traffic
detected");
Return STATUS_DROP;}}
Else
{
I+=j-TT[j];
If(j>0)
{
J+=TT[j];}}}}

```

Fig. 3 : Knuth-Morris-Pratt (KMP) Pattern Matching Algorithm

```

Dbgprint("signature match Success");
++j;
if(T[j]=='\0')
{
DbgPrint("myndis blocking-malicious traffic
detected");
Return STATUS_DROP;
}

```

Fig. 4 : Blocking Function Based on Signature

V. CONCLUSIONS

The Network Driver Interface Specification (NDIS) library abstracts the network hardware from network drivers. NDIS also specifies a standard interface between layered network drivers, thereby abstracting lower-level drivers that manage hardware from upper-level drivers, such as network transports. NDIS also maintains state information and parameters for network drivers, including pointers to functions, handles, and parameter blocks for linkage, and other system values. Malware scanning engine is the core technology of today malware protection and the first line of defence against external network attacks and system threats. Most personal scanning engine deals with the network packets under the user mode, however there are a lot of

limitation. In order to provide better protection for user, security prevention mechanisms need to be done at kernel mode. This paper clearly describes the use of NDIS intermediate driver and the development of scanning engine model at kernel model.

REFERENCES

- [1] He Chaokai, "Design and implementation of a personal firewall Based on NDIS Intermediate Drivers," IEEE Eighth ACIS International Conference, Qingdao, Software Engineering, Artificial Intelligence, Networking, and Parallel/Distributed Computing, pp. 878-882, July30 2007 – August 1 2007.
- [2] Muna M. Taher Jawhar, Monica Mehrotra, "System Design for Packet Sniffer using NDIS Hooking," International Journal of Computer Science & Communication, Vol. 1, No. 1, pp. 171-173, January – June 2010.
- [3] Walter Oney., "Programming the Microsoft Windows Driver Model", 2nd ed. Microsoft Press, A Division of Microsoft Corporation 2003.
- [4] Mark E. Russinovich, David A. Solomon, Alex Ionescu, Windows® Internals: Including Windows Server 2008 and Windows Vista, Fifth Edition, Microsoft Press, A Division of Microsoft Corporation, One Microsoft Way, 2009, pp. 1053 - 1071.
- [5] Reverend Bill Blunden, "The Rootkit Arsenal: Escape and Evasion in the Dark Corners of the System," Wordware Publishing Inc, 2009, pp. 610-616.
- [6] HanTechSnS, "SecurityStudio 2001: NDIS Intermediate Driver Operation & WDM Driver Operation," pp. 6, 2001
- [7] Printing Communications Associates, Inc. (PCAUSA), "NDIS_PACKET Discussion Part 2: NDIS_PACKET Reserved Areas," January 17, 2010.
- [8] MSDN Library, Microsoft Corporation, "NDIS-Supplied Packet and Buffer Handling Functions (NDIS 5.1)," March 6, 2010.
- [9] Greg Hoglund, James Butler, "Rootkits: Subverting the Windows Kernel," Addison Wesley Professional, July 22, 2005, Chapter 9: Covert Channels.
- [10] (2010) The Kaspersky website. [Online]. Available:<http://support.kaspersky.com/faq/?qid=208279317>

- [11] Greg Plaxton, "String Matching: Knuth-Morris-Pratt Algorithm," Theory in Programming Practise, Department of Computer Science, University of Texas at Austin, Spring 2004.
- [12] J. H. Morris, Jr and V. R. Pratt. "A linear pattern-matching algorithm," Report 40, University of California, Berkeley, 1970.
- [13] Mark Dowd, "Application-Specific Attacks: Leveraging the ActionScript Virtual Machine," IBM Internet Security Systems, April 2008. [Online]. Available: http://documents.iss.net/whitepapers/IBM_X-Force_WP_final.pdf
- [14] (2010) Adobe Systems Incorporated, "Flash Player update available to address security vulnerabilities," APSB08-11, April 8, 2008. [Online]. Available: <http://www.adobe.com/support/security/bulletins/apsb08-11.html>



Venal Pattern Generation of the Palma Dorsa

Shweta Dhawan¹ & Sandesh Gupta²

¹Engineering & Technology, Mody Institute of Technology & Science, Lakshmanagarh 332311, Rajasthan, India

²Department of Computer Science & Engineering, University Institute of Engineering & Technology, C.S.J.M. University, Kanpur 208024, India

Abstract - In this paper, we present a method to generate the vein pattern from the back of the hand. The images have been captured with near infrared imaging. The images have undergone segmentation using active contouring. Further, images are enhanced by grayscale normalization, filtering and Gaussian smoothing. The images undergo thresholding to produce a binary image. Morphological operations have been used to provide a thinned vein pattern. It has applied on the database of 1750 images with accurate results. In this work, we have used MATLAB R2009a, version 7.8.0 for coding.

Keywords - *Palma dorsa, Segmentation, Enhancement, Pre-processing, Binarization, Morphological operators, Vein pattern.*

I. INTRODUCTION

Vein pattern recognition is one of the newest biometric techniques being researched. The pattern of blood veins is unique to every individual, even among identical twins and the pattern does not change over time. The main concept behind vein pattern identification is Palma dorsa i.e. geometry of network of veins at the back of the hand. An individual's vein pattern image is captured by radiating the person's hand with near-infrared rays. The deoxidized haemoglobin in the vein vessels absorbs the infrared rays, thereby reducing the reflection rate and causing the veins to appear as a black pattern.

Vein pattern has various advantages over other biometrics. Human face is prone to changes over time - aging, facial hair, skin tone, glasses, etc. while vein patterns pattern does not change over time. Iris recognition can also be affected by certain eye problems, such as cataract, and if the user is wearing colored contact lenses or sunglasses. Fingerprints are prone to external distortion like cuts, etc. As veins are internal in the body and have a wealth of differentiating features, attempts to forge an identity are extremely difficult, thereby enabling a high level of security. While fingerprints can be duplicated using gummy fingers, that are easily made of cheap and readily available gelatin.

II. RELATED WORK

Vein pattern has seen increased attention since its inception. Many ideas have come up for vein pattern identification and authentication. The first step is to

acquire the hand vein image. For this, the thermal image of the back of the hand can be captured. Thermal images can be captured in two ways, far-infrared (FIR) and near-infrared (NIR). NIR produces good quality images when capturing the vein patterns from the back of the hand and the palm. Wang and Graham [1] studied these two thermal imaging technologies to capture vein pattern images. Lin and Fan [2] have presented a promising approach for the personal verification using palm dorsal images. The approach detailed in [2] is fully automated and uses the combination of multi-resolution representations from the post processed thermal vein patterns. Wang, Li and Cui [3] gave the concept of hand vein identification based on partitioned local binary pattern. M. Deepamalar [4] presented an improved multimodal palm vein recognition system using shape and texture features. Wang and Leedham [5] utilized the watershed algorithm to extract the skeletons of the vein patterns directly from the grayscale images. Vein pattern generation starts with pre-processing of the image acquired. Pre-processing involves segmentation of images. Badawi [6] gave the concept of active contour model or snakes for the segmentation of the images.

III. IMAGE ACQUISITION

In this work, IIT Kanpur database consisting of 1750 images has been used. The images were taken from an experimental setup of IIT Kanpur. A digital Single Lens Reflex camera combined with an infrared filter has been used. The set-up [7] is a modest wooden box with a hollow rod lodged in the middle accommodating the infrared lamp. The camera is held on a tripod attached to the box. The flat face of the night vision lamp provides for a sturdy plinth for the subject's

hand. The sensor here is kept on the opposite side of the light source. The image given in Figure 1 shows one of the samples of the vein pattern obtained.



Fig. 1 : Sample of a hand dorsal vein pattern.

IV. IMAGE PREPROCESSING

The color obtained from the above system contains some unwanted information such as background noise, noise due to the hair in the hand, intensity fluctuations. Image preprocessing involves the removal of this extra information. The region of interest has to be extracted from the acquired image and processed to obtain the vein network of the palma dorsa. It involves the following four main steps namely a) Segmentation b) Image enhancement c) Binarization d) Morphological operations e) Vein pattern generation.

A. Segmentation

Segmentation separates the skin area from the acquired image to obtain the Region of Interest (ROI). The traditional technique of Snake, i.e. Active Contouring [6] has been used for the segmentation of images. A snake is an energy-minimizing spline guided by external constraint forces and influenced by image forces that pull it toward features such as lines and edges. Snakes are active contour models [8]. Active because it is always minimizing its energy functional and therefore exhibits dynamic behavior. The way it slithers while minimizing its energy renders it the name "snake". The segmented image is shown in Figure 2.



Fig. 2 : Segmented Image

B. Image Enhancement

The image obtained after segmentation is converted to gray scale. The gray scale conversion is shown in Figure 3.

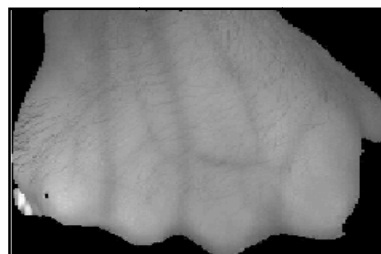


Fig. 3 : Gray scale image

As the light intensity may vary at different times, the grey scale distribution of different images is different. To reduce these differences the gray scale normalization of the image is performed as given by (1).

$$I_1 = (\text{grayimage} - \text{min}) * (255 / (\text{max} - \text{min})) \quad (1)$$

Where min and max are the minimum and maximum values of gray scale image, I_1 is the gray scale image after normalization. The image obtained after gray scale normalization is shown in Figure 4

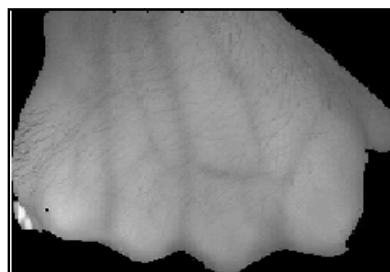


Fig. 4 : Image after gray scale normalization

The image thus obtained may contain salt and pepper noise. Median filtering is used to remove such noises. Median filter is a sliding window spatial filter that replaces the centre value in the pixel with the median of all pixel values in the window. A 5 x 5 Median filter was used here. The image obtained after median filtering is shown in the Figure 5.

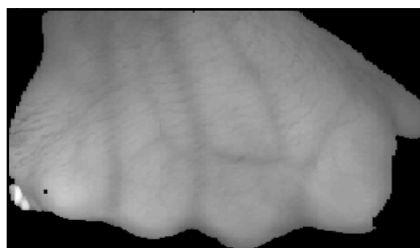


Fig. 5 : Image after median filtering

Then Gaussian smoothing [9] is applied. Gaussian smoothing is a low pass filtering which suppresses the high frequency noise while preserving low frequency parts of the image. A Gaussian low pass filter with standard deviation $\sigma=5$ was applied to the images. The image obtained after applying Gaussian filter is shown in Figure 6

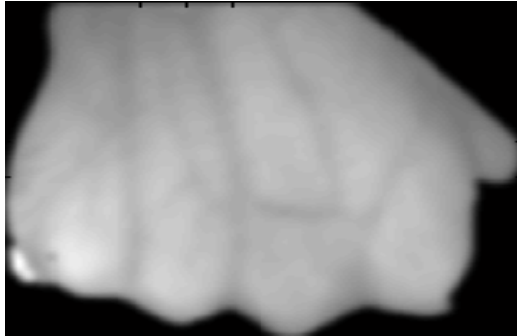


Fig. 6 : Image obtained after Gaussian filtering

Further, the variance of the image is increased to get a higher contrast between the veins and the skin in the images. The formula used is given in (2).

$$I_c(x, y) = \begin{cases} \mu_d + \sqrt{\sigma_d^2 (I_{gauss}(x, y) - \mu)^2 / \sigma^2}, & \text{if } I(x, y) > \mu \\ \mu_d - \sqrt{\sigma_d^2 (I_{gauss}(x, y) - \mu)^2 / \sigma^2}, & \text{Otherwise} \end{cases} \quad (2)$$

Where $I_c(x, y)$ is the image obtained after applying Gaussian filter, μ is the mean of $I(x, y)$, σ^2 is the variance of $I(x, y)$, μ_d is the desired mean, σ_d^2 is the desired variance. In this work, μ_d has been taken as 128 and $\sigma_d^2 = 100$. The image obtained after increasing the contrast is shown in Figure 7.

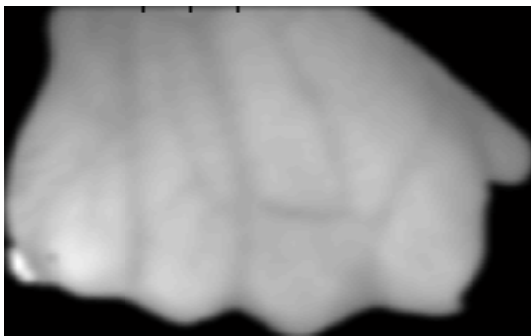


Fig. 7 : Image obtained after increasing variance

C. Binarization

Binarization is used to separate the veins from the background and to convert the image into black and white image with the help of threshold values. Different threshold values have been chosen for each pixel of the image. The value of the threshold [10] for each pixel is equal to the mean for its 25×25 neighbourhood. The formula used for Binarization is given in (3).

$$I_b(x, y) = \begin{cases} 1, & \text{if } I_c(x, y) > \mu_{xy} \\ 0, & \text{otherwise} \end{cases} \quad (3)$$

Where $I_c(x, y)$ is the image obtained after increasing the contrast, μ_{xy} is the mean value of the 25×25 neighbourhood at (x, y) and $I_b(x, y)$ is the binarized image. Sliding neighbourhood operator is used to find the mean of each 25×25 sliding block of image. Pixels in the image are marked as background pixel if their value is less than the threshold value and as “vein” pixels otherwise. Typically, a vein pixel is given a value of “1” while a background pixel is given a value of “0”. The binarized image is shown in Figure 8.



Fig. 8 : Image after Binarization

D. Morphological operations

Now morphological “dilation” operation is applied on the image using a disk of radius 1 pixel as the structural element. The resulting image is shown in Figure 9.



Fig. 9 : Dilated Image

Then morphological operation [11] of “thinning” is further applied on the image. The resulting image is shown in Figure 10. The thinned image is a skeletonised

image with vein reduced to its centre pixel and the thickness reduced to one pixel size only.



Fig. 10 : Thinned image

E. Vein pattern generation

Now the edges due to the hand boundary have to be removed. For this horizontal scanning is done, row by row. The first and last pixels encountered on each row scan is turned black. Similarly vertical scanning is done column by column. Again the first and last pixel encountered on each column scan is turned black. Thus, the hand boundary is removed and the vein pattern is found. The image after removal of hand boundary is shown in Figure 11.



Fig. 11 : Removal of hand boundary

The image may contain some small spurious edges due to the hair in the hand. These false edges have to be removed. For this all connected components are labelled and all the unconnected components of area less than 200 pixels are discarded. Thus, the vein pattern is generated as shown in Figure 12.

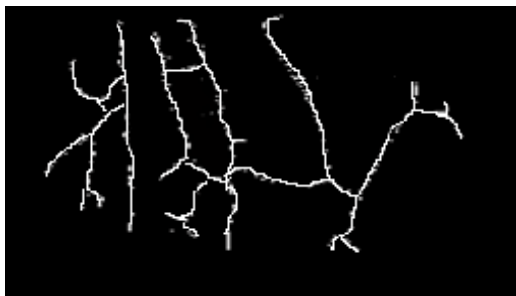


Fig. 12 : After component removal

V. CONCLUSION

In this paper, we have used active contours for the segmentation. Presence of noise leads to the application of Median and Gaussian filters. Thus, after series of processing, segmenting, gray scale conversion, normalization, filtering, smoothing, binarization, dilation, thinning, the paper obtains a clean and smooth vein pattern skeleton. The hair present in the hand poses a problem for vein pattern generation, as they lead to many small spurious, false edges. In our work, we were able to efficiently remove such false edges. Experimental results of this work shows that the vein patterns extracted are accurate and clearly depict the network of veins below the skin. Future work includes the method of feature extraction and matching with the database.

ACKNOWLEDGMENT

We express our deepest thanks to Prof. Phalguni Gupta, from Indian Institute of Technology, Kanpur, for providing us with a dataset of 1750 images of hand dorsal vein pattern.

REFERENCES

- [1] Wang Lingyu and Graham Leedham, "Near and Far-Infrared Imaging for Vein Pattern Biometrics", AVSS '06 Proceedings of the IEEE International Conference on Video and Signal Based Surveillance, pp: 52-52, Sydney, Australia
- [2] Chih-Lung Lin and Kuo-Chin Fan, "Biometric Verification Using Thermal Images of Palm-Dorsa Vein Patterns" IEEE Trans. Circuits & Sys. For Video Technology, vol. 14, pp: 199 – 213, Feb. 2004.
- [3] Yiding Wang, Kefeng Li, Jiali Cui, "Hand-dorsa vein recognition based on partition Local Binary Pattern", 2010 IEEE 10th International Conference on Signal Processing, Oct.2010,pp: 1671-1674, Beijing
- [4] M.Deepamalar and M.Madheswaran, "An Improved Multimodal Palm Vein Recognition System Using Shape and Texture Features", International Journal of Computer Theory and Engineering, Vol. 2, No. 3, June, 2010,pp:1793-8201.
- [5] Lingyu Wang and Graham Leedham, "A Watershed Algorithmic Approach for Gray-Scale Skeletonization in Thermal Vein Pattern Biometrics", Computational Intelligence and Security: International Conference, CIS 2006, Guangzhou, China, November 2006.

- [6] A. Badawi “Hand Vein Biometric Verification Prototype: A Testing Performance and Patterns Similarity” in Proceedings of the International Conference on Image Processing, Computer Vision and Pattern Recognition, pp:3-9, 2006.
- [7] Mohit Soni, Sandesh Gupta, M. S. Rao, Phalguni Gupta, “A New Vein Pattern-based verification System”, International Journal of Computer Science and Information Security, Vol.8, No. 1, pp.58-63, 2010
- [8] Ghassan Hamarneh and Tomas Gustavsson, “Statistically Constrained Snake Deformations”, IEEE Conference on Systems, Man, and Cybernetics 2000.
- [9] S. Im, H. Park, Y. Kim, S. Han, S. Kim, C. Kang, and C. Chung, “A Biometric Identification System by Extracting Hand Vein Patterns”, Journal of the Korean Physical Society, vol. 38-3, pp. 268-272, March 2001
- [10] Mehmet Sezgin and Bulent Sankur, “Survey over image thresholding techniques and quantitative performance evaluation”, Journal of Electronic Imaging 13(1), 146–165, January 2004.
- [11] Hoshyar, A.N., R. Sulaiman and A.N. Houshyar, 2011. “Smart access control with finger vein authentication and neural network”, J. Am. Sci., 7: 192-200.



Fuzzy Vault Biometric Cryptosystem : A Technical Report

Manavjeet Kaur & Supreet Kaur Gill

Dept. Computer Science, PEC University of Technology, Chandigarh, India.

Abstract - Biometrics has emerged as only technology that links authentication directly with unique characteristics of an individual and is used for many authentication processes. Though biometric authentication ensures that only legitimate user has access to system but even a biometric system itself is vulnerable to number of threats such as spoofing of user template, stealing or deleting templates from database. A rising issue in biometric system is security and privacy of user templates. To secure the biometrics – based user authentication fuzzy vault biometric cryptosystem has been proposed. These systems do not store original template but only a transformed version of it. Fuzzy vault has been shown to be an effective technique for securing user template by binding randomly generated secret key with biometrics within a cryptographic framework. This article reviews techniques adopted to implement fuzzy vault and covers various methods to enhance the performance of fuzzy vault.

Keywords - *biometric cryptosystem, fuzzy vault, minutiae, helper data, extraction, polynomial reconstruction.*

I. INTRODUCTION

Biometrics has emerged as an efficient technology that is used for authentication purposes and has been applied to many authentication processes. Biometric cryptosystem combines unique features of an individual known as biometric with secret key within a cryptographic framework. But a biometric system is vulnerable to number of threats such as spoofing of user template, stealing or deleting templates from database. So the security of this system has been on risk. Security and privacy of user template in biometrics systems has become primary concern in biometrics community. To secure the biometrics – based user authentication fuzzy vault biometric cryptosystem has been proposed. These systems do not store original template but only a transformed version of it. Fuzzy vault has been shown to be an effective technique for securing biometric templates. It uses uniform random key to secure the template by binding template with key. Hence it increases the privacy and security within a cryptographic framework.

Section II includes background, section III includes Practical implementation of fuzzy vault, IV specifies performance enhancement, V and VI describes recent work on Implementation and performance. Section VII includes security improvement and section VIII is conclusion.

II. BACKGROUND

Fuzzy vault has been originally proposed by Juels and Sudan. In their scheme using example of Alice and Bob, Alice encloses secret S in fuzzy vault and lock it

using an unordered set A. Bob using unordered set B can unlock the vault only if B substantially overlaps with A. Alice chooses a polynomial P of variable X that encodes S. The coefficients of P forms that secret key and then chaff points are added which do not lie on the chosen polynomial. Then bob tries to authenticate himself by providing an unordered set B and finding P. If this set B overlaps with unordered set A then bob is authenticated.

A. REED-SOLOMON TECHNIQUE

In their scheme Reed Solomon Technique is used to reconstruct P and decode the secret S. It is possible to construct a fuzzy vault scheme based on essentially any type of linear error-correcting code. In the simplest embodiment of such an R-S code, it is expressed as a codeword in the sequence $y_1 = p(1); y_2 = p(2); \dots; y_t = p(t)$, where $1; 2; \dots; t$ represent the first t elements of the field F. If $t > k$, then a codeword may contain some redundancy. In Reed-Solomon decoding technique input is taken as a collection of points which are presumed to lie preponderantly on a single polynomial of pre-spaced degree at most $k-1$. The decode algorithm, if successful, outputs a polynomial p giving intersection of the large majority of input points. Otherwise, the algorithm outputs null [1].

III. PRACTICAL IMPLEMENTATION OF FUZZY VAULT

Clancy et al proposed a fingerprint vault based on fuzzy vault of Juels and Sudan. He used multiple minutiae locations as elements of locking set. This paper describes the use of random points known as chaff

points which do not lie on polynomial. These points along with the minutiae points that lie on the polynomial become vault. Minutiae points are concealed by these chaff points even if the vault is exposed and prevents the misuse of vault. As the no. of chaff point increases the security of vault increases. But the method assumed that fingerprints one required to form vault and other for query are prealigned [2].

To introduce alignment in fuzzy vault system for fingerprints Yang and Verbauwhede proposed the use of reference minutiae extracted during vault encoding and decoding. The alignment is established if these two references are same and thus the origins of coordinate frames to be used[3]. Uludag proposed a method which eliminated this feature characteristic of minutiae for alignment and used simple translation and rotation between template and query because reference minutiae cannot be same at enrolment and verification. The algorithm used cyclic redundancy check and Lagrange Interpolation instead of Reed Solomon decoding. The main drawback of Reed Solomon coding scheme assumes

- (i) The input data set S only contain integer within limited range.
- (ii) Vault may also leak some information because it is stored without transformation. This algorithm decodes several candidate sets of size n+1(n is degree of polynomial) which are generated from the unlocking set. These sets are input to Lagrange interpolation to reconstruct the polynomial which hides the secret. Cyclic redundancy is used to identify the correct polynomial. Reconstructed polynomial is compared by using CRC and if CRC renders zero means correct else it denies the candidate set [4].

A. LARANGE INTERPOLATION

Lagrange polynomials are used for polynomial interpolation. For a given set of distinct points x_j and numbers y_j , the Lagrange polynomial is the polynomial of the least degree that at each point x_j assumes the corresponding value y_j (i.e. the functions coincide at each point).

$$L(x) = \sum_j^k y_j l_j(x) = \frac{(x-x_0)}{(x_j-x_0)} \cdots \frac{(x-x_{j-1})}{(x_j-x_{j-1})} \frac{(x-x_{j+1})}{(x_j-x_{j+1})} \cdots \frac{(x-x_k)}{(x_j-x_k)}$$

IV. PERFORMANCE ENCHANCEMENT

A. HELPER DATA

Anil k Jain and Uludag further carried this technique and enhanced performance of fuzzy vault by introducing helper data. In this system template is stored in transformed domain to provide security but it then becomes difficult to align query with stored template. Helper data helps the template in transformed domain for alignment and comparison with the query data. It does not leak minutiae information while aligning the query template. The technique used here is OOF(Orientation Field Flow Curves) which are set of piece wise linear segments. The maximum curvature points and corresponding values constitute the helper data.[5]

Karthik Nandkumar and Anil k Jain further improved fuzzy vault by using

- (i) Minutiae matcher during decoding to compensate for non-linear distortion in fingerprints. The minutiae matcher uses the adaptive box technique that accounts for distortion.
- (ii) Along with the location of the minutiae points orientation field is also considered. This increases the number of chaff points to be added whose location is close to a true minutiae but with different direction.
- (iii) It also used local image quality index estimated from fingerprint in to select the most reliable minutiae. This significantly improved the GAR(genuine accept rate). This steps for extraction of helper data are firstly estimating the orientation of field secondly extraction of flow curves thirdly determination of maximum curvature points and lastly clustering of high curvature points. Then ICP algorithm is used for alignment using helper data [6].

B. FUZZY COMMITMENT SCHEME

This work is carried further by implementing fuzzy commitment scheme to improve the security of fuzzy vault system. In this paper the polynomial is that evaluation using helper data are encrypted. Minutiae descriptor uses two attributes, orientation and ridge frequency information in a minutiae neighbourhood for securing polynomial evaluations.

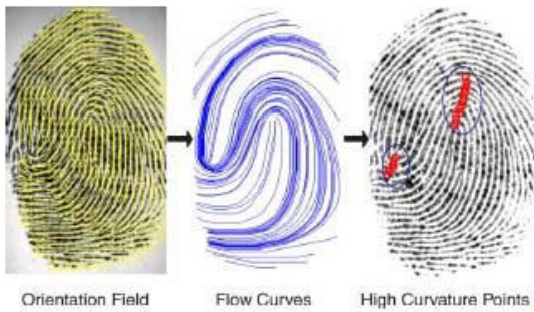


Fig. 1: Helper Data Extraction [6]

In this technique helper data constitutes A- abscissa points of minutiae and G- Secure ordinate points. This G is obtained by XORing descriptor values and C codeword. Codeword is in turn generated by adding error bits to 16 bit ordinate values.

$$G = (D \text{ XOR } C)$$

During authentication again a XOR operation is applied between new found descriptor of query D' and secure ordinate value G of vault.

$$C = (D' \text{ XOR } G)$$

If $D = D'$ then C' is same as C, the original value is extracted and hence the polynomial otherwise it is rejected [7].

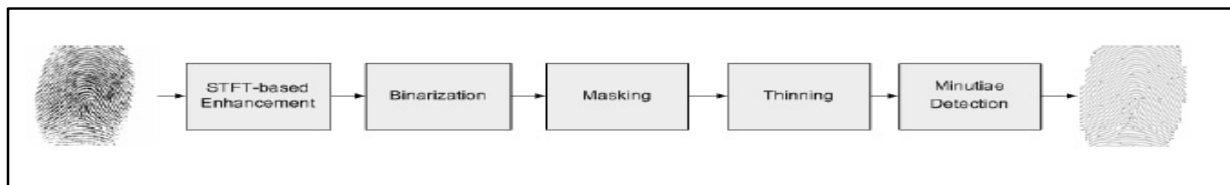


Fig. 2 : Minutiae Detection [7]

C. CHAFF PLACEMENT

Alper Kanak and Ibrahim Sogukpinar used the Clancy method to add chaff points but in different way. This scheme combines the fingerprint minutiae with the user specific pseudo random data to enhance security. A set of user specific randomly selected chaff minutiae features are stored and subset of only this set is used at each acquisition. Predefined chaff minutiae are used in these vaults. This reduces the time to calculate chaff points each time for enrolment. In order to improve image quality such as reducing the space requirement and time consumption and to improve accuracy STFT-based enhancement is applied. Intrinsic images like ridge orientation, frequency and region mask are estimated simultaneously from STFT analysis [8].

Orencik, Pederson, Savas and Keskinoz discuss the location of chaff points which may leak information about the genuine points and proposes a technique that makes difficult to distinguish genuine points. The distance between a chaff point and a genuine point or another chaff point is t but the distance between two genuine points is not fixed and can be less than t which makes the detection of minutiae easy. So Chaff points should be placed at a distance t' which is less than t . To improve security of chaff generation scheme these points are chosen such that it lies on fake polynomial.

This creates the false impression of genuine image points [9].

D. GEOMETRIC HASHING

The alignment problem is also handled by another method i.e. geometric hashing technique. In this approach the transformed template is aligned automatically. This technique uses hash table for fingerprint matching and verification purposes. The enrolment stage stores the transformed version of templates in the hash tables. In the verification stage, after aligning the input query it is matched against hash table values. For every recorded pair a vote is collected. The slot getting maximum number of votes is taken as matching candidate [10][11].

V. RECENT WORK ON ITS IMPLEMENTATION

Another approach for alignment is that instead of using hash tables, prealignment can be resolved by using only properties intrinsic to minutiae sets. The role of these structures in matching algorithms is to align the enrolment and verification minutiae sets. Three structures used for alignment are Five Nearest neighbour, Voronoi Neighbour and Triangle Based structures. Out of these triangle based structures has proved as efficient structures for alignment. But it has certain limitations. Firstly need to construct a vault for every structure, secondly the value of N is required to be

determined to ensure atleast one structure leads to unlocking of the vault where N is the no. of particular structures and the value of N may reveal too much information [12].

Peng Li and Xin Yang laid emphasis on the alignment of the transformed template but have no alignment algorithm and propose alignment free system. The problems in using alignment scheme explicitly is that alignment data should not leak any information, may reduce the security of the system and moreover not much effective in real time systems. The features selected for alignment free fuzzy vault need to be invariant to rigid transformation and not leak any significant information. So preffably minutiae descriptor and minutiae local structures are used. In this technique no alignment is used at all and the security lies in only chaff points. The features used are fused with three different rule to encode and decode alignment free fuzzy vault. Among three fusion strategies sum rule works best. In this case hash check is used instead of CRC [13].

VI. RECENT WORK ON ITS PREFORMANCE

Hiroaki Kikuchi, Yasunori Onuki and Kei Nagai worked on decoding which is complex because it makes necessary to test all possible combinations of minutiae detected from query to reconstruct polynomial and decreases the effectiveness of the performance. The basic idea is to assign index to each minutiae and then rearrange them and perform error-correction by using Reed Solomon Code. No exhaustive search is required as in previous decoding. The error correcting blocks decides the performance of scheme. As their no. increases, the randomness increases and also the performance [14].

The chaff generation portion is the most computationally intensive part of the whole system. This paper addresses that problem. It proposed algorithm which is based on circle packing theorem which is less intensive than existing methods. The existing system uses Euclidean distance but the proposed method uses geometrical mathematical theorem. In this scheme instead of circle square is used. The chaff points are generated by simply comparing distance between selected chaff point and neighbouring genuine points or chaff points. It uses simple operation like $+$, $-$ as compared to square and square root so decreases the consumption time. But this scheme increases the uniformity among genuine points and chaff points [15].

VII. SECURITY IMPROVEMENT

To increase the security of the fuzzy vault proposed a technique by Peng Li and Xin Yang is integrating

minutiae's local ridge orientation information. In this scheme following things are introduced

- (i) Minutiae descriptor is used to derive invariant values. Then these descriptor are transformed into deformation domain using these invariant values (translation and rotation)
- (ii) Transformation amount is measured by using designed changing function for each minutiae and changing function is generated using Hermit's interpolation.
- (iii) A two factor authentication is used, a password and a fingerprint.
- (iv) Invariant value corresponding to each minutia is input to changing function whose output determines the transformation.
- (v) Invariant value is determined from the password given by the user and minutiae descriptor.
- (vi) In decoding fingerprint and password both are required. If the password is known then it is less risky new password is issued. But if fingerprint is known then it creates issues. But new vault using another transformation version of image is forward and new password is assigned. So this deals with the irrevocability of the biometric template [16].

Another method proposed for applying the fingerprint having a few minutiae to the fuzzy vault and along with it enhancing the security to implement a practical fuzzy fingerprint vault with multiple polynomials in the locking process in using only one polynomial. That is, each real minutiae is projected on the two different polynomial $p1(x)$ and $p2(x)$. Since these two polynomials are independent of each other, it is difficult for an attacker to generate the two polynomials correctly. Chaff minutiae also have two y values that do not lie on both $p1(x)$ and $p2(x)$ in the proposed method [17].

Another technique is to encrypt Fuzzy Vault. The secret key is encrypted by the key derived from a set of random data in locking phase. Then these data are encoded on the fingerprint minutiae. At last, the minutiae are encrypted by the private list. To construct the vault, instead of generating many chaff points, we use a private list to encrypt the locking data units randomly and less storage is required, but the higher level of security is achieved [18].

The proposed hybrid cryptosystem improves the matching performance as well as security of the vault. The technique incorporates minutiae descriptors which capture ridge orientation and frequency information in a minutia's neighbourhood. Instead of explicitly storing the minutiae descriptors in the vault, the ordinate values

corresponding to the minutiae are encrypted using the associated minutiae descriptors. Due to the intra- user variations in the minutiae descriptor values, standard cryptographic algorithms such as the (AES) cannot be used. Therefore, another bio-crypto algorithm called the fuzzy commitment technique is used to associate the ordinate value which in turn serves as the key with a minutia descriptor. Since only actual matching descriptors will be able to “decrypt” the ordinate values rather than a non-matching descriptor and hence decode fuzzy vault correctly [19].

VIII. CONCLUSION

Various mathematical methods have been used to implement fuzzy vault in better way. Some method focussed on practicality in system and how to make it efficient as real time application and some methods increased the performance of the system by increasing GAR and FRR rate. But still there are issues to be solved more importantly regarding the security of this system. Researchers are working in this direction to resolve this issue and to emerge with more efficient and secured fuzzy vault biometric cryptosystem.

REFERENCES

- [1] Juels A and Sudan M, “A fuzzy vault scheme,” in Proc. IEEE Int. Symp. Inform. Theory, Lausanne, Switzerland, 2002, p. 408.
- [2] Clancy T, Lin D, and Kiyavash N, “Secure smartcard-based fingerprint authentication,” in Proc. ACM SIGMM Workshop on Biometric Methods and Applications, Berkley, CA, Nov. 2003, pp. 45–52.
- [3] Yang S and Verbauwhede I, “Automatic secure fingerprint verification system based on fuzzy vault scheme,” in Proc. IEEE ICASSP, Philadelphia, PA, Mar. 2005, vol. 5, pp. 609–612.
- [4] Uludag U, Pankanti S, and Jain A.K, “Fuzzy vault for fingerprints,” in Proc. Audio- and Video-Based Biometric Person Authentication, Rye Town, NY, Jul. 2005, pp. 310–319.
- [5] Uludag U and Jain A.K, “Securing fingerprint template: Fuzzy vault with helper data,” in Proc. CVPR Workshop Privacy Research Vision, New York, Jun. 2006, p. 163.
- [6] Nandakumar K, Jain A K and Pankanti S, "Fingerprint-based fuzzy vault: implementation and performance," IEEE Trans. Information Forensics & Security, 2(4):2007, pp. 744-757,
- [7] Nagar A., Nandakumar K., Jain A.K., Securing fingerprint template: Fuzzy vault with minutiae descriptors. In: Internat. Conf. for Pattern Recognition, Tampa, 2008
- [8] Kanak A, Sogukpinar I, Fingerprint hardening with Randomly Selected Chaff Minutiae, CAIP Springer, 2007, pp. 383-390
- [10] Chung Y, Moon D, Lee S, Jung S, Kim T, and Ahn D, “Automatic alignment of fingerprint features for fuzzy fingerprint vault,” in Proc. Conf. Information Security Cryptology, Beijing, China, Dec. 2005, pp. 358–369.
- [11] Moon D, Lee S, Chung Y, Pan S B, Moon K, Implementation of Automatic Fuzzy fingerprint Vault, IEEE 2008
- [12] Jeffers J, Arakala A, Fingerprint Alignment for a Minutiae-Based Fuzzy Vault, IEEE, 2007
- [13] Li P, Yang X, Cao K, Tao X, Wang R, Tian J, An Alignment-free Fingerprint Cryptosystem based on Fuzzy Vault Scheme., Journal of network and Computer Applications, 2009 pp. 207-220
- [14] Kikuchi H, Onuki Y and Nagai Kei, Evaluation and Implement of Fuzzy Vault Scheme using Indexed minutiae, 2007, IEEE
- [15] Khalil-Hani M, Bakhteri R, Securing Cryptographic Key with Fuzzy Vault based on a New Chaff Generation Method, 2010, IEEE, pp.259-265.
- [16] Li P, Yang X, Cao K, Shi P, and Tian J, Security-Enhanced Fuzzy Fingerprint Vault Based on Minutiae’s Local Ridge Information 2009, ICB 2009, LNCS 5558, pp. 930–939
- [17] Daesung Moon, Woo-Yong Choi, Kiyong Moon, Fuzzy Fingerprint Vault using Multiple Polynomials, 2009, IEEE, Page(s): 290 – 293
- [18] Feng Quan, Su Fei and Cai Anni, Encrypted Fuzzy Vault Based on Fingerprint, Beijing, China, International Conference, 2009, , Page(s): 137 – 140
- [19] Abhishek Nagar ,Karthik Nandakumar , Anil K. Jain ,A hybrid biometric cryptosystem for securing fingerprint minutiae templates ,a Michigan State University, 2009, Pages 733-741.



Constraint Optimised Path Tracking for Social Robots

Kumar Ayush & Navin Kumar Agarwal

Electrical and Electronics Engineering, Birla Institute of Technology, Mesra, Ranchi, India

Abstract - The paper gives a mathematical model to efficiently implement social constraints in mobile robots and accordingly control its' tracking. A generalized constraint set including minimizing distance, obstacle avoidance, social avoidance, personal space and their applications such as real time planning, person detection and tracking are demonstrated hereby. Social conventions are implemented using weighted constraint method resulting in human-like behavior. Related simulation-based experiments, performed for verification of the conclusions drawn, are suitably described.

Keywords - Human robot interaction, tracking, social robot, mapping, motion planning, obstacle detection

I. INTRODUCTION

Most traditional robots consider all the obstacles alike for their path planning. With this paper we give a methodology to distinctively identify any person based on algorithms as mentioned further for social robots. Also traditional robots have been considered insensitive to social conventions which points towards a considerable scope for research and development to instill human like behavior in robots. e.g. - a robot might be conventionally expected to move being towards the left side of the path when in an environment where it works along with humans [1]. The algorithms previously developed for producing conventional behavior generally did not result in a precise social behavior [2]. Also they are typically not extensible to further constraints. Some common errors in traditional robots include halting amidst its path, processing delay leading to path blockage and colliding with people in unanticipated situations.

In our method we represent social constraints as mathematical cost functions [3] which are appropriately weighted to produce a balanced response set by the robot. An important aspect of our work is combination of path planning with social convention [4]. E.g. if there is a crowded path full of obstacles then the robot looks for alternative paths to reach its destination. This behavior can be attributed as human-like. The robots reacting in accordance to the defined cost functions are considered to be socially correct. Hence we have simulated and implemented basic human behavior which is globally recognized into mobile robots.

A proper emphasis on efficiency constraints is laid with respect to generic parameters as well as social parameters. The rest of the paper demonstrates modeling for individual constraints. Following it are our

experiments with conclusive observations in accordance with the methodology followed. The applications and future works are thereafter mentioned encouraging further research in this area.

II. ORIGIN AND APPROACH

The main aim of this research is to give socially acceptable behavior to robots while interacting with people. The normal navigation of the robot change by providing specific constrains to make it a social robot. These constrains are derived from different field including social psychology [4], path planning, obstacle avoidance [5] and human-robot collaboration.

We are interested in our robot working in human environment with humans, for this we need to know how humans behave. The robot's behavior is drawn from human sociology. Humans follow many social conventions such as keeping fixed distance while walking, walking left in a pathway [6].

Types of distances	Distances (in cm)	
	Close phase	Far Phase
Intimate distance	0-15	15-46
Personal distance	46-76	76-120
Social distance	120-210	210-370
Public distance	370-760	760 or more

Table 1 : Proxemic distance data

The concept of proxemics (the study of measurable distances between people as they interact) [7] can be

implemented in social robots. The proxemics distances can be observed from the TABLE I. The shape and size of personal space changes with changed situation.

A person-tracking [8] system was designed and two people were analyzed and studied how people walk in pairs.

Person tracking is important for a social robot to distinguish between normal obstacles and persons. Our tracker is similar to that of Topp and Christensen (2005) [9].

The algorithm used for tracking person is that the scanned image is divided into segments; if the distance between points is less than 10 cm then it is considered as same segment. Similarly if the points are more than 3 m apart they are discarded. The potential legs are the segments with width greater than 20 cm and less than 60 cm. If two such leg segments are separated less than 40 cm then they are classified as a person else potential leg is classified as potential person. Potential persons are tracked with standard particle filter algorithm [10]. This algorithm is robust and can track person coming toward or away from the robot. The robot sensors must be reliable enough for tracking a person in order to remain useful and keep safety of people. The robot must ensure the person's safety at all the times and maintain distance from person. The scanning laser range-finder was used to track people.

III. STRUCTURE

Social behavior is a mindset and it is not absolute or rule that must be followed. Instead social conventions are flexible. We are using cost functions to model social convention similar to the way as humans do unknowingly.

A. Approximate path tracker

For the social robot to navigate like people it must have an approximate path plan to the destination. This plan neglects smaller obstacles and moving persons. It takes into account larger obstacle e.g. If there is crowd in the pathway, the robot has two paths either it can trace its shortest part dogging through the crowd which is difficult and may lead to mission failure else it can follow a different new path without the hallway. To produce human like path navigation heuristic planner A* [11] with cost functions is used for task and social convention implementation.

B. Constraints and cost functions

Constraints may be hard with absolute limits or soft with variable limits which may be neglected. A cost function is a mathematical function whose value can be optimized to a lower value. Soft constraints can be mathematically collected into cost function. The

constraints have two aspects task and social. The minimizing distance and obstacle avoidance are tasks of travelling to goal. The remaining ones are related to social aspect of travelling like person avoidance, default velocity, inertia.

1) *Optimizing Distance* : To save time and energy people take short cuts and often take the shortest path possible. Thus, one part of robots objective should be to minimize overall path length.

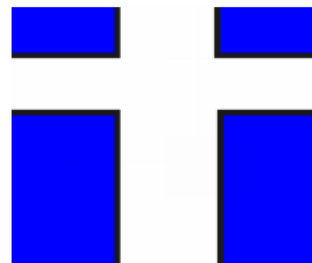
Distance used as heuristic function for the A* planner is :

$$h_{\text{distance}}(s) = \sqrt{(s_{\text{goal}} \cdot x - s \cdot x)^2 + (s_{\text{goal}} \cdot y - s \cdot y)^2}$$

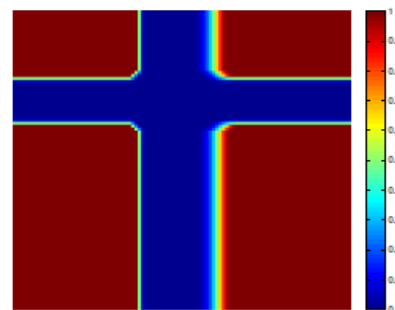
2) *Obstacle Avoidance* : Obstacle avoidance technique involves two aspects: a hard constraint against colliding with obstacles and a function to avoid coming too close to things.

a) *Hard Constraint* : The robot is constrained not to collide with stationary objects and walls.

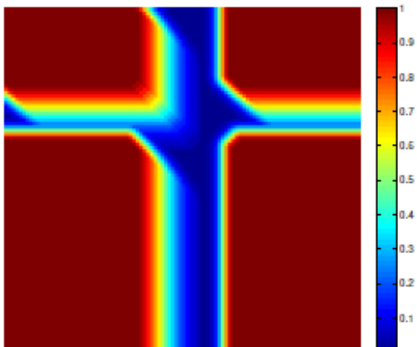
b) *Buffer Constraint* : The robot should keep a safe distance from the obstacles. The cost for this varies in accordance with the speed and angle of approach. This creates a buffer around the obstacle for the robots safety.



(a) Map of simple environment, composed of intersecting pathways



(b) Obstacle buffer cost for the simple map shown in (a), for the robot travelling at a velocity of 0.3 m/s at $\alpha = 0$ (i.e., to the right).



(c) Obstacle buffer cost region for the simple map shown in (a), for the robot travelling at 1 m/s at $\alpha = 3\pi/4$ (i.e., towards the upper left-hand corner).

Figure 1. Shows how the obstacle buffer changes with angle of robot's velocity, obstacle buffer cost region for two robot velocities and directions, where the shading corresponds to the cost of encountering that spot on the map. Furthermore, the robot's direction of travel influences the width of the cost region, so that the robot incurs a higher cost when driving directly toward an obstacle rather than alongside one

3) *Human Avoidance* : With obstacle avoidance, robot also has to avoid person. These are different category of obstacle having hard constrains and other cost functions.

a) *Absolute Avoidance* : The robot must never plan a path through a person. The robot should reject the paths intersecting with people's path.

b) *Personal Space* : Proxemics is the space around the person. It is not constant and differs across cultures and changes with situations and speed of walking.

The personal space can be modelled as two halves of 2D Gaussian functions [12]: an elliptical from the front and symmetrical from the behind. Figure 2 shows the cost function for a person moving along the positive Y-axis, either a relative velocity of 1 m/s toward the robot.

c) *Pass on Left* : When approaching a person travelling in the opposite direction, according to Indian conventions, people typically avoid collision by moving left. This can be modelled by increasing the cost to the left. As with personal space, the convention to pass the left can be modelled as a mixture of Gaussian functions, as shown in Figure 3.

4) *Default Velocity* : The robot should keep constant velocity. Changes to the default velocity should result in cost to the robot; it should have to trade between slowing and travelling greater distances around a person or obstacle. This cost is proportional to the absolute

difference between the chosen velocity and default velocity.

5) *Inertia* : The robot should prefer to move in a straight line.

IV. IMPLEMENTATION

In implementation, we used many methods for path tracker, person-tracking and robot navigation. The following will through some light on the methods used:

1) *Path Tracking*: The reaction time of the robot should be very fast. A plan to the goal should be generated as soon as the environment conditions change in order to ensure a safe, low cost path plan.

We use the heuristic planner A* to produce paths.

a) *Variable Grid* : Rather than planning on single resolution grid, our approach uses variable grids of decreasing resolution. The plan needs to be of high resolution near the robot and less resolution away from the robot.

b) *Objective Function* : All the constrains must be put in a single function for the A* planner to work. We combine each cost function with linear waiting for each constraint. The total cost can be defined as:

$$y = \sum p_i \cdot f_i(y)$$

Where $f_i(y)$ is the action cost of constraint I and p_i is the weight associated with that constraint. Additional constraints can be added in a similar fashion.

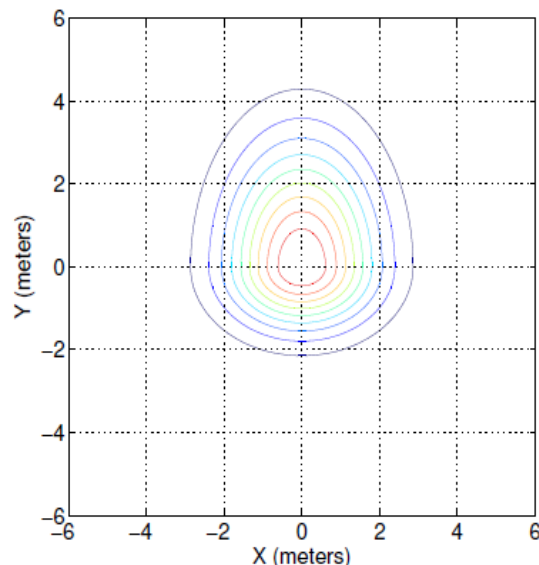


Fig. 2(a) : Personal space cost for a person moving at 1.0m/s along the positive Y axis.

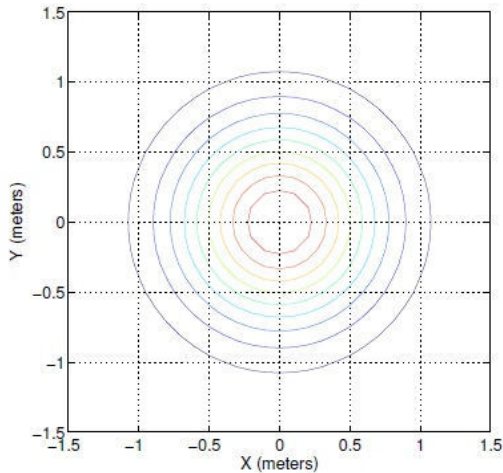


Fig. 2(b) : Personal space cost for a stationary person. The cost function is symmetrical because the robot cannot reliably detect person's orientation.

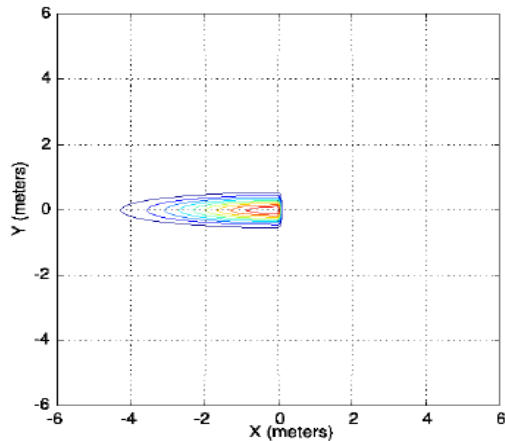


Fig. 3 : Contour map. Tends to the left cost for a person moving along the positive y axis (up). The person is centred at (0, 0). The robot can freely pass on the person's right. But incurs a cost for travelling on the person's left.

2) *Person tracking*: We use laser-based person-tracking method similar to that of Topp and Christensen (2005). The tracker is modified to use map of the environment and better smooth the tracked velocities.

a) *Map-based tracking*: It is assumed that the robot has an earlier map of the environment. The robot scans to find the changes as obstacles or persons.

b) *Velocity smoothing*: Because several of the social constraints in our framework depend on the person's direction of travel. For the robot to know persons velocity we use a linear least-squares regression on the person's tracked positions over time.

3) *Tracking*: Paths are framed continuously, and the robot is expected to update its navigation map accordingly. The Pure Pursuit path-following algorithm [13] is used along with mapping, to redirect the robot in case it travels off in stray directions or new path is framed.

V. RESULT

Carmen simulator has been used to simulate all our works. We simulate a round robot that uses scanning laser range finder. Virtual people are created by adding pair of legs. Real world environment is generated by the simulator as noise added to the readings of the scanner.

Experiments were conducted to verify the implementation of the algorithm.

Experiment: The experiment is performed to observe the path tracking of the social robot influenced by the destination and the obstacles, obstacles may be human or non human and maybe stationary or moving. The moving obstacle may or may not follow the social convention of moving towards the left when crossing. The pathway is broad enough for the robot to pass on either side of the obstacle.

In most of the cases the robot moved to the left when it faced people in its path which is socially correct in accordance with the Indian convention. 70 percent of the time robot behaved in this correct manner. When the person was travelling on the wrong side i.e. the right side, the robot should have turned to its right to avoid the person. Unexpected behaviour was observed when a person was standing towards the left of the robot, and the robot in forward motion.

VI. INFERENCE

From the above experiments, the robot is observed to follow social conventions as expected such as left alignment along the path, maintenance of buffer distance from obstacles including humans. It conforms to optimum speed with respect to human and non human obstacles accordingly. In order to reduce overall costs, the robot may choose different paths even when minor changes are made to the robot's speed or person's position.

Constant weights were used for the different cost functions. In case we want to considerably increase the cost of *pass on left*, the robot mostly moves towards the left and may not choose the shortest path. Thus by varying the weights, different constraints can exemplified accordingly. Further studies are under progress with exceptions being added by varying the number of person and their speed.

VII. CONCLUSION

Human social conventions are hereby successfully represented by mathematical cost functions and the robot traces its path accordingly and so they are recognized by the people as social. We have hence emphasized on technology to distinguish humans from other obstacles and suitably work the robot according to social conventions. This research developed a method for socially acceptable and preferred path tracking for robots. This can be further utilized for more effective human environment interactions.

We believe this adaptation of robots to human environment can be a boon to robot's flexibility and efficiency in future applications. This work will be beneficial for futuristic robots working more closely to human sensitivities.

VIII. FUTURE PROSPECTS

There is a need for improving search speed and person tracking. These limitations arise during implementation and are not fundamental to the overall framework. We believe that a wide variety of other social tasks can be implemented using this method. Robots with different behaviour can be developed using definite constraint weights.

ACKNOWLEDGEMENT

We appreciate the comments and suggestions of our Robotics professor Dr. Vijaylakshmi and Department Head Dr. T. Ghosh who supported our work in futuristic technologies.

REFERENCES

- [1] Olivera, V. M. and Simmons, R. (2002). Implementing human-acceptable navigational behavior and a fuzzy controller for an autonomous robot. In Proceedings WAF: 3rd Workshop on Physical Agents, Murcia, Spain.
- [2] Prassler, E., Bank, D., and Kluge, B. (2002). Key technologies in robot assistants: Motion coordination between a human and a mobile robot. Transactions on Control, Automation and Systems Engineering.
- [3] Bradley, S.; Hax, A.; Magnanti, T. (1977). Applied mathematical programming. Addison Wesley.
- [4] Patterson, M. L., Webb, A., and Schwartz, W. (2002). Passing encounters: Patterns of recognition and avoidance in pedestrians. Basic and Applied Social Psychology.
- [5] Marcelo Becker, Carolina Meirelles Dantas, Weber Perdigão Macedo, Obstacle avoidance Procedures for Mobile Robots, 18th International Congress of Mechanical Engineering.
- [6] Ducourant, T., Vieilledent, S., Kerlirzin, Y., and Berthoz, A. (2005). Timing and distance characteristics of interpersonal coordination during locomotion. Neuroscience Letters.
- [7] Hall, E. T. (1974). Proxemics. In Weitz, S., editor, Nonverbal Communication: Readings with Commentary, pages 205–227. Oxford University Press, New York.
- [8] Schulz, D., Burgard, W., Fox, D., Cremers, A.B.: Tracking multiple moving targets with a mobile robot using particle filters and statistical data association. In: IEEE Intl. Conf. on Robotics and Automation (ICRA). (2001)
- [9] Topp, E. A. and Christensen, H. I. (2005). Tracking for following and passing persons. In Proceedings of the IEEE/RSJ International Conference on Intelligent Robots and Systems (IROS), pages 70–76, Edmonton, Alberta, Canada.
- [10] Gockley, R. (2007). Developing spatial skills for social robots. In Proceedings of the AAAI Spring Symposium on Multidisciplinary Collaboration for Socially Assistive Robotics, pages 15–17, Palo Alto, CA.
- [11] Hart, P. E.; Nilsson, N. J.; Raphael, B. (1972). "Correction to "A Formal Basis for the Heuristic Determination of Minimum Cost Paths"". SIGART Newsletter 37: 28–29.
- [12] Arulampalam, S., Maskell, S., Gordon, N., and Clapp, T. (2002). A tutorial on particle filters for on-line non-linear/non-Gaussian Bayesian tracking. IEEE Transactions of Signal Processing, 50(2):174–188.
- [13] R. C. Coulter, "Implementation of the pure pursuit Path tracking algorithm," Robotics Institute, Carnegie Mellon University, Pittsburgh, PA, Tech. Rep. CMU-RI-TR-92-01, Jan. 1992.



An Application of MATLAB/SIMULINK for Speed Control of DC Series Motor using IGBT-DIODE Bridge

Joy Bandopadhyay, Swaraj Banerjee & Suman Ghosh

Electrical Engineering Dept., Dr. B.C Roy Engineering College, Durgapur, India

Abstract - This paper aims at employing an IGBT-DIODE bridge for speed control of dc series motor as well as simulating the power flow from source to load as well as from load to source but without impairing the performance of dc series motor. The mechanical input used for motor is torque which is applied in a step increasing form. In case of dc series motor when load is increased its speed and torque get affected but with the help of this simulink circuit a controlled operation is obtained which not only makes sure that in spite of increase in load the motor's speed increases and settles down to become constant as well as its output torque but also the motor can be used as generator if an application of that sort is required.

I. INTRODUCTION

Industrial applications nowadays have become increasingly complex and demanding. In the field of drives, power systems, power electronics, machines, controls all of them need to be workable, efficient. Before installing these in industries that is the practical models they are basically tested with the help of hardware as well as software integration. Simulink is highly versatile software which is used to simulate many industrial applications relating to electrical as well as electronics technologies. This paper aims at controlling the speed of dc series motor with the help of an IGBT-DIODE bridge and as well as provide generator action for the dc series motor with the help of simulink. Simulink, an add-on product to MATLAB, provides a graphical, interactive environment for modeling, simulating, and analyzing of dynamic systems. It makes sure of rapid construction of virtual prototypes to explore design concepts at any level of detail with minimal effort [2]. For modeling, Simulink provides a graphical user interface (GUI) for building models as block diagrams. It includes a comprehensive library of predefined blocks that can be used to develop graphical models of systems using drag-and-drop mouse operations. It supports linear and nonlinear systems, modeled in continuous-time, discrete time sampled time [3]. The user is able to produce an up-and-running model that would basically require hours or days or may be even longer to build in the laboratory environment. The interactive nature of Simulink encourages users to try out several things like instant changing of parameters, replacement of blocks, changing

configuration of the circuits, and several other things within very short period of time and also see out the consequences and results instantly. Even through these techniques students can learn efficiently with frequent feedback. Simulink enables proper coordination between the circuit and MATLAB program thereby ensuring controlling of block and parameters if so required

II. DC SERIES MOTOR

The DC series motor provides high starting torque and is able to move very large shaft loads when it is first energized. Figure 1 shows the wiring diagram of a series motor. From the diagram it's obvious that the field winding in this motor is connected in series with the armature winding. This is the feature that gives the series motor its name. The field is made from heavy-gauge wire that is large enough to carry the load as the series field winding is connected in series with the armature, it will carry the same amount of current that passes through the armature. For this reason the wire gauge is so large, the winding will have only a few turns of wire. In some larger DC motors, rather than conventional round wire used for power distribution the field winding is made from copper bar. The square or rectangular shape of the copper bar stock makes it fit more easily around the field pole pieces. It can also radiate more easily the heat that has built up in the winding due to the large amount of current being carried. Since the series field is made of large conductors, it can carry large amounts of current and produce large torques. The amount of current that passes

through the winding determines the amount of torque the motor shaft can produce. For example, the starter motor that is used to start an automobile's engine is a series motor and it may draw up to 500 A when it is turning the engine's crankshaft on a cold morning. Series motors used to power hoists or cranes may draw currents of thousands of amperes during operation.

III. CIRCUIT DESCRIPTION

Here a 200 H.P. dc series motor rated 550V 1750 r.p.m. (revolutions per minute) field voltage 150V is used. A pulse generator is used for triggering of the IGBTs. The pulses are fed to the individual gate terminals of the IGBTs as per fig 1. The function of a switch is to Pass through input 1 when input 2 satisfies the selected criterion; otherwise, pass through input 3. The inputs are numbered top to bottom (or left to right). The input 1 pass-through criteria are input 2 greater than or equal, greater than, or not equal to the threshold. The first and third input ports are data ports, and the second input port is the control port [1]. Here the threshold value is 0.5. Here the load applied to the series motor is increased in step form. Now as per this circuit configuration there will be two modes of current obtained positive as well as negative and the target is to make sure that motor speed rises and becomes constant at the end of simulation time 4 secs in spite of step increase in motor's mechanical torque input. Here collector voltage is 550v dc. Simulation is started and IGBTs Q1 and Q4 operate together (fig 5 and fig 6) to maintain positive armature current of 0.9 amperes at 0.5 secs, (fig 3) and when they are turned off this positive current freewheels and linearly drops to 0 at 0.66 secs and reverses through diodes D2 and D3 (fig 7 and fig 8). Up to 0.66 secs of time speed of motor rises up to 1.5 r.p.m. (fig 2) and the torque output of the motor rises up to 2 Nm up to 0.5 secs (fig 4) the period during which armature current stays positive, and after 0.5 secs when armature current starts dropping towards zero the torque output of the motor starts dropping and reaches zero at 0.66 secs the period at which the armature current of the motor becomes zero and starts reversing as IGBTs Q2 and Q3 (fig 9 and fig 10) come into operation maintaining negative current and diodes D1, D4 direct the output current from load to source (fig 11 and fig 12) which finally settles down to -1.7 amperes. Now after 0.66 secs the motor armature current reverses in negative direction but speed of series motor continues to rise after a brief interval, had it been a shunt motor the speed and torque of motor would have followed the current to become negative but for applications requiring speed and torque to remain in same direction series motor is chosen where speed of motor continue to follow up in the same direction even after the armature current reverses. Therefore the torque after reaching

zero at 0.66 secs starts rising up in the positive direction alongside with the speed whereas the armature current has already reversed with the mechanical torque input being raised in step time of 0.1 secs. The torque output reaches 7.3 Nm at 3 secs and becomes constant settling down at 7.3 Nm with the speed of motor rising and settling at 60.1 r.p.m. So when the motor feeds back the armature current to source it can be used as generator too.

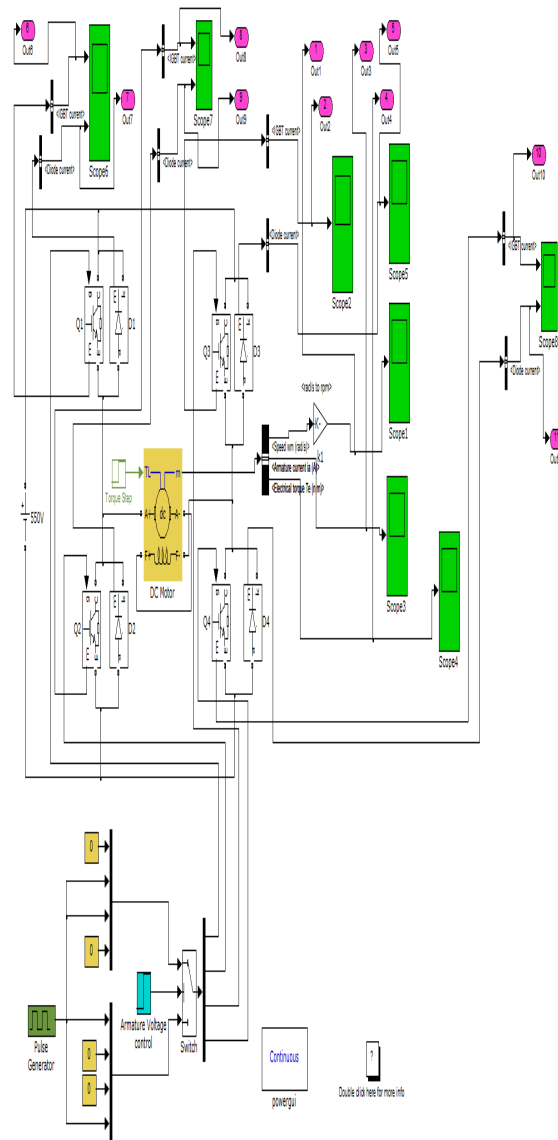


Fig. 1 : Simulink model of IGBT-DIODE Bridge for speed control of dc series motor

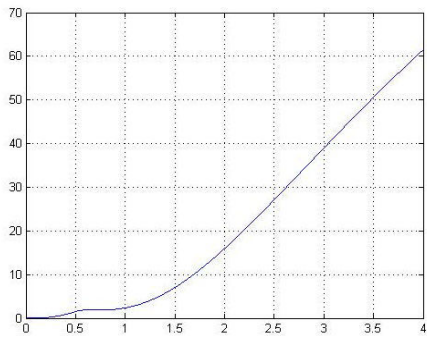


Fig 2. Speed of DC series motor.

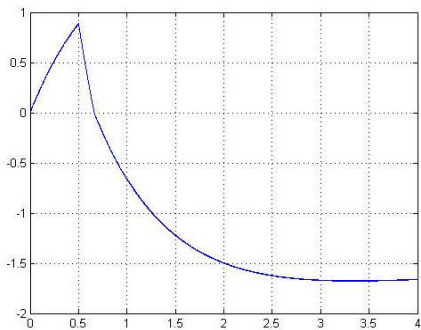


Fig. 3 : Armature current of DC series motor.

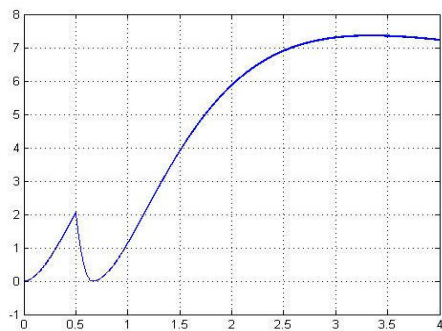


Fig. 4 : Electrical torque of DC series motor

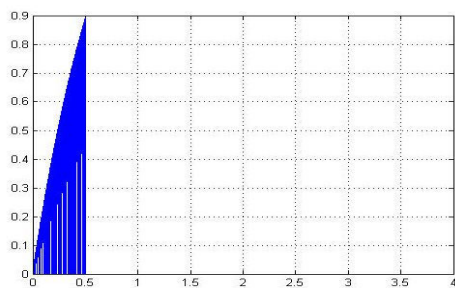


Fig. 5 : IGBT Q1 current.

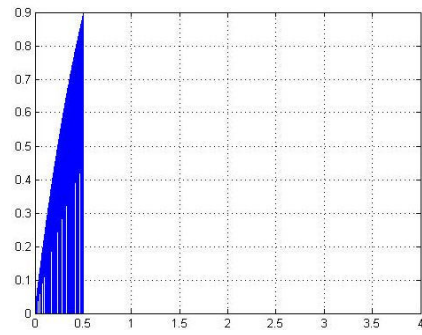


Fig. 6 : IGBT Q4 current

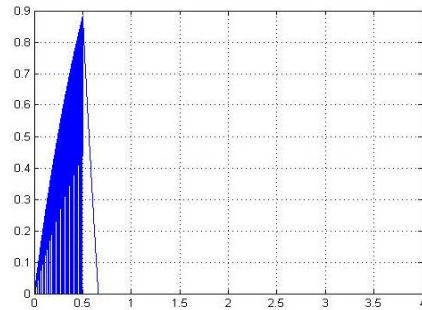


Fig. 7 : DIODE D2 current

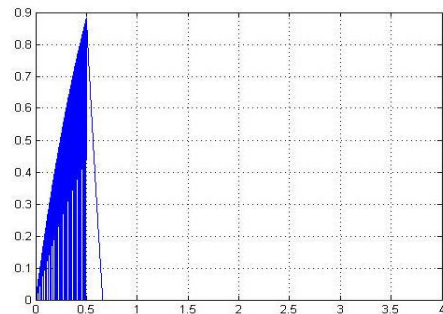


Fig. 8 : DIODE D3 current.

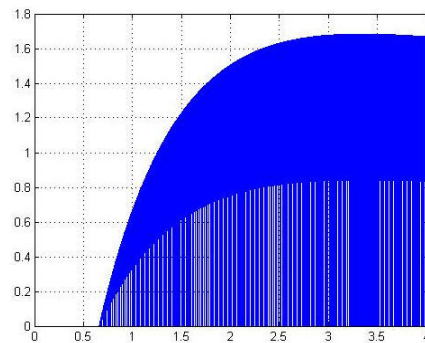


Fig. 9 : IGBT Q2 current.

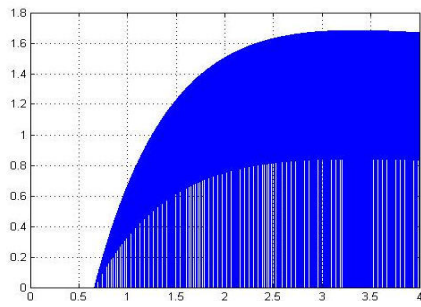


Fig. 10 : IGBT Q3 current.

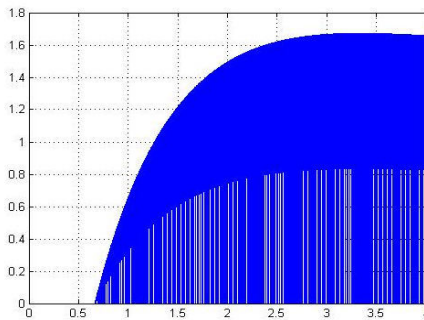


Fig. 11 : DIODE D1 current

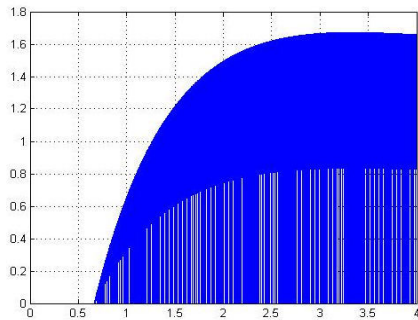


Fig. 12 : DIODE D4 current.

IV. OBSERVATION TABLES

A. Time (t) Vs Speed (N)

Time t (secs)	Speed N (r.p.m)
0.0	0.0
0.5	1.5
1.0	1.6
1.5	9.0
2.0	18.5
2.5	29.0
3.0	39.5
3.5	50.0
4.0	60.1

B. Time (t) Vs Torque (T)

Time t (secs)	Torque T (Nm)
0.0	0.0
0.5	2.0
1.0	1.0
1.5	4.0
2.0	5.9
2.5	7.0
3.0	7.3
3.5	7.3
4.0	7.3

V. ABBREVIATIONS AND ACRONYMS

- Revolutions per minute (r.p.m.)
- Newton meter (Nm).
- Time in (secs).

VI. CONCLUSION

As per this paper the circuit configuration can be used for dc series motor to continue to run in same direction with constant speed. The motor doesn't reverse its direction after current through both armature and field reverses and continues to run in same direction. This type of circuit configuration enables better speed control of dc series motor as well as its torque and armature current control. If desired can be used to act as generator and provide supply to a dc motor.

VII. ACKNOWLEDGEMENT

It is with our deepest gratitude and appreciation which we offer to our respected Professor Sushanta Dutta of Dr. B.C. Roy Engineering College who's advice on the making of this paper has been of great help.

REFERENCES

- [1] SIMULINK, Model-based and system-based design, using Simulink, Math Works Inc., Natick, MA, 2000.
- [2] SimPowerSystems for use with Simulink, users guide, Math Works Inc., Natick, MA, 2002.
- [3] Leonhard, W., Control of Electric Drives. New York, Springer-Verlag, 2001.
- [4] Bimbhra, P.S., Power Electronics. New Delhi, Khanna Publishers, 2006.
- [5] Mohan, Ned, Power Electronics, John Wiley and Sons, 1989.

□□□

Implementation of Probabilistic Neural Network using Approximate Entropy to Detect Epileptic Seizures

Sachee¹, Roohi Sille², Garima Sharma³ & N. Pradhan⁴

^{1,2&3}Dept. of Biomedical Engineering, Bundelkhand University, Jhansi, India

⁴Dept. of Psychopharmacology, National Institute of Mental Health and Neurosciences, Bangalore, India

Abstract - Epileptic seizures detection is largely based on analysis of Electroencephalogram signals. The ambulatory EEG recordings generate very lengthy data which require a skilled and careful analysis. This tedious procedure necessitates the use of automated systems for epileptic seizure detection. This paper proposes one such automated epileptic seizure detection technique based on Probabilistic Neural Network (PNN) by using a time frequency domain characteristics of EEG signal called Approximate Entropy (ApEn). Our method consists of EEG data collection, feature extraction and classification. EEG data from normal and epileptic subjects was collected, digitized and then fed into the PNN. For feature extraction, the wavelet coefficients are derived using Discrete Wavelet Transformation. For the feature selection stage a new methodology is proposed, which is, comparing the ApEn values of wavelet coefficients of different EEG data. The experimental results portray that this proposed approach efficiently detects the presence of epileptic seizures in EEG signals and showed a reasonable accuracy.

Keywords - *Electroencephalogram, Epilepsy, Approximate Entropy, Epileptic Seizure, Probabilistic Neural Network, Discrete Wavelet Transformation.*

I. INTRODUCTION

Epilepsy is a disorder of the brain characterized by an enduring predisposition to generate unprovoked, recurring epileptic seizures that disturb the nervous system¹. Seizures or convulsions are temporary alterations in brain functions due to abnormal electrical activity of a group of brain cells that present with apparent clinical symptoms and findings. Epilepsy may be caused by a number of unrelated conditions, including damage resulting from high fever, stroke, toxicity, or electrolyte imbalances. Nearly 1% of world's total population experience at least one seizure in its life time². Unfortunately, the occurrence of an epileptic seizure is not predictable and its process is not completely understood yet. Electroencephalogram (EEG) as a representative signal of the electrical activity of the nerve cells, has been the most utilized signal to clinically assess brain activities, and the detection of epileptic discharges. However the detection of epilepsy, which includes visual scanning of EEG recordings for seizures, is very time consuming especially in the case of long recordings. Automated diagnostic systems for epilepsy have been developed using different approaches. Earlier methods of automatic seizure detection using EEG were based on Fourier transformation which detects some characteristic waveforms that fall primarily within four frequency bands. Though useful for various EEG characterizations,

but fast Fourier transform (FFT), suffer from large noise sensitivity. Other methods like parametric method for power spectrum estimation, reduces the spectral loss problems and gives better frequency resolution. Being non stationary signals, the parametric methods are not suitable for frequency decomposition of EEG. The discrete wavelet transform is a powerful method proposed in the late 1980s to perform time-scale analysis of non-stationary signals and well suited to locate transient events like epileptic seizures².

Several workers have proposed Artificial neural network (ANN) based detection systems for epileptic diagnosis. Amplitude of EEG, Average duration, average power spectrum, dominant frequency, spike amplitude and spike rhythmicity are some of the previously described inputs to an adaptive structural neural network³⁻⁷. The method proposed by N. Pradhan *et al.*, uses a raw EEG signal as an input to a learning vector quantization (LVQ) network⁸. This paper discusses an automated epileptic EEG detection system using probabilistic neural networks (PNN), and a time-domain feature of the EEG signal called approximate entropy (ApEn) that reflects the nonlinear dynamics of the brain activity. ApEn drops abruptly due to the synchronous discharge of large groups of neurons during an epileptic activity. So, it is a suitable feature for using it in the implementation of automated detection of epilepsy⁹⁻¹⁰. ApEn is a statistical parameter

to quantify the randomness of a time series data of physiological signals. The entropy estimators are broadly classified into two categories -spectral entropies and embedding entropies. The spectral entropies use the amplitude components of the power spectrum of the signal as the probabilities in entropy calculations. It quantifies the spectral complexity of the time series. The embedding entropies use the time series directly to estimate the entropy. Approximate Entropy is a kind of embedding entropies.

In this paper, approximate entropy based epileptic detection system of wavelet transformation proposed by Muthanantha et al is used with modified approach¹¹. The methodology is applied to two different groups of EEG signals and its 5 constituent EEG sub bands. The approximate entropy of the wavelet coefficient are used to represent the time frequency distribution of the EEG signals in each sub band and PNN is used to detect epileptic EEG signals.

II. METHODOLOGY

Fig. 1 shows the flow diagram of the proposed neural network based automated epileptic detection system.

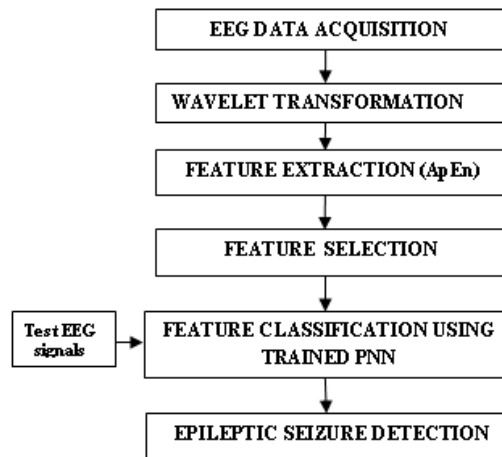


Fig. 1 : Data flow diagram of the proposed system

As shown in Figure 1 the epileptic seizure detection system consists of three main modules: a feature extractor that generates a wavelet based feature from the EEG signals, feature selection that composes composite features, and a feature classifier (PNN) that outputs the class based on the composite features.

A. EEG data acquisition:

Two sets of EEG data corresponding to the healthy and epileptic subjects collected at NIMHANS, Bangalore were used as the experimental data set for the study. The signals were analyzed in three groups: group H (healthy subjects) and group GE generalized epilepsy and EE ECT epileptic subjects. Group H contains 50 single channel EEG segments and group GE, EE in total contains 50 single channel EEG segments of 8sec duration each sampled at 128Hz. As such, each data segment contains $N=1024$ data points collected with 25 channels. Each EEG signal is considered as a separate EEG signal resulting in a total of 100 EEG signals. These data were loaded and saved in the working directory for the testing and training of PNN. The EEG data were collected using the standard electrode placement technique from the surface. Fig. 2 shows a representative signal of healthy subject and epileptic subject from each group.

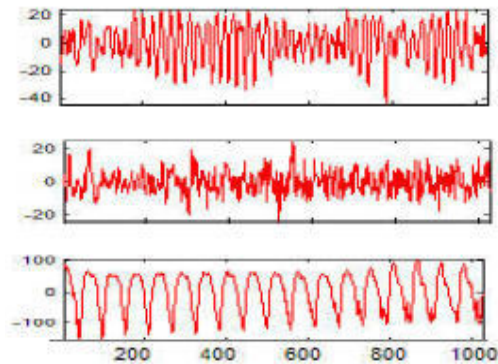


Fig. 2 : Sample unfiltered EEGs Healthy H , ECT Epilepsy EE and generalized epilepsy GE (from top to bottom)

B. Wavelet transformation:

Wavelet transform (WT) forms a general mathematical tool for signal processing with many applications in EEG data analysis. Its basic use includes time-scale signal analysis, signal decomposition and signal compression. The multi scale feature of WT allows the decomposition of a signal into a number of scales, each scale representing a particular coarseness of the signal under study. Discrete wavelet transformation (DWT) employs two sets of functions called scaling functions and wavelet functions, which are associated with low-pass and high-pass filters, respectively. The decomposition of the signal into the different frequency bands is simply obtained by successive high-pass and low pass filtering of the time domain signal. Therefore the signal can be reconstructed as a linear combination

of the wavelet functions weighted by the wavelet coefficients. The key feature of wavelet is the time – frequency localization. It means that most of the energy of the wavelet is restricted to a finite time interval. The wavelet technique applied to the EEG signal will reveal feature related to the transient nature of the signal. The wavelet transformation analyses the signal at different frequency bands, with different resolutions by decomposing the signal into a coarse approximation and detail information¹². All wavelet transforms can be specified in terms of a low pass filter, which satisfies the standard quadrature mirror filter condition. The procedure of multi resolution decomposition of a signal $x(n)$ is schematically shown in the Figure 3. The down-sampled outputs of first high-pass and low-pass filters provide the detail, D1 and the approximation, A1, respectively. The first approximation, A1 is further decomposed and this process is continued till 5th level approximation d5 is achieved. The number of decomposition levels is chosen based on the dominant frequency component in the signal. In the present study, the number of decomposition levels was chosen to be 5 as the EEG signals having epileptic seizures are extracted and saved in graphical form in .dat file after sampling at 128 Hz.

The smoothing feature of Daubechies wavelet for order 4 (Db4) made it more appropriate to detect changes of EEG signal. Hence, the wavelet coefficients were computed using db4 in present study. The proposed method was applied on all data sets; (group H, GE and EE). The EEG sub bands of a5, d5, d4, d3, d2 and d1 are shown in Figure 4.

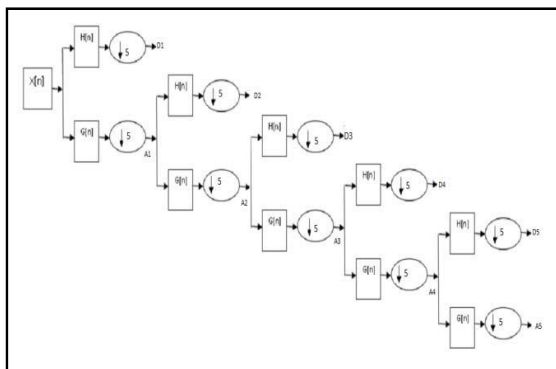


Fig. 3 : Scheme of five level wavelet decomposition

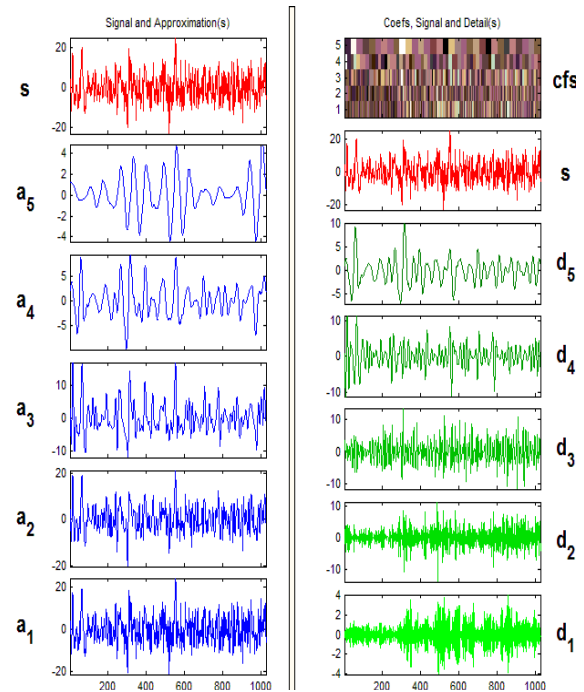


Fig. 4 : A multi resolution Wavelet Decomposition up to five levels

The detail at level j is defined at

$$D_j = \sum a_j \cdot k \cdot \Psi_j \cdot k(t)$$

And the approximation at level J is defined as

$$A_j = \sum D_j$$

It becomes obvious that

$$A_{j-1} = A_j + D_j$$

$$\text{and } f(t) = A_j + \sum_{j \leq J} D_j$$

C. Feature Extraction

The proposed system makes use of a single feature called ApEn for the epileptic detection. The ApEn is a wavelet domain feature that is capable of classifying complex systems. The value of the ApEn is determined as following^{11, 13-14}.

- 1) Let the data sequence containing N data points be $X = [x(1), x(2), x(3), \dots, x(N)]$.
- 2) Let $x(i)$ be a subsequence of X such that $x(i) = [x(i), x(i+1), x(i+2), \dots, x(i+m-1)]$ for $1 \leq i \leq N - m$, where m represents the number of samples used for the prediction.

- 3) Let r represent the noise filter level that is defined as: $r=k \times SD$ for $k = 0, 0.1, 0.2, 0.3, \dots, 0.9$ where SD is the standard deviation of the data sequence X .
- 4) Let $\{x(j)\}$ represent a set of subsequences obtained from $x(j)$ by varying j from 1 to N . Each sequence $x(j)$ in the set of $\{x(j)\}$ is compared with $x(i)$ and, in this process, two parameters, namely $C_i^m(r)$ and $C_{i+m+1}(r)$ are defined as follows:

$$C_i^m(r) = \frac{\sum_{j=1}^{N-m} k}{N-m}$$

$$\text{where } k = \begin{cases} 1, & \text{if } |x(i) - x(j)| \leq r \text{ for } 1 \leq j \leq N-m \\ 0, & \text{otherwise} \end{cases}$$

$$\text{and } C_{i+m+1}(r) = \frac{\sum_{j=1}^{N-m} k}{N-m}$$

- 5) We define $\Phi_m(r)$ and $\Phi_{m+1}(r)$ as follows:

$$\Phi_m(r) = \frac{\sum_{i=1}^{N-m} \ln(C_i^m(r))}{N-m}$$

$$\Phi_{m+1}(r) = \frac{\sum_{i=1}^{N-m} \ln(C_i^{m+1}(r))}{N-m}$$

The values of ApEn indicates the irregularity of the system as small values imply strong regularity and large values imply substantial fluctuations. In the proposed approach, ApEn is calculated for one approximation and for detailed information such as D4 and D5.

D. Feature Selection

For feature selection, we divided data into two different sets: the training set and the testing set.

In the training set we have 14 different EEG signals from channel 1 belonging to the general EEG signals and ECT EEG signals in which nZ1, nZ2, nZ3, nZ4, nZ5, nZ6, nZ7 are the normal EEG signals Z1,Z2 are generalized epileptic EEG signals and Z3,Z4,Z5,Z6,Z7 are ECT epileptic EEG signals. Now we decomposed the signal up to 5 levels and calculated the ApEn values of all the coefficients (A2,D4,D5). Hence, we get 42 ApEn values for the training set.

In the testing set there are 100 EEG signals of which there are 50 normal EEG signals, 20 generalized epileptic signals and 30 ECT epileptic signals for different odd channels. These signals were again decomposed up to 5 levels and hence the 300 ApEn values were calculated for the testing set. Table 1 shows

extracted feature (mean ApEn) for the subbands of training set.

Table 1 Feature extraction of sample data set

Set	Wavelet Sub bands	ApEn
GENERALISED EPILEPSY (GE)	A2	-0.0042
	D4	0.1430
	D5	0.31335
ECT EPILEPSY (EE)	A2	-0.0042
	D4	0.06838
	D5	0.32742
HEALTHY (H)	A2	-0.0042
	D4	0.1686714
	D5	0.3039429

E. Probabilistic Neural Network Classifier (PNN)

The classification of EEG signals into healthy and epileptic signals is done using the probabilistic neural work. The three layers of PNN are: Input Layer, the Radial Basis Layer which evaluates distances between the input vector and rows in the weight matrix, and the Competitive Layer which determines the classification with maximum probability of correctness (Figure 5). Dimensions of matrices are marked under their names.

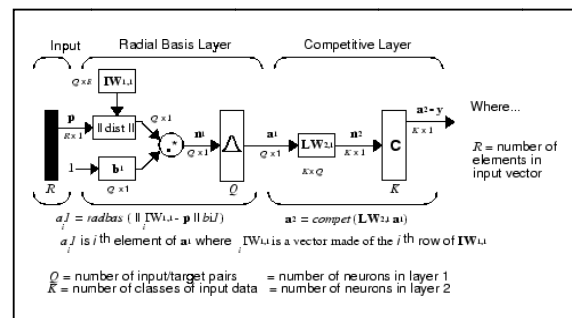


Fig. 5 : PNN Classifier

- 1) **Input layer** : The input vector, denoted as p , is presented as a black vertical bar in Figure 5. The input layer unit simply distributes the input to neurons in the pattern layer. On receiving a pattern x from input layer, the neuron x_{ij} of the pattern computes its output using the below formula

$$\phi_{ij}(x) = \frac{1}{(2\pi)^{0.5d} \sigma^d} \exp\left(-\frac{(x - x_{ij})^T (x - x_{ij})}{2\sigma^2}\right)$$

Where d denotes dimension of the pattern vector x , is the smoothing parameter and x_{ij} is the neuron vector.

2) Radial Basis Layer : In the Radial Basis Layer, the vector distances between input vector p and the weight vector, made up of each row of the weight matrix QXR are calculated. Here, the vector distance is defined as the dot product between p and the i^{th} row of W produces the i^{th} element of the distance vector matrix, denoted as $\|\mathbf{dist}\|$. The bias vector b is then combined with $\|\mathbf{dist}\|$ by an element-by-element multiplication, represented as “ \cdot ” in Figure 5. The result is denoted as $n = \|\mathbf{dist}\| \cdot b$. The transfer function in PNN has built into a distance criterion with respect to a center. In this paper, we define it as $\text{radbas}(n) = e^{-n^2}$. Each element of n is substituted into the transfer function and produces corresponding element of a , the output vector of Radial Basis Layer. We can represent the i^{th} element of a as $a_i = \text{radbas}(\|\mathbf{dist}\| \cdot b_i)$. Where W_i is the i^{th} row of W , and b_i is the i^{th} element of bias vector b .

3) Competitive Layer : There is no bias in the Competitive Layer. In this layer, the vector a is first multiplied by the layer weight matrix M , producing an output vector d . The competitive function C produces a 1 corresponding to the largest element of d , and 0's elsewhere. The index of the 1 is the class vectors. If the i^{th} sample in the training set is of class j , then we have a 1 on the j^{th} row of the i^{th} column of M . The decision layer classifies the pattern x in accordance with Bayes decision rule based on the output of all summation layer neurons using

$$\hat{C}(x) = \arg \max \{p_i(x)\}, i=1,2,3,\dots,m$$

Where \hat{C} denotes the estimated class of pattern x , and m is total number of classes in training samples. Hence, PNN employed in this work possesses 30 nodes in the input layer and 2 nodes in the output layer (the number of nodes in the output layer is the number of classifications of EEG signals). The performance of the PNN model was evaluated in terms of training performance and classification accuracies and the results confirmed that the proposed scheme has potential in classifying the EEG signals.

III. RESULTS AND DISCUSSION

ApEn values are computed for healthy, generalized epileptic and ECT epileptic signals and are fed as inputs to the two neural networks. This is achieved by using $m=3$, $r=3$ and $N=1024$ where m is no. of groups, r is similarity criterion between repetitive patterns of length m in total data points i.e. N . Among the available 100 EEG signals 21 are used for training and remaining are used for testing the performance the neural network. The potentiality of the ApEn to discriminate the two signals namely healthy, generalized epileptic and ECT epileptic EEG signals depends on the values of m , r and N . Table 2 shows the results of overall accuracy of this PNN

classifier system in detecting healthy, generalized and ECT epileptic EEG signals.

Table 2 Accuracy of PNN classifier in detecting EEG signals

Sl. N		Total	Correctly detected	Incorrectly Detected	Accuracy (in %)
1	Generalized epilepsy	20	18	2	90
2	ECT epilepsy	30	23	7	73
3	Healthy	50	34	16	68

As the table 2 shows, the designed PNN classifier has a very high accuracy of 90% in detection of generalized epilepsy whereas the accuracy for detecting healthy EEG signals was slightly lower (68%). Table shows that our wavelet based ApEn classifier has good potential in the characterization of the generalized epileptic patterns and ECT epilepsy. The results suggest that wavelet based system ApEn as the input feature is best suited for the real time detection of the epileptic seizures in less time and less computation burden. When the signals are fed to the PNN model, some are correctly detected, and some are incorrectly detected. The results of this study are based on data sets corresponding to seven different subjects only. By increasing the number of subjects the detection accuracy of the classifier may even be improved. The optimum ApEn parameter values obtained may not be useful for a generalized case where no. of subjects are large. This problem will not arise in the proposed PNN-based method as it has performed well irrespective of the ApEn parameter values used.

REFERENCES

- [1] “Epilepsy” from <http://neurology.health-cares.net/epilepsy-seizures.php>.
- [2] Hamid R. Mohseni¹, A. Maghsoudi and Mohammad B. Shamsollahi, “Seizure Detection in EEG signals: A Comparison of Different Approaches” in proceedings of 28th Annual IEEE International Conference on Engineering in Medicine and Biology Society, Aug. 30-Sept. 3 2006, pp: 6724-6727.
- [3] M.K. Kiyimik, M. Akin, and A. Subasi, "Automatic recognition of alertness level by using wavelet transform and artificial neural network," Journal of Neuroscience Methods, vol. 139(2), pp. 231–240, 2004.
- [4] E. Haselsteiner, and G. Pfurtscheller, "Using time-dependent neural networks for EEG classification," IEEE Transactions on Rehabilitation Engineering, vol. 8, pp 457–463, 2000.

- [5] J. Gotman, "Automatic recognition of epileptic seizures in the EEG, Electroencephalogram". Clin. Neurophysiol, vol. 54, pp. 530–540, 1982.
- [6] Nicolaos B. Karayiannis, Amit Mukherjee, "Detection of Pseudo sinusoidal Epileptic Seizure Segments in the Neonatal EEG by Cascading a Rule-Based Algorithm with a Neural Network" IEEE Transactions on Biomedical Engineering, vol. 53, no. 4, April 2006.
- [7] Vairavan Srinivasan, Chikkannan Eswaran, and Natarajan Sriraam, "Approximate Entropy-Based Epileptic EEG Detection Using Artificial Neural Networks", IEEE Transactions on Information Technology in Biomedicine, vol. 11, no. 3, May 2007.
- [8] N.Pradhan, P.K Sadasivan, and G.R.Arunodaya Detection of seizure activity in EEG by an Artificial Neural Network: A preliminary study. Computers and Biomedical research. vol. 29, pp. 303–313, 1996.
- [9] L. Diambra, J. C. Bastos de Figueiredo, and C. P.Malta, "Epileptic activity recognition in EEG recording," Phys. A: Stat. Mech. Appl., vol. 273, pp. 495–505, 1999.
- [10] M. Gayatri, Arun Kumar, Manish Janghu, Mandeep Kaur and T.V. Prasad. Implementation of Epileptic EEG using Recurrent Neural Network. International Journal of Computer Science and Network Security, VOL.10 No.3, March 2010. Pp 290-296.
- [11] Muthanantha Murugavel, A.S. and Ramakrishnan S. Wavelet Domain Approximate Entropy-Based Epileptic Seizure Detection, Proceedings of the 5th International Conference on Information Technology.
- [12] Guler I, Ubeyli ED. Application of adaptive neuro-fuzzy inference system for detection of electrocardiographic changes in patients with partial epilepsy using feature extraction. Expert Syst Appl; 27(3):323–30, 2004.
- [13] Subasi, A. Automatic recognition of alertness level from EEG by using neural network and wavelet coefficients. Expert Systems with Applications, 28, 701–711, 2005.
- [14] Kandaswamy, A., Kumar, C. S., Ramanathan, R. P., Jayaraman, S., & Malmurugan, N. Neural classification of lung sounds using wavelet coefficients. Computers in Biology and Medicine, 34(6), 523–537, 2004



Dynamic Channel Allocation Considering Random User Distribution and Mobility

Rushabh Vora, Sagar Tamboli, Priyanshu Shah & Sukanya Kulkarni

Department of Electronics and Telecommunication, Sardar Patel Institute of Technology, Mumbai, India

Abstract - Recently, heavy traffic in the spectrum with interference being the most prohibiting factor has given rise to the need for efficient channel assignment techniques to increase the overall system capacity. In this paper using MATLAB we provide a comparison between fixed channel allocation (FCA) and dynamic channel allocation (DCA) which attempts to allocate channels to users in such a way so that the average blocking probability and forced termination in the entire system is minimized. Further in contrast to traditional DCA schemes we have considered random user mobility and traffic variations to study forced termination probability.

Keywords - Cellular network, dynamic channel allocation, random user distribution, user mobility.

I. INTRODUCTION

The exponential increase in the number of users and the paucity of wireless spectrum poses a challenge for the technicians to increase the system efficiency so as to accommodate as many users as possible in the available limited but very precious spectrum. The increasing number of higher data rate devices clearly states that dynamic channel allocation with some innovative techniques will help solve the problem of spectrum efficiency. With these DCA schemes, spectrum will be allocated dynamically depending on need of the service and providers that in turn depends on end users' demands in a time and space variant manner. Here, each node performs rapid spectrum sensing to detect spectrum holes and distributed coordination to use them.

A. Channel allocation

A given radio spectrum can be divided into a set of disjoint or non interfering radio channels. All such channels can be used simultaneously while maintaining an acceptable received radio signal. Reliable and efficient channel allocation management as given in [1] is vital for the growth and innovation of wireless technologies and services in Next Generation Wireless Networks.

B. Types of channel allocation

Fixed channel allocation (FCA) - Here the area is partitioned into a number of different cells and a number of channels are assigned to each cell according to some reuse pattern depending upon the reuse quality. FCA schemes are very simple, however they do not adapt to

changing traffic conditions and user distribution. In order to overcome these FCA deficiencies DCA strategies have been introduced.

Dynamic channel allocation (DCA) - As opposed to Fixed Channel Allocation (FCA), in Dynamic Channel Allocation (DCA) as given in [2] there is no fixed relationship between channel and cells. All channels are kept in a central pool and are assigned dynamically to radio cells as new calls arrive in the system. In DCA as given in [3], a channel is eligible for use in any cell provided that signal interference constraints are satisfied.

C. Proposed method

In contrast to traditional call-by-call DCA schemes, where the channel assignment is based only on current channel usage conditions in the service area, in this work we considered a mobility-aware DCA algorithm in which the channel assignment is adaptively carried out using varying positions of users in the system. Also it has the main feature of reallocating a channel to an ongoing call if the quality of the communication channel decreases below certain level based on the interference level experimented at the receiver; this is made without disconnecting the call. Hence, in this paper we present work in progress about dynamic channel allocation considering the mobility of users along with interference in such a way that average blocking probability and forced termination in entire system is minimized.

II. SYSTEM MODEL

A. Interference

Interference is a fundamental nature of wireless communication systems, in which multiple transmissions often take place simultaneously over a common communication medium. It can stem from a variety of causes. Generally, the interference starts at a base-station transmitter (Tx), either from the same cellular system or from a nearby Tx. The interference can result in dropped calls, decreased receiver (Rx) sensitivity (and range), increased Rx noise figure and desensitization of receive-system active components.

Two metrics are used to evaluate system performance: Blocking probability and Forced Termination probability. The blocking probability is defined as statistical probability of losing a call either due to the lack of available channels or that available channels are experiencing too much interference. The forced termination probability is statistical probability of a call that is forced to terminate prematurely either due to non-availability of channel in new cell or excess interference on existing channel.

B. Carrier to noise interference ratio (CNIR)

The ratio between the power of the carrier signal and the power of all interfering users plus noise (CNIR) is a measurement used to determine the interference levels experienced in some point of communication link. The CNIR is calculated according the following expression:

$$CNIR = \frac{P_t d_t^{-\alpha} 10^{\frac{\epsilon_0}{10}}}{N_0 + \sum_{i=1}^k P_i d_i^{-\alpha} 10^{\frac{\epsilon_0}{10}}} \quad (1)$$

Where P_t is transmitter power, d_t is the distance between transmitter and receiver, α is an attenuation factor, the term $10^{\frac{\epsilon_0}{10}}$ denotes the loss due to log-normal shadowing, N_0 corresponds to noise power. The sum term represents the total interference due to the k users using the same channel, transmitting with a power P_i at a distance d_i from receiver. As is previously mentioned, the algorithm proposed allocates and re-allocates channels based on a measurement of interference levels and user. In this algorithm, CNIR measurement is used in order to make decisions on whether a channel can be assigned to a call or not.

C. Channel allocation to new calls

When a user requests for a channel, the base station checks for its availability. If a channel is available, the base station calculates the CNIR of the particular channel in the cell. If the $CNIR > \text{threshold} (\delta)$ then the channel is assigned else checks for other channels. If no channel is available then the call is blocked.

D. Channel re-allocation of ongoing calls

When a user starts a call, it remains connected for some time. During this period, several events may occur affecting the communication between transmitter and receiver. Some of these events are: mobility of the transmitter, the emergence of other transmitters within the network, even the emergence of transmitters coming from other networks. All these events may degrade the quality of the communication channel. In order to avoid force termination, a channel re-allocation strategy is proposed. In this strategy, every user connected within every cell is evaluated. If interference condition is not satisfied, channel reallocation is implemented.

III. SIMULATION AND RESULTS

The main aim of the simulation is to study and compare DCA and FCA algorithm under various traffic patterns and user mobility in MATLAB. We have considered a cellular system of 19 cells of unit radius. In our case as shown in Fig. 4 the distribution of user in the system is random in nature. The user can be at any position in any cell. Every call request is subject to a Poisson process, with mean arrival rate $\lambda = 6$ calls per hour. The holding time is a random variable exponentially distributed with mean $1/\mu = 120$ s. To allocate and re-allocate channels the algorithm considers a CNIR threshold $\delta = 15$ dB. As shown in the fig. 1, in every time period the following events take place:

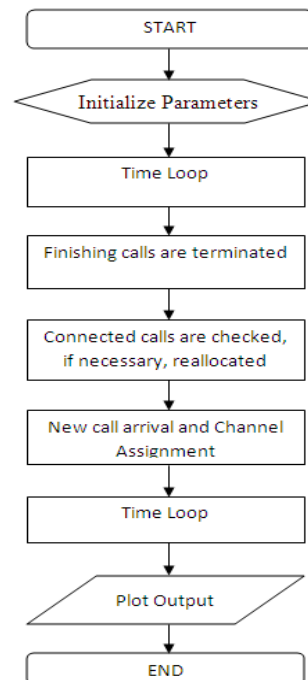


Fig. 1 : Main loop

A. Simulation of DCA

In the proposed work we have considered 19 channels for the system. Hence each cell in DCA can access 19 channels. Number of users varies from 200 to 1000. In each time period each user undergoes following events.

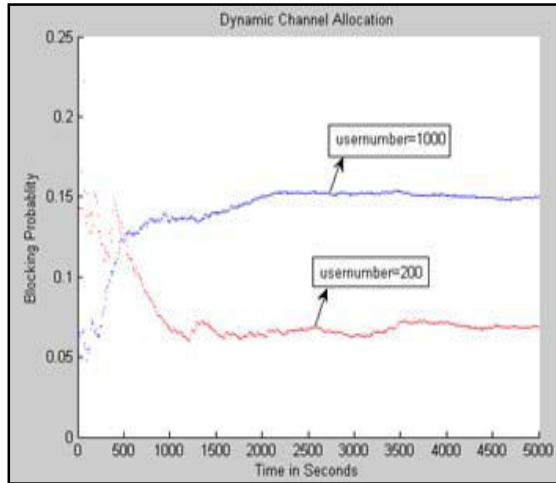


Fig. 2 : Transient response for DCA

- a) *Call termination*: Calls of connected users are terminated if the holding time is completed.
- b) *Channel re-allocation*: Calls of the still connected users are examined as given in [4]. They are re-allocated under following two conditions:
 - i) If the user has moved out of the cell (user mobility), the probability that the user moves out of the cell is considered to be 0.1. If the user moves out of the cell, then it moves into random surrounding cell to a random location in it. It checks whether a channel is available and calculates CNIR. If the $CNIR > \text{threshold} (\delta)$ then the channel is assigned, else force terminated.
 - ii) If the desirable interference condition is not satisfied then for every user we check if the $CNIR > \text{threshold} (\delta)$. If it is less than threshold it checks for other channels in the same cell which satisfies CNIR condition. If no such channel is available then it is force terminated.
- c) *Channel allocation*: In every time period each user is checked whether he is connected, if not we check for available channels which satisfies CNIR condition. If no such channel is available then it is blocked as shown in (2).

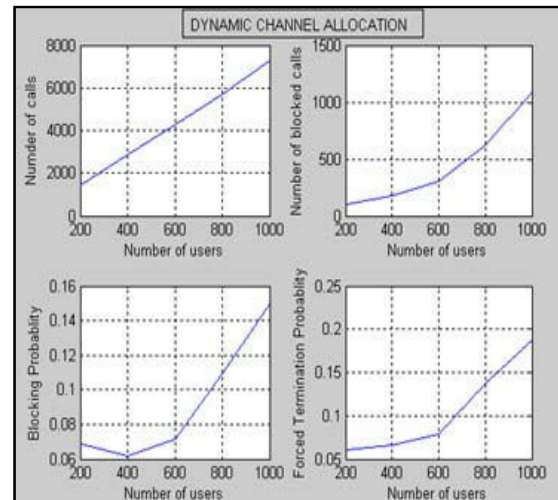


Fig. 3 : Parameters of DCA

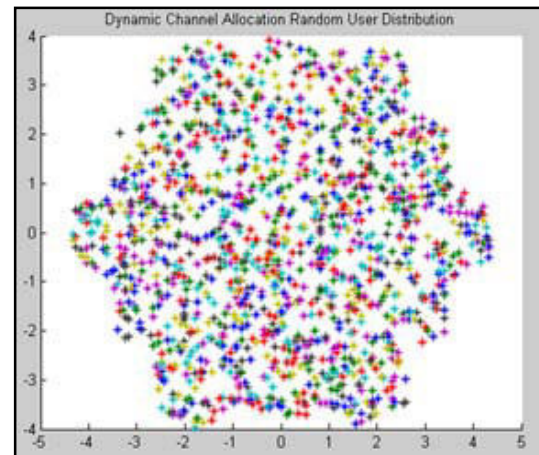


Fig. 4 : Random user distribution

B. Simulation of FCA

In the proposed work we have considered 19 channels for the system for simulation. Hence each cell in FCA can access only 1 channel because number of channels per cell is fixed. Number of users varies from 100 to 500. In each time period each user undergoes following events:

- a) *Call termination*: Calls of connected users are terminated if the holding time is completed.
- b) *Channel re-allocation*: Calls of the still connected users are examined. They are re-allocated under following two conditions:

- i) If the user has moved out of the cell (user mobility), then it moves into random surrounding cell to a random location in it.
- ii) If the desirable interference condition is not satisfied then for every user we check if the $C/N >$ threshold (δ). If it is less than threshold it checks for other channels in the same cell which satisfies C/N condition. If no such channel is available then it is force terminated.
- c) *Channel allocation*: In every time period each user is checked whether he is connected, if not we check for available channels which satisfies C/N condition. If no such channel is available then it is blocked.

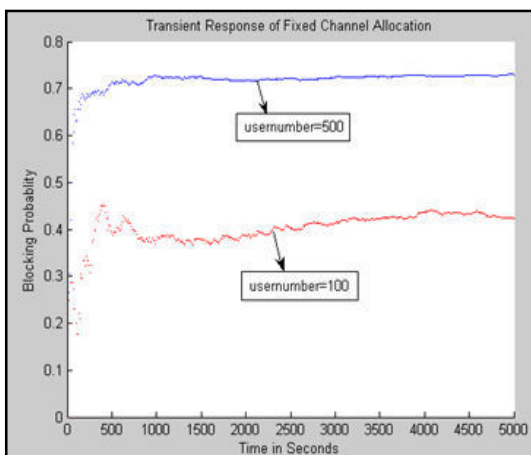


Fig. 5 Transient response for FCA

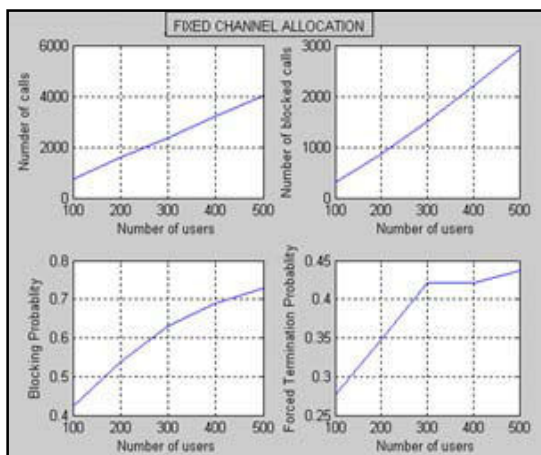


Fig. 6 : Parameters of FCA

C. Comparison between DCA and FCA

From fig. 2 and fig. 5 we can conclude that as number of users' increases blocking probability also increases. As seen from fig. 3 and fig. 6, for same

number of channels the performance of DCA is much better than FCA. Number of blocked calls in DCA is far less than those in FCA and hence the blocking probability in DCA is much less than in FCA. The forced termination probability in DCA is less than that in FCA because of channel reuse. Hence DCA outperforms FCA in most parameters except for complexity. The formula in equation (2) evaluates theoretical value of blocking probability according to Engset's Loss formula [1].

$$P_b = \frac{\binom{M-1}{k} \rho^k}{\sum_{i=0}^k \binom{M-1}{i} \rho^i} \quad (2)$$

IV. CONCLUSION AND FUTURE WORK

The wireless resource allocation has received a tremendous attention due to rapidly growing interest in wireless communications. Spectral efficiency is playing an increasingly important role as future wireless communication systems will accommodate more and more users and high performance services. In this paper we have provided an extensive survey of the resource allocation problem in wireless communications and presented a detailed and comparative discussion of the major allocation schemes. With recent trends in micro-cellular networks and access-broadband networks where multimedia applications will be extended to end users using microwave links, we are faced with new, interesting and important challenges to the wireless resource allocation problem. These emerging new areas will introduce a new set of constraints in channel allocation problems. The solution to these problems will play an important role in providing ubiquitous access to multimedia applications in wireless networks.

REFERENCES

- [1] W.C.Y. Lee, Mobile Cellular Communication Systems, 1989.
- [2] Z. Qing, M. Salder, "A survey of Dynamic Spectrum Access," IEEE Signal Processing Magazine, Vol.70, No.5, pp.78-89, May 2007.
- [3] L. Li, J. Tao and T. Xiaofong, "Dynamic Channel Assignment performance in multiservice hierarchical wireless networks." IEEE Intl Symp on Personal, Indoor and Mobile Radio Comm., pp.1-5, May 2006.
- [4] S.Yubin, "The performance simulation of Dynamic Channel Allocation in different cellular topologies," Control Conf., 27th Chinese, pp. 330-333, 16-18 July 2008.

□□□

Image Fusion Using Frequency and Algorithm

Nisha & Harpal Singh

Department of Computer Science & Engineering, Jalandhar, India

Abstract - This paper contains multifocus image fusion using spatial frequency and genetic algorithm. We are to divide the source images into blocks divide the source images into blocks. The blocks with higher spatial frequency are chosen. Suitable sizes of blocks are determined. Image fusion is based on artificial neural network.

Keywords - component; (Image fusion, Frequency, Genetic algorithm)

I. INTRODUCTION

Due to the limited depth-of-focus of optical lenses it is often not possible to get an image which contains all relevant objects in focus. One possibility to overcome this problem is to take several pictures with different focus points and combine them together into a single frame, which contains the focused regions of all input images 1to3

A. Image fusion

Image fusion provides an effective way of reducing this increasing volume of information while at the same time extracting all the useful information from the source image. Image fusion apart from reducing the amount of data is to create new image. Figure 1 Image fusion is the process by image is combined into a single image retaining the important feature from each of the original images. It is often required foe images acquired from different instrument modalities or capture techniques of the same scene or objects

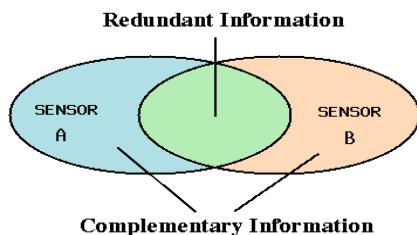


Fig. 1

The image fusion techniques allow the integration of different inputs. The fused image can have spatial and spectral quality. Numerous fusion applications have appeared in medical imaging like simultaneous evaluation of CT, MRI and PET images. That is more suitable for the purpose of human perception and for

further image processing tasks such as segmentation, object detection or target recognition in application such as remote sensing and medical imaging.

Multi view fusion, a set of images of the same scene taken by the same sensor but from different viewpoints is fused to obtain an image with higher resolution than the sensor normally provides or to recover the 3D representation of the scene. Images of the same scene are acquired at different times either to find and evaluate changes in the scene or to obtain a less degraded image of the scene. The former aim is common in medical imaging, especially in change detection of organs and tumors, and in remote sensing for monitoring land or forest exploitation.

A. Image fusion using artificial neural network

Image fusion is based on artificial neural network. An artificial neural network is a system based on the operation of biological neural networks; it is an emulation of biological neural system. A neural network can perform tasks that a linear program cannot. When an element of the neural network fails, it can continue without any problem by their parallel nature. A neural network learns and does not need to be reprogrammed. It can be implemented in any application without any problem.

B. Artificial neural network

An artificial neural network is a system based on the operation of biological neural networks, in other words, is an emulation of biological neural system. A neural network can perform tasks that a linear program cannot. When an element of the neural network fails, it can continue without any problem by their parallel nature. A neural network learns and does not need to be reprogrammed. It can be implemented in any application without any problem

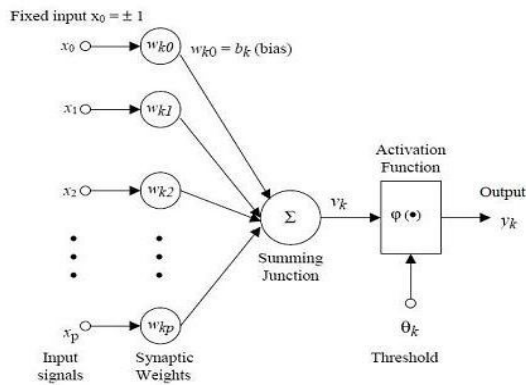


Fig. 2 : ANN

ANN represents a highly connected network of neurons - the basic processing unit it is a good system for image processing and has been processing such as image segmentation, Image fusion, and Image compression. Image fusion can be usually carried out in levels: Pixel level. Feature level image processing requires high spatial and high spectral resolution in a single image. The simplest image fusion method is to take average of two (or multiple) original images pixel by pixel. However when this direct method is applied, the contrast of features uniquely presented in either of the images is reduced. In order to solve this problem, several sophisticated approaches based on multistage transform, such as Paldian pyramid, gradient pyramid, ratio-of-low-pass pyramid, morphological pyramid, and multiresolution wavelet transform have been proposed. The basic idea of most of the multistage transform-based methods is to perform multiresolution decomposition on each source image, then integrate a composite multiresolution representation from these. Subsequently, the fused image is reconstructed by performing an inverse multiresolution transform. The fusion method, originated from human visual perception principle, is suitable to merge images with diverse focuses. Two spatially registered images with different focuses are decomposed into several blocks. Then, three features reflecting the clear level of every block are calculated. Finally, artificial neural networks are used to recognize the clear level of the corresponding blocks to decide which blocks should be used to construct the fusion result. The proposed method is computationally simple and can be applied in real time. Compared to the method based on discrete wavelet transform (DWT), the proposed method can achieve better results in some situations both in visual and quantitative measure. Ann represents a highly connected network of neurons - the basic processing unit it is a good system for image processing and has been processing such as image segmentation,

Image fusion and image compression. Image fusion can be usually carried out in levels: Pixel level. Feature level image processing requires high spatial and high spectral resolution in a single image. The pixel based fusion scheme the sub band signal of the fused image is simply acquired by picking the high frequency coefficient with greater absolute value. This fusion scheme is the weighted average scheme. The salient feature is first identified in each source image. The salience of a feature is computed as a local energy in the neighborhood of a coefficient. A pixel level image fusion algorithm based on artificial neural networks is considered. The Fusion method which was originated from perception is appropriate to merge images. Two spatially registered images with different focuses are decomposed into several blocks. Then, features reflecting the clear level of every block are calculated. Finally, artificial neural networks are used to recognize the clear level of the corresponding blocks to decide which blocks should be used to construct the fusion result.

II. RELATED WORK

Image fusion is an important is an important research field of image processing. How to get the best fusion quality is not an easy problem for the research. The work in [1] proposed nonsampled contour let transform is a multiresolution tool for image fusion For NSCT how to get a better focus measurement is an important research content. The experiment result that the dual layer PCNN model is a good focus measurement foe NSCT and the method proposed in this study has better fusion performance than the other classical method. The present paper proposes multifocal image fusion algorithm by using MPCNN. EOL and SF are used to measure the clarity of the image blocks of different sizes. The proposed method requires no training because of the linking ability of PCNN. Two different types of kernel matrix Gaussian and $1/r$ distribution have been used for different linking held evaluations of MPCNN. The value of b is decided by using the iteration method. The fusion of the images comes under the category of multi focus images fusion. In the existing method of images on their clarity measure, PCNN plays an important role in the image fusion process in choosing the best quality images block for fused image. Fusion method becomes tedious end time consuming because of the inherent complexity of PCNN. [2] Proposed Image fusion methods which are basically pixel by pixel approach. Pixels of the two images are compared and based on this comparison either average or maximum has taken. However when this direct method is applied the contrast of features uniquely presented in either of the images is reduced. The work in paper [3] proposes multifocal image fusion

algorithm by using MPCNN. EOL and SF are used to measure the clarity of the image blocks of different sizes. The proposed method requires no training because of the linking ability of PCNN. Two different types of kernel matrix Gaussian and $1/r$ distribution have been used for different linking field evaluations of MPCNN. The value of b is decided by using the iteration method. The fusion of the images comes under the category of multi focus image fusion. In the existing method of images on their clarity measure, PCNN plays an important role in the image fusion process in choosing the best quality images block for fused image. Fusion method becomes tedious end time consuming because of the inherent complexity of PCNN.

III. PROPOSED WORK

A. Spatial Frequency:-

The row and column frequencies of an image block are given by

$$RF = \sqrt{\frac{I}{MN} \sum_{m=1}^M \sum_{n=2}^N [F(m, n) - F(m, n - 1)]^2}$$

$$CF = \sqrt{\frac{I}{MN} \sum_{n=1}^N \sum_{m=2}^M [F(m, n) - F(m - 1, n)]^2}$$

B. Total Spatial frequency is given as

$$SF = \sqrt{RF^2 + CF^2}$$

Genetic Algorithm:-

We employ HA to search for the largest fitness value with a given fitness function. HA is the core components are depicted as.[5]

- a) Select mate: A large portion of the low fitness individuals is discarded through in natural selection step. N individuals in one iteration only the top Good individuals survive for mating and the bottom N Bad $=N-N$ good ones are discarded to make room for the selection rate is $N \text{ good} / n$.
- b) Crossover: Crossover is the first way that a HA explores a fitness surface. Two individuals are chosen from N good individuals to produce two new offspring's crossover point is selected between the first and last chromosomes of each

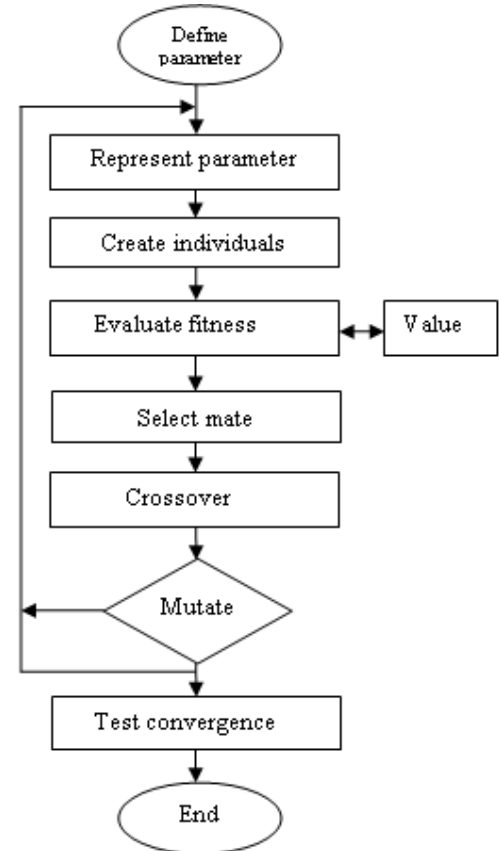
individual after the crossover point are exchanged and two new offspring are produced.

- c) Mutate: Mutation is the second way that a HA explores a fitness surface. It introduced traits not the original individuals and keep HA from converging too fast. The pre determined mutations rate should be low. Mutations deteriorate the fitness of an individual; however, the occasional improvement of the fitness adds diversity and strengthens the individual. After obtaining the fundamental concepts in HA, we are able to design an optimized fusion system with the aid of HA.

C. Multi-focus image fusion

We have to combine two or more images of a stationary camera. The fusion algorithm can be extended to handle more than two source images.

- a) Decompose the source images A and B into blocks of size $M*N$ blocks of A and B are denoted by A and B.



- b) Spatial frequency of A and B are denoted by SF and SF
- c) Fused image of the block F1 by comparing spatial frequencies of blocks A and B.
- d) Verify and correct the fusion result in step(3) We use a majority filter together with a 3*3 window.
- e) HA is employed to search for optimized sizes of block.

IV. CONCLUSION

Special frequency is used for a block based multi focus image fusion algorithm. The basic idea is to divide source images into blocks. The resultant based image is construct with higher spatial frequency value. For the sizes of block HA is brought forward

V. REFERENCE

The work in [1] proposed nonsubsampling contourlet transform is a multiresolution tool for image fusion For NSCT how to get a better focus measurement is an important research content. [2] Proposed Image fusion methods which are basically pixel by pixel approach. Pixels of the two images are compared and based on this comparison either average or maximum has taken. However when this direct method is applied the contrast of features uniquely presented in either of the images is reduced. The work in paper [3] proposes multifocal image fusion algorithm by using MPCNN. EOL and SF are used to measure the clarity of the image blocks of different sizes.

- [1] Beiji Zou, J. Asian network for scientific information. A school of information science and engineering Central South University Changsha ISSN 1812-5638.[2011].
- [2] Ping-Cheng Hsieh. and Pi-Cheng Tung,.. A novel hybrid approach based on sub-pattern technique and whitened PCA for face recognition,[2009].
- [3] K.G. Baum and M.Helguera, J.P. Hornak ,. A Techniques for fusion of multimodal images Application to breast imaging,. Proceedings of IEEE International Conference on Image Processing, pp 2521–2524.[2006]
- [4] Yang-Ping. And Wang , Multimodal medical image fusion using fuzzy radial basis function neural networks. Technical Report. University of Maryland at College Park. [2007].
- [5] Sasikal, . A Technique for fusion of multimodal images. Department of instrument of instrument engineering. Madras Institute of technology.[2007].
- [6] Shaohui Chen and Hongbo Su, . Decomposition Using Support Vector Machines for Multifocus Image Fusion. ISSN 1424-8220.[2008].
- [7] Li, S.and B.yang.,. Milt focus image fusion using region segmentation and spatial frequency. IEEE sensors j.,” 10:1519-1526,[2008].
- [8] Jun Kong†.and Kaiyuan Zheng, IJCSNS International Journal of Computer Science and Network Security. VOL.8 No.2.[2008]
- [9] D. Agrawal. and J. Singhai, Image Process., Iet Vol. 4, Iss. 6, pp. 443–451,[2010]
- [10] Jiang Dong and Dafang Zhuang,. Advances in Multi-Sensor Data Fusion: Algorithms and Applications. ISSN 1424-8220.[2007].

□□□

Mathematical Computation of Bit Error Rate for Different Fading Channels Using MATLAB

Mayank Jain¹, Sanjay Sharma² & R. P. Agarwal³

¹Department of Electronics & Communication Engineering, Vidya College of Engineering ,
Vidya Knowledge Park, Meerut, India

²Electronics, Informatics & Computer Engineering, Shobhit University, Meerut, India,

³Shobhit University, Meerut, India

Abstract - There are a number of factors that enter into the choice of a modulation scheme for use in a wireless application. Performance of a cellular system is dependent on the efficiency of the modulation scheme in use. Here we have discussed Multiple Input Multiple Output(MIMO) in Wireless medium by using Spatial Multiplexing technique for the calculation of the Bit Error Rate (BER). This gives the best BER performance in a multipath fading environment using computer simulation (MATLAB). Each digital modulation are modeled and simulated under Rayleigh, Rician & Nakagami fading channel conditions. Subsequently, a comparison study is carried out to obtain the BER performance for each modulation scheme under Rayleigh, Rician & Nakagami fading conditions and to identify which modulation scheme gives best BER performance.

Keywords - Rayleigh, Rician & Nakagami Fading.

I. INTRODUCTION

The requisite for wireless communication and its abstruse nature is upsurging from the past few decades [1]. In future it is believed to be more challenging and complicated with the evolution of different types of fading model. There are different types of fading models striving in urban and rural areas [2]. Rayleigh fading model is considered to be most common fading model, found in urban environment. In Rayleigh fading model there is no line of sight communication, where the signal is received after several reflections and scattering. Rician fading consists of line of sight communication and found to be more applicable for satellite communication. Nakagami fading model is mostly suited for urban multipath propagation and it is sought to be most practical model, specially used in mobile communication [3]. In a digital system, the capacity for a channel of bandwidth W perturbed by white thermal noise of power N , with an average transmits power of P , is given by

$$C=B \log_2 (1+ S/N) \quad (1)$$

The Multi-Input and Multi- Output (MIMO) communication systems provide very high data rates with low error probabilities[4]. In communication, multiple-input and multiple-output, or MIMO, is the use of multiple antennas at both the transmitter and receiver to improve communication performance.

It is one of several forms of smart antenna technology.

MIMO technology has attracted attention in wireless communications, since it offers significant increases in data throughput and link range without additional bandwidth or transmit power[5]. It achieves this by higher spectral efficiency[6] (more bits per second per hertz of bandwidth) and link reliability or diversity (reduced fading). Because of these properties, MIMO is a current theme of international wireless research.

In this paper, we describe a wireless transmission in which we have used the concept of MIMO .Spatial multiplexing technique has been used to increase the channel capacity significantly[7]. BPSK, QPSK, M-PSK & 8-QAM[8] are the modulation techniques which are studied in the Rayleigh, Rician & Nakagami channel. A comparative study of various modulation schemes for MIMOs and results are shown in the next sections .BER is calculated and analyzed for comparison.

II. SYSTEM MODEL

Rayleigh-fading is a multiplicative process, its simulation involves generating the Rayleigh fading process and multiplying it with the transmitted signal. The generation part directly follows from the fact that the envelope of a complex Gaussian random process

(with independent real and imaginary parts) has a Rayleigh distribution[9]. In cases when the fading process with a specific correlation needs to be generated, we have to use a Spectral Shaping filter for shaping the PSD of the fading process. Once the Rayleigh fading signal is generated, it can be multiplied with the transmitted signal to simulate the Rayleigh fading channel[10]. The Rayleigh distribution can be given by

$$P_z(z) = \frac{2z}{P_r} \exp\left[-\frac{z^2}{P_r}\right], z \geq 0 \quad (2)$$

If in addition to the scattering, there is a line of sight signal at the receiver, then the mean of the random process will no longer be zero. Such a situation may be better modelled as Rician fading[11]. For a multipath fading channel containing a specular or LOS component, the complex envelope of the received signal can be given by the Rician distribution,

$$p_z(z) = \frac{z}{\sigma^2} \exp\left[-\frac{(z^2 + s^2)}{2\sigma^2}\right] I_0\left(\frac{zs}{\sigma^2}\right), z \geq 0 \quad (3)$$

As some of our data does not fit in Rayleigh and rician faded model so a well general model called Nakagami faded model come in to existence [12],[13]. The Rayleigh distribution can be given by

$$P_z(z) = \frac{2k^k z^{2k-1}}{\Gamma(k)P_r^k} \exp\left[-\frac{kz^2}{P_r}\right], k \geq .5 \quad (4)$$

Where k is measure of fading.

III. SIMULATION DETAILS

Firstly, single bit data transmission was achieved assuming the channel to be Rayleigh faded with zero mean and variance. However, crucial data may be lost if there is a deep fade in the channel, hence the received signal is error prone. Secondly, these bits were retransmitted using blocks of certain length, over which the channel is assumed to be stationary and undergoes a slow fading, and the performance was found to be better than the earlier case. The procedure was repeated for the Rician fading channel which contains atleast one line of sight (LOS) path and also for Nakagami faded channel. As modulation schemes helps in signal to be error free, so the single bit and block bit transmission is carried under BPSK, QPSK, M-PSK & 8-QAM modulation schemes, to get signal error free at receiver.

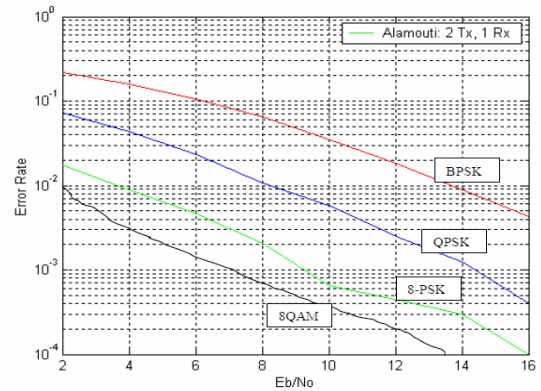


Fig. 1: BER performance of RAYLEIGH fading using different modulation techniques.

The figure - 1 shows that for RAYLEIGH fading environment 8-QAM modulation technique has the lowest BER as compared to the other three modulations i.e.: BPSK, QPSK and M-PSK. So the performance of 8-QAM modulation technique is best under these conditions.

Table-1: BER performance under RAYLEIGH fading at SNR of 8db

Modulation Technique	Bit Error Rate
BPSK	0.031
QPSK	0.01
M-PSK	0.0012
8-QAM	0.0010

Table-1 shows that in case of 8-QAM modulation technique the value of bit error rate is least i.e. :0.001 under RAYLEIGH fading environment as compared to other modulations. So, the performance of 8-QAM modulation technique is better in comparison to BPSK, QPSK and M-PSK.

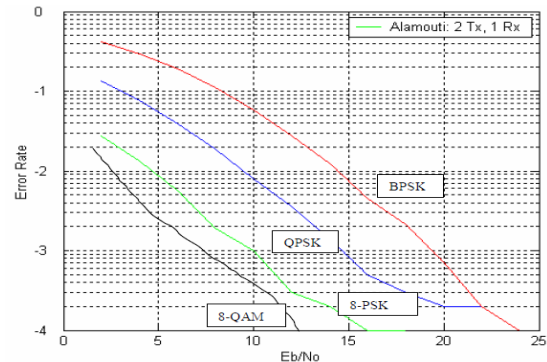


Fig. 2 : BER performance of RICIAN fading using different modulation techniques.

The figure - 2 shows that for Rician fading environment 8-QAM modulation technique has the lowest BER as compared to the other three modulations i.e.: BPSK, QPSK and M-PSK. So the performance of 8-QAM modulation technique is best under these conditions.

Table-2: BER performance under Rician fading at SNR of 10db.

Modulation Technique	Bit Error Rate
BPSK	0.0398
QPSK	0.006
M-PSK	0.0012
8-QAM	0.0011

Table-2 shows that in case of 8-QAM modulation technique the value of bit error rate is least i.e.:0.0010 under Rician fading environment as compared to other modulations.

So, the performance of 8-QAM modulation technique is better in comparison to BPSK, QPSK and M-PSK.

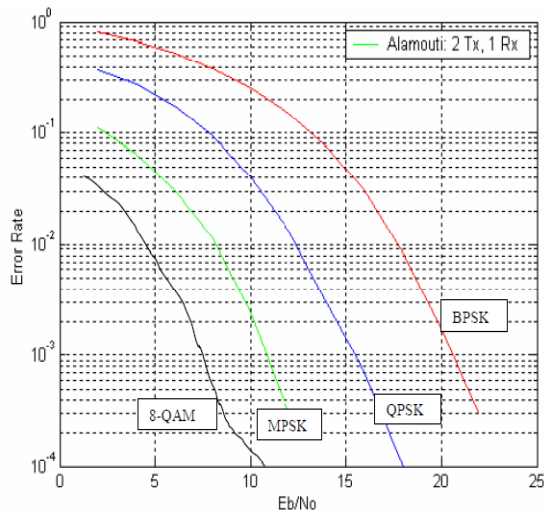


Fig. 3: BER performance of NAKAGAMI fading using different modulation techniques

The figure-3 above shows that under NAKAGAMI fading environment 8-QAM modulation technique has the lowest BER as compared to the other three modulations i.e.: BPSK, QPSK and M-PSK. So the performance of 8-QAM modulation technique is best under these conditions.

Table-3: BER performance under NAKAGAMI fading at SNR of 10db.

Modulation Technique	Bit Error Rate
BPSK	0.1412
QPSK	0.0251
M-PSK	0.0012
8-QAM	0.0010

Table-3 shows that in case of 8-QAM modulation technique the value of bit error rate is least i.e.:0.0010 under NAKAGAMI fading environment as compared to other modulations. So, the performance of 8-QAM modulation technique is better in comparison to BPSK, QPSK and M-PSK.

III. CONCLUSION

In this paper a comparative study of different modulation techniques with MIMO system under different fading environments is done. The study of ALAMOUTI SCHEME is also carried out. The figures 1 shows that in case of RAYLEIGH fading channel the bit error rate (BER) is least i.e.: 0.001 for 8-QAM modulation technique as compared to the other three modulation techniques i.e.: BPSK, QPSK, M-PSK. Hence the performance of the Quadrature Amplitude Modulation is best when RAYLEIGH fading is present in MIMO system. The figures 2 show that in case of Rician fading the bit error rate (BER) is again least for QAM modulation technique as compared to the other three modulation techniques i.e.: BPSK, QPSK, 8-PSK. Hence the performance of the Quadrature Amplitude Modulation is best when Rician fading is present in MISO systems.

It is also seen that in case of all the modulation techniques, for a bit error rate of 10^{-2} , MIMO system with NAKAGAMI fading requires approximately 3db less power as compared to the system with RAYLEIGH fading. The performance of Rician fading lies in between NAKAGAMI and RAYLEIGH fading.

REFERENCES

- [1] Theodore S. Rappaport, Wireless Communications, chapter 1.
- [2] Theodore S. Rappaport, Wireless Communications, chapter 7.
- [3] Siavash M. Alamouti, "A Simple Transmit Diversity Technique for Wireless Communications", IEEE journal on select areas in communications, vol.16, no.8, October 1998

- [4] Ilan Hen, "MIMO Architecture for Wireless Communication", Intel Technology Journal, Vol. 10, Issue 2, 2006.
- [5] Major Harinder Singh Sandhu, Thesis of Master of Technology: Power Efficient Free Space Optical Multiple Input Multiple Output Wireless Communication, Department Of Electrical Engineering, Indian Institute Of Technology Delhi, May 2008
- [6] G.D. Golden, G. J. Foschini, R. A. Valenzuela and P.W. Wolniansky "Detection Algorithm and Initial Laboratory Results using VBLAST space time communication Architecture" Electronics letters, 7th January 1999, Vol.35 No.1
- [7] T. Eng and L. B. Milstein, "Partially coherent DS-SS performance in frequency selective multipath fading," IEEE Trans. Commun., vol. 45, pp. 110-118, Jan. 1997.
- [8] M. A. Smadi and V. K. Prabhu, "Performance analysis of generalized- faded coherent PSK channels with equal-gain combining and carrier phase error," IEEE Trans. Commun., vol. 5, pp. 509-513, Mar. 2006.
- [9] J. K. Cavers, "An analysis of pilot symbol assisted modulation for Rayleigh fading channels," IEEE Trans. Commun., vol. 40, pp. 686-693, Nov. 1991.
- [10] X. Tang, M.-S Alouini, and A. J. Goldsmith, "Effect of channel estimation error on M-QAM BER performance in Rayleigh fading," IEEE Trans. Commun., vol. 47, pp. 1856-1864, Dec. 1999.
- [11] S.Seo, C.Lee & S. Kang, "Exact performance analysis of M-ary QAM with MRC diversity in Rician fading channels", Electronics Letters, vol. 40, no. 8, April 2004.
- [12] V. A. Aalo, "Performance of maximal ratio diversity systems in a correlated Nakagami-fading environment," IEEE Trans. Commun., vol.43, pp. 2360-2369, Aug. 1995.
- [13] C. M. Lo and W. H. Lam, "Error probability of binary phase shift keying in Nakagami-m fading channel with phase noise," Electron. Lett., vol. 36, pp. 1773-1774, Oct. 2000.

□□□

Inclined Slot Loaded Proximity-Coupled Microstrip Antenna for WLAN

Milind Thomas, Vikas Chelani, Rahul Ramesh, Sanjay Sukumar & Saurav Singh

Electronics and Communication Engineering Department, New Horizon College of Engineering,
Marthahalli, Bangalore – 560103, Karnataka, India

Abstract - The design of a miniaturized proximity-coupled microstrip antenna (PCMA) is presented here. The antenna has very small size, wide bandwidth and moderate gain and may be used as small, compact antenna for 5GHz band wireless local area network (WLAN). Simulated results using IE3D software are verified by measurement.

Keywords - Proximity-Coupled, Slot-Loaded, 2:1 VSWR Bandwidth, Broadside Direction.

I. INTRODUCTION

Planar, thin, light weight antennas are attractive for wireless applications. There are various types of wireless local area network (WLAN) standards, like, Bluetooth, WiFi, WiMAX, High Performance LAN (HIPERLAN) etc. For next generation wireless networking, high speed broadband systems HIPERLAN/, HIPERLAN/2 are proposed, which uses frequency band of 5.470 GHz – 5.725 GHz. The objective is to design a broadband miniaturized planar antenna for HIPERLAN/2 with moderate gain. Here, the bandwidth is defined as the frequency range for which return loss is -10 dB or less and gain is 4 dBi or more. Here, the design and parametric studies of an inclined slot-loaded proximity-coupled microstrip antenna (PCMA) are described. Single layer Microstrip antennas have very narrow bandwidth because of their inherent properties, but using multilayered proximity coupling, higher bandwidth can be achieved. In PCMA, the radiating patch, fabricated on a dielectric substrate, is excited by a microstrip line on another substrate, as shown in Figure 1.

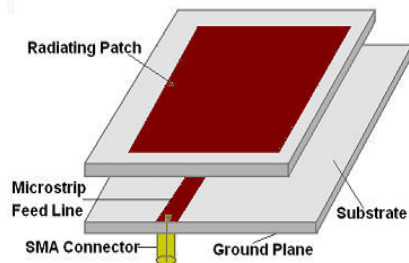


Fig. 1: Proximity-Coupled Microstrip Antenna

In wireless environment, signals are scattered from various structures and reach the receiving terminal from any unpredicted direction (Figure 2).

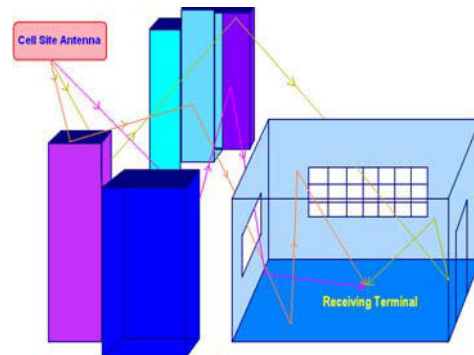


Fig. 2 : Signal Scattering in Wireless Environment

Thus directional antennas may be used. An omnidirectional antenna not only receives signal from all directions but also receives noise from all directions. A directional antenna receives noise only from a particular direction, resulting in better communication.

II. ANTENNA STRUCTURE

Slot is inclined at an angle Φ with respect to the microstrip feed line, just below the centre of the radiating patch (Figure 3).

This microstrip line is fed by a co-axial SMA connector in the second substrate. Patch dimensions are 12mm X 4.4mm. Dimensions of the feed line are 5mm X 1mm. Part of the feed line which appears beyond the centre of the radiating patch is stub line and this stub line is important for impedance matching. Here, stub

line length is 2.5mm. Dimensions of the inclined slot are 1.5mm X 0.5mm.

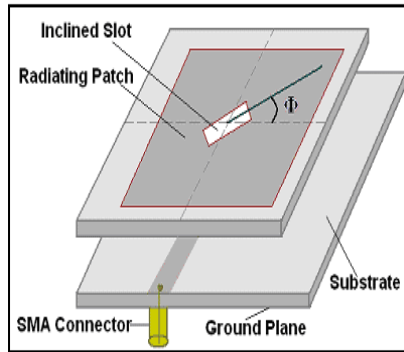


Fig. 3 : Inclined-Slot Loaded PCMA

After a large number of simulations, best results are obtained when inclination of the slot (Φ) is 45° with respect to the feed line. The dimensions of the ground plane of the fabricated antenna are 30mm X 25mm.

III. SIMULATED & MEASURED RESULTS

For antenna simulation, IE3D software is used and for measurement, Vector Network Analyzer (N5230A, Agilent Technologies). Antenna is fabricated on glass epoxy substrate with dielectric constant 4.36 and loss tangent of 0.01 and height of the dielectric substrate is 1.57mm. Optimum dimensions of the patch, slot, feed line and angle of inclination of the slot are determined after a large number of simulations, to achieve miniaturized size, broad bandwidth, best impedance matching and good gain of the antenna. Simulated radiation pattern of the antenna is shown in Figure 4, which is in broadside direction.

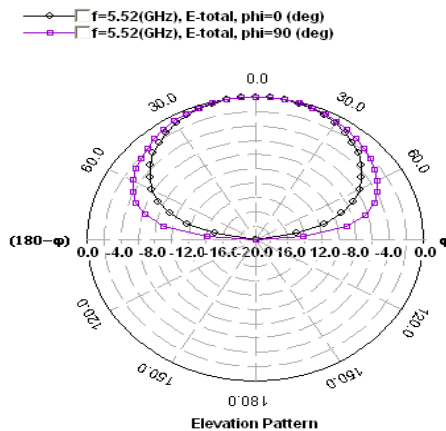


Fig. 4 : Radiation Pattern of the Inclined-Slot Loaded PCMA

Simulated and measured return losses are compared in Figure 5. Return loss (-10dB) bandwidth is 290MHz [5.40GHz – 5.69GHz].

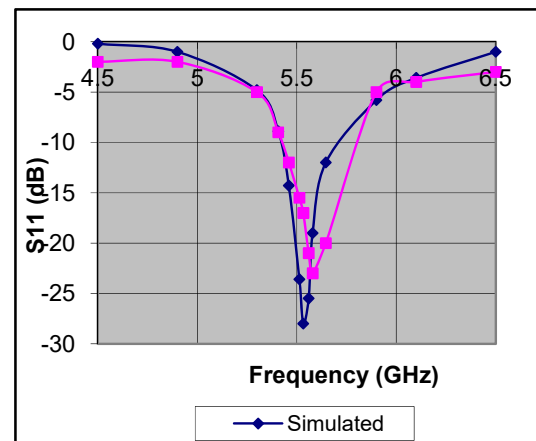


Fig. 5 : Simulated and Measured Return Losses

Simulated and measured return losses are compared in Figure 6. Over the bandwidth minimum and maximum gains of the antenna are 4.2 dBi and 5.1 dBi.

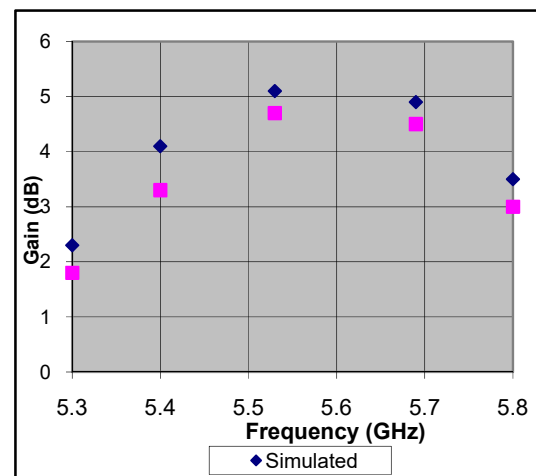


Fig. 6 : Simulated and Measured Gains of the Antenna

Gain of the antenna is measured at discrete frequencies by measuring transmission coefficient parameters (S_{21}) and using Friis transmission formula. Transmitted power (P_t) and Received power (P_r) can be related to the S_{21} by the expression $P_r/P_t = |S_{21}|^2$. According to Friis transmission formula,

$|S_{21}|^2 = (G_r^2 \lambda^2) / (4 \pi r)^2$, where gain of transmitted (G_t) and received antenna (G_r) are same. That is, gain of the receiving antenna is $G_r = (4 \pi r / \lambda) |S_{21}|$, where 'r' and ' λ ' are the separation between the antennas and the free-space wavelength respectively.

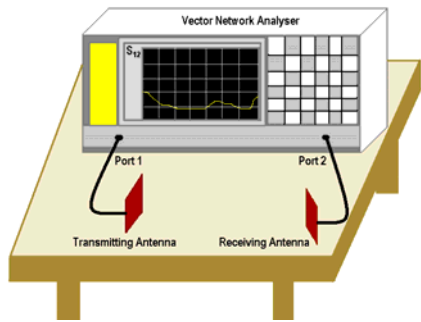


Fig. 7 : Experimental Setup for Gain Measurement

In simulation, the angle of inclination of the slot (Φ) is varied to observe the effect of inclination on the performance of the antenna (Figure 8).

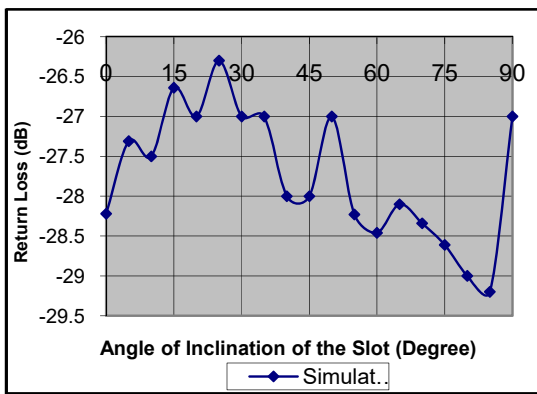


Fig. 8. Simulated Return Loss vs Inclination of the Slot

The variation of 2:1 VSWR bandwidth with angle of inclination is also investigated (Figure 9). Good impedance matching and highest bandwidth are achieved when the angle of inclination of the slot is 45 degree.

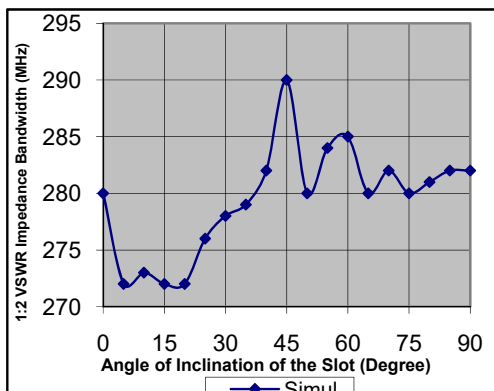


Fig. 9 : Simulated 2:1 VSWR vs Inclination of the Slot

Due to the variation of inclination of the slot, there are very small changes in resonance frequency, antenna efficiency and gain of the antenna, because these parameters principally depend on the peripheral dimensions of the antenna, which are kept constant.

IV. CONCLUSIONS

Performance of a miniaturized microstrip antenna for WLAN application is reported here. The simulation using IE3D shows that in order to achieve same characteristics, in the same frequency range, using PCMA, without loading by any slot, the required dimension of patch, on the same substrate, should be 12mm X 10mm and for proper impedance matching the dimension of the microstrip feed line should be 15mm X 4mm. Therefore using the proposed inclined-slot loaded PCMA the peripheral area of the patch is reduced by 65%. The feed line dimension is reduced by 90%. Due to miniaturization of the antenna, bandwidth also decreases. Here, after a large number of simulations, a miniaturized broadband antenna is designed at 5 GHz band.

REFERENCES

- [1] F. Yang, X-X Zhang, X. Ye and Y. Rahmat-Samii, "Wide-band E-shaped patch antennas for wireless communications", IEEE Trans. Antennas and Propagation, vol. AP-49, pp. 1094– 1100, 2001.
- [2] K. L. Wong, Planar Antennas for Wireless Communications, John Wiley & Sons, New Jersey, 2003.
- [3] J. S. Roy, N. Chattoraj and N. Swain, "Short circuited microstrip antennas for multiband wireless communications", Microwave & Optical Technology Letters, vol. 48,no. 12, pp. 2372 – 2375, Dec.2006.
- [4] J. S. Roy, and M. Thomas, "Design of a circularly polarized microstrip antenna for WLAN", Progress In Electromagnetic Research, PIER M, vol. 3, pp. 79 – 90, 2008.
- [5] B.-H. Sun, J.-F. Li, Q.-Z. Liu, "Compact broadband printed antenna for multi-functional mobile terminals", Journal of Electromagnetic Waves and Applications, JEMWA, Vol. 22, 1292 – 1298, 2008.
- [6] J. Ghosh and J. S. Roy, "Design of a wideband microstrip antenna", Journal of Electromagnetic Waves and Applications, JEMWA, vol. 22, pp. 2379-2389, 2008.
- [7] L. Varshney and J. S. Roy, "A broadband stepped-slot antenna", Microwave Review, Vol. 5, No.2, pp. 33-36, Dec. 2009
- [8] J. S. Roy and M. Thomas, "Investigations on a new proximity coupled dual-frequency microstrip antenna for wireless communication", Microwave Review, vol. 13, no. 1, pp. 12 – 15, June 2007.

Image Processing Based Intelligent Traffic Controller

Vikramaditya Dangi, Amol Parab, Kshitij Pawar & S.S Rathod

Electronics and Telecommunication Dept., Sardar Patel Institute of Technology, Mumbai, India

Abstract - The frequent traffic jams at major junctions call for an efficient traffic management system in place. The resulting wastage of time and increase in pollution levels can be eliminated on a city-wide scale by these systems. The paper proposes to implement an intelligent traffic controller using real time image processing. The image sequences from a camera are analyzed using various edge detection and object counting methods to obtain the most efficient technique. Subsequently, the number of vehicles at the intersection is evaluated and traffic is efficiently managed. The paper also proposes to implement a real-time emergency vehicle detection system. In case an emergency vehicle is detected, the lane is given priority over all the others.

Keywords - Adaptive Background Subtraction, Edge Detection, Emergency vehicles, Image Processing, Traffic Management.

I. INTRODUCTION

Current traffic control techniques involving magnetic loop detectors buried in the road, infra-red and radar sensors on the side provide limited traffic information and require separate systems for traffic counting and for traffic surveillance.

Inductive loop detectors do provide a cost-effective solution, however they are subject to a high failure rate when installed in poor road surfaces, decrease pavement life and obstruct traffic during maintenance and repair. Infrared sensors are affected to a greater degree by fog than video cameras and cannot be used for effective surveillance.

In contrast, video-based systems offer many advantages compared to traditional techniques. They provide more traffic information, combine both surveillance and traffic control technologies, are easily installed, and are scalable with progress in image processing techniques. This paper tries to evaluate the process and advantages of the use of image processing for traffic control. Implementation of our project will eliminate the need of traffic personnel at various junctions for regulating traffic. Thus the use of this technology is valuable for the analysis and performance improvement of road traffic.

Also priority to emergency vehicles has been the topic of some research in the past. A proposed system for detection of these vehicles as in [1] is based on Radio-Frequency Identification (RFID). However, the use of this technology necessitates unnecessary extra hardware to be installed both at every junction and in every vehicle. There have also been studies to recognize these vehicles by analysis of the sound of their siren as

shown in [2]. However, this technology is also easily influenced by noise and requires additional hardware at every traffic signal.

II. PROPOSED SYSTEM

A. System Overview

The various steps of our proposed system are described in Fig 1. A camera is fixed on poles or other tall structures to overlook the traffic scene as seen in [3]. Images extracted from the video are then analysed to detect and count vehicles. Then depending on the signal-cycle (we have taken it to be 3 minutes), time is allotted to each lane. For example, if the number of vehicles in a four-lane intersection is found to be 10, 30, 20 and 20, then time allotted to each lane is in the ratio 1:3:2:2. The system also takes into account the emergency vehicles at the intersection. If such a vehicle is detected, the lane is given priority over the others.

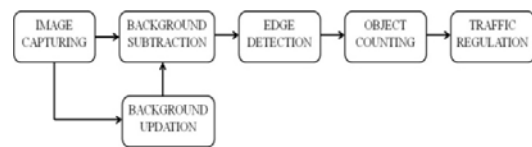


Fig. 1 : System Overview.

B. Background Subtraction

Static background subtraction' has been the traditional method for real-time segmentation of an object in video based system. The technique is based on computing the error between a constant background frame and the current one. Video-based techniques for outdoor environments are easily influenced by factors such as weather, change in illumination and motion.

Hence, a static background proves insufficient and a robust background model is necessary to deal with change of luminance.

We propose the use of the adaptive background technique as described in [4]. Generating the current background image based on segmentation results extracted from differencing the image with the previous extracted background is the basic idea of our method. The updated background (B_{new}) is computed as a function of current background (B_o) and current frame I through the equation:

$$B_{new} = \begin{cases} (\alpha * B_o) + (1 - \alpha) * I & \text{if } RES = 0 \\ B_o, & \text{otherwise} \end{cases} \quad (1)$$

Where RES is the result of subtraction of consecutive frames, and the value of α is 0.5.

The model hence accounts for the changes in background and reduces the error caused by them as shown in (1).

Once we have developed an adaptively changing background model, our next step is to separate the foreground from the background of the image. This is done by a pixel-by-pixel comparison of the current frame with the background at that instant. A pixel would be part of the foreground, when its value is different enough from its corresponding value in the background model. The edges and objects are then recognized on the basis of a predefined threshold.

C. Edge Detection

After separating the foreground objects, we need to define their edges in the subtracted image. This is done by using an edge detection algorithm. There are a variety of edge detection techniques that have been used in the past [5]. Simple techniques such as the Boolean edge detector converts a window of pixels into a binary pattern based on a local threshold, and then applies masks to determine if an edge exists at a certain point or not. In the Marr-Hildreth Edge Detector, we smoothen the image using a Gaussian and Laplacian function. This takes the second derivative of an image. If there is a step difference in the intensity of the image, it will be represented in the second derivative by a zero crossing.

The Sobel operator is a discrete differentiation operator, computing an approximation of the gradient of the image intensity function. At each point in the image, the result of the Sobel operator is either the corresponding gradient vector or the norm of this vector. The operator consists of a pair of 3×3 convolution kernels designed to respond maximally to edges running vertically and horizontally relative to the pixel grid, one kernel for each of the two perpendicular orientations.

The method finds edges using the Sobel approximation to the derivative. It then returns edges at those points where the gradient of the image is the maximum. Prewitt operator is similar to the Sobel operator used for detecting vertical and horizontal edges in images. It is a fast method only suitable for well-contrasted noiseless images.

The Canny edge detector is considered to be one of the most widely used edge detection algorithms in the industry. It works by first smoothing the image and finds the image gradient to highlight regions with high spatial derivatives. It then tracks along these regions to suppress any pixel that is not at the maximum. Finally, through hysteresis, it uses two thresholds and if the magnitude is below the first threshold, it is set to zero. If the magnitude is above the high threshold, it is made an edge and if the magnitude is between the two thresholds, it is set to zero unless there is a path from this pixel to a pixel with a gradient above the second threshold. That is to say that the two thresholds are used to detect strong and weak edges, and include the weak edges in the output only if they are connected to strong edges.

D. Background Subtraction

After finding the edges the next stage is to count the number of objects as defined by the edges. There have been many algorithms suggested for object detection and contour tracing. These include the commonly used Radial Sweep method, Theo Pavlidis' Algorithm and Square Tracing Algorithm. However, in this paper we have implemented the Moore-neighbourhood algorithm based on a similar method as in [6]. The algorithm starts by choosing a random start point. When the current pixel 'p' is black, the Moore neighbourhood of 'p' is examined in clockwise direction starting with the pixel from which 'p' was entered and advancing pixel-by-pixel until a new black pixel in 'p' is encountered. The algorithm terminates when the start pixel is visited for the second time. The black pixel walked over will be the contour of the pattern. The efficiency of the algorithm improves greatly when we stop only after entering the start pixel in the same manner as entered initially. This is known as Jacob's stopping criteria. We have implemented this algorithm which does a decent job of identifying the number of cars in a given picture.

The contour tracing algorithm enables us to define the boundary of the object as well as their size. We specify different size ranges to classify the various types of vehicles. This gives us a measure of the traffic density on each road at the intersection (refer Fig. 3(d)). The traffic light is then regulated by allotting variable time according to the measured density and size of the vehicles.

E. Emergency Vehicle Condition

In case a red beacon is detected, the next step is to identify whether it is from an emergency vehicle or not. This is done by identifying the blinking frequency of red light detected in the image sequence and comparing it to the standard used by the emergency vehicles.

The conditions for detection of red light beacon during various periods of the day are shown below. Once they are satisfied, we scan the intermediate frames for the absence of the beacon by the condition as shown below.

Night time conditions:

For red light: $R > 230$, $G < 250$, $B < 250$

In the intermediate frames: $R < 230$, $G > 230$, $B > 230$

Day time conditions:

For red light beacon: $R > 230$, $G < 250$, $B < 250$

In the intermediate frames: $R < 230$, $G < 230$, $B < 230$

If matched, the normal system is overridden and the lane is given priority over all the others. The lane is turned green until the vehicle has passed the intersection.

III. RESULTS AND DISCUSSIONS

To compare between various types of edge detection algorithms we tested their performance for ten images taken from real traffic intersections. After finding the edges, the picture was subjected to an object counting algorithm. The performance of the edge detector algorithms was defined by the number of vehicles accurately detected. The results are shown in Table I. Canny Edge detector was found to be the best among those compared (93.47%).

The Boolean edge detector performs a decent job of marking the locations of edges, however it failed to complete the edges making object detection difficult. The Sobel and Prewitt operators are more adept at recognizing edges that are horizontal or vertical and are susceptible to noise (refer Fig 2), as also found in [7]. The Marr-Hildreth was found to be the most susceptible to noise and gave a lot of false results. The use of two thresholds by Canny edge detector makes it less likely to be fooled by noise, and more likely to detect true weak edges, providing a better and fairly noise resistant method for the detection of edges. Hence we have used this method of detection in the paper, along with Moore neighbourhood method to count the vehicles marking the final step of our system.

TABLE I : COMPARISON OF EDGE DETECTION TECHNIQUES

Image no	Actual no. of objects	Boolean	Marr Hildreth	Sobel	Prewitt	Canny
1	4	2	6	2	2	4
2	3	0	4	1	1	2
3	4	2	3	2	3	4
4	5	2	3	2	3	6
5	5	2	3	3	3	5
6	7	3	5	3	2	6
7	4	1	5	1	1	4
8	5	2	5	3	2	5
9	3	0	3	0	1	2
10	6	4	3	2	3	6
Accuracy %		39.13	84.78	41.30	45.65	93.47

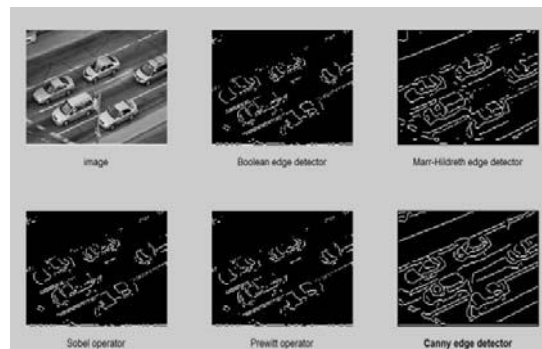


Fig. 2 : Output of various edge detection techniques.

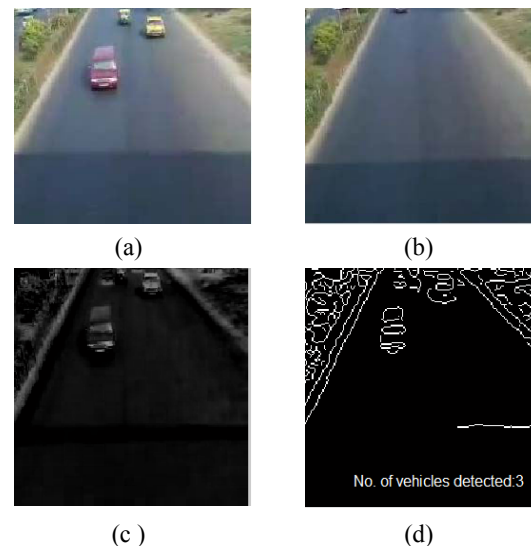


Fig. 3 : (a)Real-time image (b)Background image (c)Subtracted image (d)No. of vehicles = 3

The proposed system is used to analyze a real time traffic scene for a road (Fig 3(a)). The adaptive background, updated from the scenes is shown in Fig. 3(b). The subtracted image then contains only the foreground objects (vehicles) as seen in Fig 3(c). Using image processing algorithms (Fig 3(d)), the number of vehicles in the lane can be found out. In this case, the number of vehicles is 3.

The video is also analysed for the detection of emergency vehicles through their flashing red lights. By specifying a threshold, we have isolated the areas with high intensity of red light and comparatively lesser intensity of blue and green colour. The resultant image is shown in Fig. 4(b). As we can see, the headlights of the vehicle were also detected, which led to an erroneous output. Hence the red light must satisfy the additional condition of blinking. This is achieved by taking account for the fact that the red light shall appear in every third frame only. The other lights do not appear in the image sequence with this frequency and hence are eliminated. This leads to the conclusion of the presence of an emergency vehicle as shown in Fig. 4(c).

Our model was tested for ambulance during various times of the day and was found to be successful. In addition, the beacon can be identified even if the emergency vehicle is in an inclined position with respect to the camera as seen in Fig. 4(c).



Fig. 4 : a) Image of a vehicle during daytime, (b) Detection of all lights, (c) Emergency vehicle detected

IV. CONCLUSION

In this project, we have successfully implemented an algorithm for a real-time image processing based traffic controller. Upon comparison of various edge detection algorithms, it was inferred that Canny Edge Detector technique is the most efficient one. Analysis of various contour tracing and object counting methods

revealed the Moore neighbourhood technique to be more robust when compared to the others. The paper demonstrates that image processing is a far more efficient method of traffic control as compared to traditional techniques. We have also implemented a system for emergency vehicle detection based on image processing techniques. The use of our algorithm removes the need for extra hardware such as sound sensors or RFID tags. The increased response time for these vehicles is crucial for the prevention of loss of life.

V. FUTURE WORK

The focus shall be to implement the controller using DSP as it can avoid heavy investment in industrial control computer while obtaining improved computational power and optimized system structure. The hardware implementation would enable the project to be used in real-time practical conditions. More information about this method can be found in [8]. In addition, we propose a system to identify the vehicles as they pass by, giving preference to emergency vehicles and assisting in surveillance on a large scale.

REFERENCES

- [1] Ahmed S. Salama, Bahaa K. Saleh, Mohamad M. Eassa, "Intelligent Cross Road Traffic Management System (ICRTMS)," 2nd Int. Conf. on Computer Technology and Development, Cairo, Nov 2010, pp. 27-31.
- [2] B. Fazenda, H. Atmoko, F. Gu, L. Guan1 and A. Ball, "Acoustic Based Safety Emergency Vehicle Detection for Intelligent Transport Systems," ICCAS-SICE, Fukuoka, Aug 2009, pp.4250-4255.
- [3] Y. Wu, F. Lian, and T. Chang, "Traffic monitoring and vehicle tracking using roadside camera," IEEE Int. Conf. on Robotics and Automation, Taipei, Oct 2006, pp. 4631– 4636.
- [4] Z. Jinglei, L. Zhengguang, and T. Univ, "A vision-based road surveillance system using improved background subtraction and region growing approach," Eighth ACIS Int. Conf. on Software Engineering, Artificial Intelligence, Networking, and Parallel/Distributed Computing, Qingdao, August 2007, pp. 819-822.
- [5] M. Siyal, and J. Ahmed, "A novel morphological edge detection and window based approach for real-time road data control and management," Fifth IEEE Int. Conf. on Information, Communications and Signal Processing, Bangkok, July 2005, pp. 324-328.

- [6] K. Wang, Z. Li, Q. Yao, W. Huang, and F. Wang, "An automated vehicle counting system for traffic surveillance," IEEE Int.Conf. on Vehicular Electronics and Safety, Japan, Dec 2007, pp. 1-6.
- [7] M. Juneja, P. Sandhu, "Performance evaluation of edge detection techniques for images in spatial domain," Int. Journal of Computer Theory and Engineering, Singapore, vol. 1, no. 5, Dec 2009, pp. 1793-8201.
- [8] K. Hang, "Real-time image acquisition and processing system design based on DSP," The 2nd IEEE Int. Conf. on Computer and Automation Engineering (ICCAE), Singapore, Feb 2010, pp. 492-496.



Wireless Real Time Atmospheric Data Acquisition and Analysis using MATLAB

Boddu Varun Reddy, Ch. Vivek, Tarigopula Sanjeev & Vinoth Babu Kumaravelu

SENSE, VIT University, Vellore, India

Abstract - Real time wireless atmospheric data acquisition has always been necessary for weather scientists and environmental engineers, especially atmospheric data from 1-50KM above the surface of the earth. The weather balloons with payloads available in the market are expensive and require a lot of effort to launch. We have discussed an affordable and efficient way of doing this with help of MATLAB GUI. The authors have integrated hardware that is the ground station with MATLAB via the RS232 port and analyzed the income data and plotted each of them w.r.t height obtained from the onboard GPS.

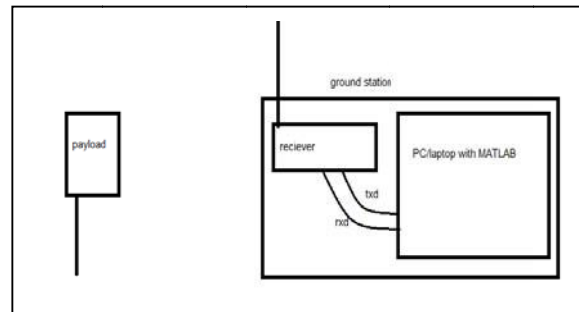
Keywords - component; weatherballoon; MATLAB GUI; RS232.

I. INTRODUCTION

There are two parts to this paper, in the first part we discuss the design of the hardware and the second we discuss how we have integrated the hardware to software which is MATLAB and developed a GUI. This system can be used by weather scientists, environmental engineers in colleges to collect atmospheric data like temperature, pressure, humidity, altitude and also the location and use it for their research. MATLAB is a versatile tool for any engineer; one can also communicate with external devices (hardware) with the help of rs232 port of the computer. We have used this to our advantage and received data directly into MATLAB and analyzed it. We have also developed a graphical user interface to help us easily setup the communication system and calibrate the sensors. All in all this complete setup well help gather data from any payload wirelessly and efficiently. We have tested the system for a range of 1-1.5Km in height. We have depended on LOS communication. The range of the system can be improved with properly designed antennas and using a high sensitivity receiver.

II. BASIC BLOCK DIAGRAM

A basic block diagram of operation is given below

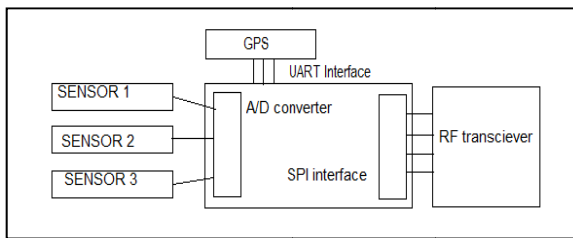


III. PAYLOAD DESIGN AND DEVELOPMENT

The payload is basically an embedded system with sensors, GPS, and RF transceiver. The microcontroller we chose for this payload is ATMEGA 8535 it has all the regular ports and communication interface. The advantage is that the interrupts are executed faster in this microcontroller with only 8kbytes of flash available. The sensors integrated to this microcontroller are LM35 for temperature because of its wide range, Freescale absolute pressure sensor MPX6115A and a humidity sensor. We have used a GPS module with a MTK MT3318 chipset which has a sensitivity of -151.6db and 51 channels for more accuracy. The mother board, sensors signal conditioning circuit, the RF board were designed in eagle and fabricated. The RF daughter board contains a CC1100 low power RF IC from Texas Instruments and a power amplifier PA649 which increases the power output of the RFIC to 1W, which is more than enough for a range upto 1km if we are using the same RFIC at the receivers end. The GPS is connected to the UART port, the RF board to the SPI and sensors to ADC of microcontroller. The software was developed using AVR studio 4. The CC1100 is

operated in the slave mode. The register values for the initial configuration were obtained from RF Studio 7. The CC1100 is configured such that it has a data rate of 9600 baud per sec and operates at a frequency of 433MHz with GFSK modulation. The data is arranged in form of data packet which includes the height, date, time ,sensor data and then sent to the RFIC. All the electronic components are fixed in a rugged mechanical structure which can withstand heavy vibrations. This payload is launched into the atmosphere using a helium balloon and ascends at a rate of 1m/s. The payload is switched on before it is launched and starts transmitting data continuously.

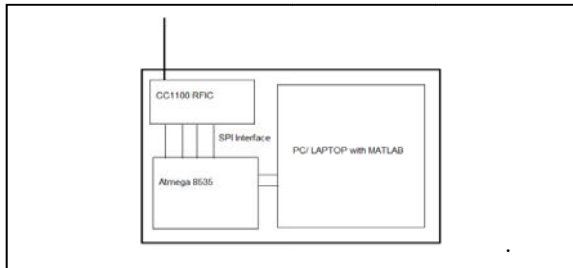
IV. PAYLOAD BLOCK DIAGRAM



V. GROUND STATION DESIGN

The ground station was developed using the same microcontroller and RFIC that is the ATMEGA 8535 and CC1100. The RFIC is configured with the same settings which were used in the payload design the transmitter and receiver mode are activated in both the cases. The interesting part of the ground station is that it is connected to a PC via the RS232 cable with a max232 level converter. The RS232 port hereon referred to as the com port is accessed through MATLAB. The main idea behind the ground station was to make it as light as possible.

VI. BLOCK DIAGRAM OF GROUND STATION

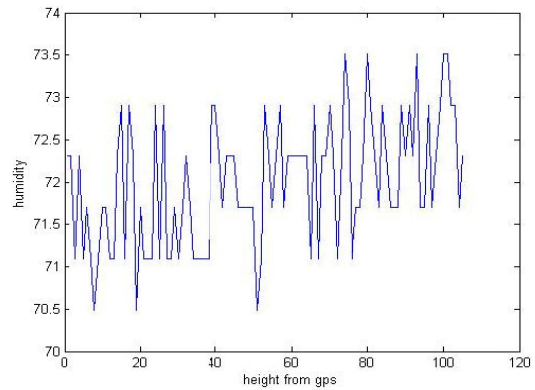


VII. MATLAB INTERFACE

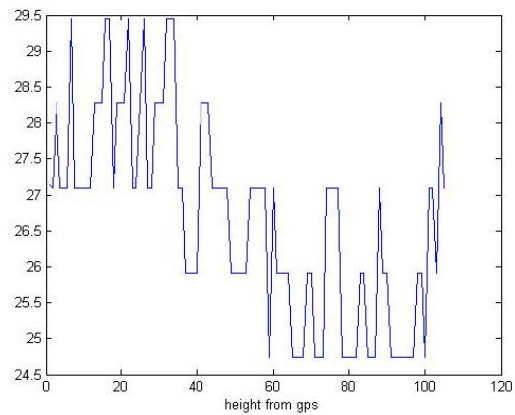
We have developed a Graphical user interface which allows us to calibrate the sensors to the ground value and also start the communication all the data is received in an array. The data packet received from the microcontroller of the ground station serially has been decoded as follows: Height, date, time, temperature,

pressure, humidity. The GUI that has been developed is very user friendly showing the real time plots of the data received. The GUI shows the real-time variation in the graphs accurately. The GUI is developed for simplex communication in case of a packet error a message indicating the error will be displayed on the screen thus avoiding the data loss. The MATLAB GUI makes use of the various radio buttons, push button, axes, edit text and static text in regard to perform various functions in the GUI.

VIII. PLOTS OBTAINED IN MATLAB



Above is the plot of humidity v/s height obtained in MATLAB



Above is the plot of temperature v/s height obtained in MATLAB

IX. CONCLUSION

In this paper we have designed and implemented a wireless data acquisition system exploiting MATLAB’s GUI development kit. We have also successfully tested this system for a range of 1 to 1.5Km. Real time plots were obtained and manipulated using the GUI developed.

REFERENCES

- [1] Moore, "Matlab for Engineers" 3e, copyright 2011J.
- [2] Siri Namtvdet, "Application note AN047", texas instruments.
- [3] Online: <http://www.mathworks.com/products/matlab/>, website of The Math Works, Inc., developer and distributor of technical computing software Matlab (access link for Matlab product information).
- [4] Application Note 460 LM34/LM35 Precision Monolithic Temperature Sensor , texas instruments.
- [5] Sang-Hoon Lee, Yan-Fang Li, and Vikram Kapil"Development of MATLAB based graphical user interface environment for PIC microcontrolers". "Proceedings of the 2004 American Society for Engineering Education Annual Conference & Exposition"

□□□

Performance Comparison of Fuzzy Logic Controller with Different Types of Membership Function using Matlab Tools

Shikha Rao¹, Lini Mathew² & Rahul Gupta³

^{1&3}Electronics and Instrumentation Deptt., Vidya College of Engineering, Meerut, India

²Electrical Engineering Deptt., N.I.T.T.R. Chandigarh, India

Abstract - In this work a straightforward approach for designing a fuzzy logic based controller is presented using Matlab/Simulink module. The objective of this paper is to evaluate the effect of membership function in fuzzy logic controller. This work presents the performance comparison of fuzzy logic controller with two different types of membership function. In the present work, an attempt has been made to develop a fuzzy based control system for a DC position control system. Now the main aim is to design a control system that will ensure good transient and steady state response of the system. Basically three steps are carried out to implement this work: Firstly a Fuzzy logic controller is designed using triangular membership function. Secondly a fuzzy logic controller is designed using Gaussian membership function. In last performance of fuzzy controller with triangular membership function is compared with fuzzy controller with Gaussian membership function. For the implementation of this work MatLab/Simulink Module and MatLab/Fuzzy Toolbox are used.

Keywords - Matlab, Simulink, Fuzzy logic Controller (FLC), Fuzzy Set, Membership function, Gaussian function, Triangular function.

I. INTRODUCTION

MATLAB is a high-performance language for technical computing integrates computation, visualization, and programming in an easy-to-use environment where problems and solutions are expressed in familiar mathematical notation. This paper presents a simple approach to design fuzzy logic based controller for Matlab/Simulink environment. For implementation of this work Matlab-Simulink and Matlab-Fuzzy logic toolbox are used. The Fuzzy Logic Toolbox is collection of functions built on the Matlab numeric computing environment. Fuzzy Logic Toolbox provides Matlab functions, graphical tools, and a Simulink block for analyzing, designing, and simulating systems based on fuzzy logic. It provides tools to create and edit fuzzy inference systems within the framework of Matlab, and it is also possible to integrate the fuzzy systems into simulations with Simulink[1]. This toolbox relies heavily on graphical user interface (GUI) tools. GUI-based tools provide an environment for fuzzy inference system design, analysis, and implementation. The Fuzzy Logic Toolbox for use with MATLAB is a tool for solving problems with fuzzy logic. Fuzzy logic is a fascinating area of research because it does a good job of trading off between significance and precision. Fuzzy controllers are used to control consumer products, such as washing machines, video cameras, and rice cookers, as well as industrial processes, such as cement

kilns, underground trains and robots. Fuzzy control is a control method based on fuzzy logic. A fuzzy logic can be described simply as “*computing with words rather than numbers*”; similar a fuzzy control can be described simply as “*control with sentences rather than equations*”. A fuzzy controller can include empirical rules, and that is especially useful in operator controlled plants.

When compared to the conventional controller, the main advantage of fuzzy logic is that no mathematical modelling is required. Since the controller rules are especially based on the knowledge of the system behaviour and the experience of the control engineer. The FLC requires less complex mathematical modelling than classical controller does[2].

In this paper, a fuzzy controller is presented for a position control system. In this work two Fuzzy logic controllers are designed with different types of membership functions using GUI tools supported by the Fuzzy-Toolbox in Matlab and then, simulation results of these controllers are compared with each other.

II. SYSTEM DESCRIPTION

In this work fuzzy logic controller is designed for a servo system. Servo systems are typical motion control systems having non-linearities such as friction and saturation. The motion control systems are also characterized by parameter uncertainties. The parameter

uncertainties are caused by estimation errors and/or parameter variations. Two major sources of the parameter variations in positioning systems are inertia and friction variations. Inertia of the positioning systems may vary due to payload variation. Friction variation may occur due to variations of the lubrication condition and/or inertia. Inertia variation can cause variation of the Coulomb friction as well. Therefore, the robustness of the control system is also an important requirement of the motion control systems. Fig.1 shows a Simulink based position control system and fig.2 shows its time response[5].

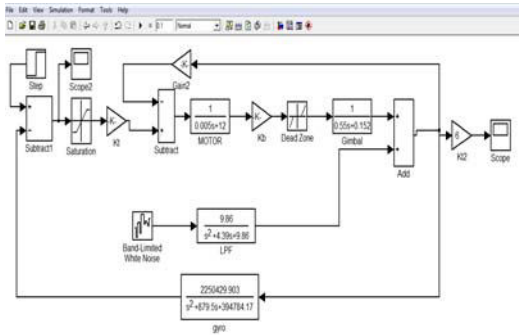


Fig.1 : Simulink based block diagram of position control system

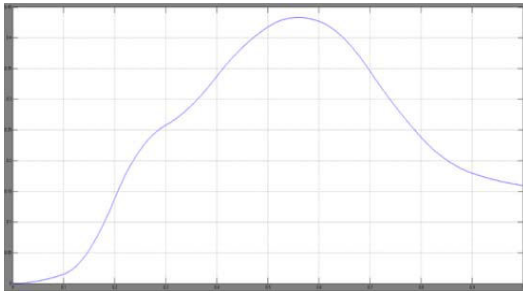


Fig. 2 : Unit step response

Fig. 2 shows that the system response is highly affected by these non-linearities. Now the main aim is to design a control system that will attenuate the effect of these non-linearities and ensure good transient and steady state response of the system.

Given servo system is a highly complex, non-linear and uncertain system. For such applications, a knowledge base controller is needed. The field of fuzzy has been making a rapid progress in recent years. Fuzzy based control system has been widely exploited for non-linear, high order and uncertain system. Therefore, in this work a fuzzy based controller is presented for a given servo system.

III. FLC DESIGNING

The main of this work is to design a fuzzy logic controller using Matlab based Fuzzy logic tool box which will improve the transient and steady state behaviour of the system. The control input variables for the proposed fuzzy controller are chosen as error (e) and change of error (Δe). The control output variable (U) is defined as the output for fuzzy controller. They are fuzzy linguistic variable represent the actual speed error (e), change of actual speed error (Δe) and the output control effort (u) respectively. The actual variable expression is given as:

$$e(k) = r(k) - y(k) \quad (1)$$

$$\Delta e(k) = e(k) - e(k - 1) \quad (2)$$

$$u(k) = f[e(k), \Delta e(k)] \quad (3)$$

Where $r(k)$ and $y(k)$ are the set-point and the actual output value at the k^{th} sampling interval, respectively and $f(,)$ denotes the input-output relation function.

The time responses of error signals can be used to represent information related to the system output responses. As the error signals approach zero the output signals move towards reference. Depending on the performances of controllers used, the error signals may or may not become zero. The error signal of a controlled system will be sufficient to derive the controller rules since it contains the necessary information about the outputs[1].

After evaluating the input and output variables of the controller, it is required to convert each piece of input and output data into degrees of membership by a lookup in one or several membership functions. For each input and output variable described by seven fuzzy sets: NB, NM, NS, Z, PS, PM and PB[3]. When the membership function has been designed, the following has been taken into consideration:

- i. Choose the membership function curve with low resolution when the error is large and high one when error is small.
- ii. The degree of interaction between different fuzzy sets is generally given between 0.4-0.8.

The fuzzy logic controller is a rule-based controller and the rules are in the *if-then* format e.g. “If error is A_i and change in error is B_i then output is C_i ”.

The rules to designed fuzzy controller are given in the Table I. Table I uses seven linguistic variables for the error and change in error with 49 rules.

Table 1 : Rule base of fuzzy-logic controller

Error (e)/	NB	NM	NS	Z	PS	PM	PB
------------	----	----	----	---	----	----	----

Derivative of error (Δe)							
NB	NB	NB	NB	NB	NM	NS	Z
NM	NB	NB	NB	NM	NS	Z	PS
NS	NB	NB	NM	NS	Z	PS	PM
Z	NB	NM	NS	Z	PS	PM	PB
PS	NM	NS	Z	PS	PM	PB	PB
PM	NS	Z	PS	PM	PB	PB	PB
PB	Z	PS	PM	PB	PB	PB	PB

From the rule table, the rules are manipulated as - *If error is NB and change in error is NB, then output is NB.* The actual motor speed is fed back and is compared with set speed. After comparison, error signal and the change in error are calculated and are given as input to fuzzy controller. In this work, the error is normalized to per unit value with respect to the set speed. This helps in using the fuzzy controller for any set speed. The fuzzy controller will attempt to reduce the error to zero by changing firing angle of switching signal.

In this work firstly a fuzzy logic controller is designed using triangular membership function and then using a Gaussian membership function. These membership functions are building using the graphical user interface (GUI) tools provided by the Fuzzy Logic Toolbox. There are five primary GUI tools for building, editing, and observing fuzzy inference systems in the Fuzzy Logic Toolbox: the Fuzzy Inference System or FIS Editor, the membership Function Editor, the Rule Editor, the Rule Viewer and Surface viewer, shown in fig.3

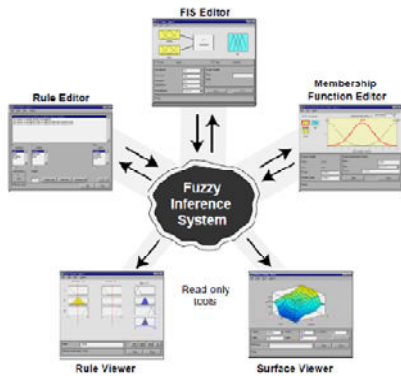


Fig. 3 : Fuzzy inference system with five GUI tools

A fuzzy controller uses several membership functions and from these functions triangular membership function is the simplest membership function. Fig. 4(a), 4(b) and 4(c) show the membership function editor window where input and output variables are designed using triangular membership function.

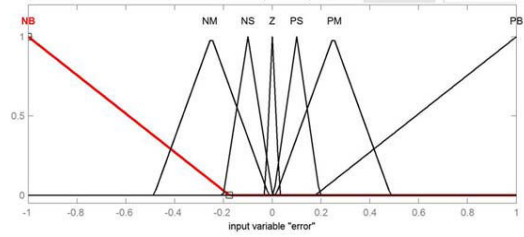


Fig. 4(a) : Triangular membership function for input variable error (e)

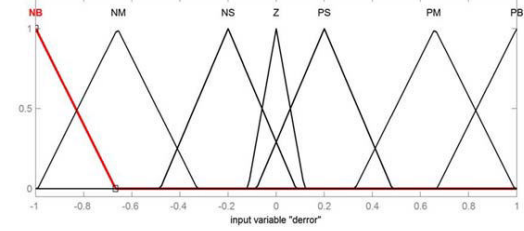


Fig.4(b) Triangular membership function for input variable error change in error (Δe)

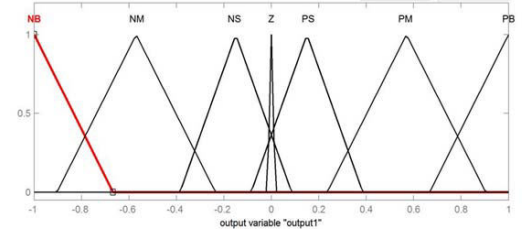


Fig. 4(c) : Triangular membership function for output variable (U)

The Gaussian type membership function is chosen for each variable and universe of discourse is defined from -1 to 1. The Gaussian membership function is expressed as follows:

$$f(x, c, \sigma) = \exp \left[-\frac{(x - c)^2}{2\sigma^2} \right]$$

Where c is the centre of Gaussian curve and σ is the width of Gaussian function. The Gaussian membership function of each input and output variable with seven fuzzy sets (NB, NM, NS, Z, PS, PM, & PB) is shown in fig.5(a), fig.5(b) and fig.5(c).

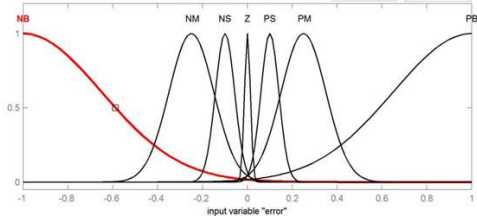


Fig. 5(a) : Gaussian membership function for input variable error(e)

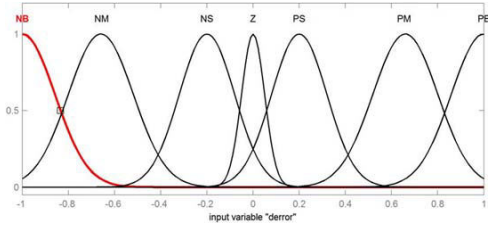


Fig. 5(b) : Gaussian membership function for input variable change in error(Δe)

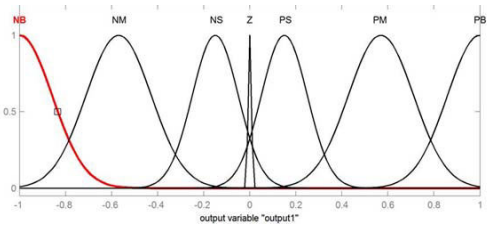


Fig. 5(c) : Gaussian membership function for output(U)

Based on the descriptions of input and output variables defined with FIS Editor, the Rule Editor allows constructing the rule statements automatically in *if-then* format. Similar to FIS editor and Membership function editor, Rule editor has the menu bar and the status line. The menu items allow to open, close, save and edit a fuzzy system using five basic GUI tools. Based upon the rule base given in table1, Rule-Editor is used to view and edit fuzzy rules. Rule editor for FLC is shown in fig.5.

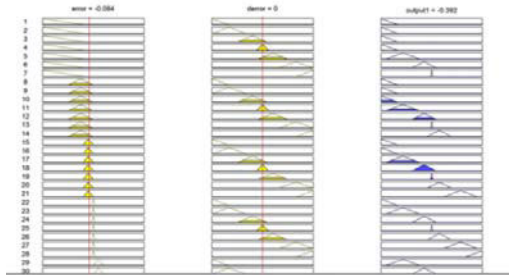


Fig. 5 : Rule editor of FLC

Surface viewer of fuzzy logic toolbox generates and plots an output surface map for the system with one or more inputs and outputs. This is read only tool. The surface view of FLC with triangular membership function is shown in fig.6 and with Gaussian membership function is shown in Fig.7

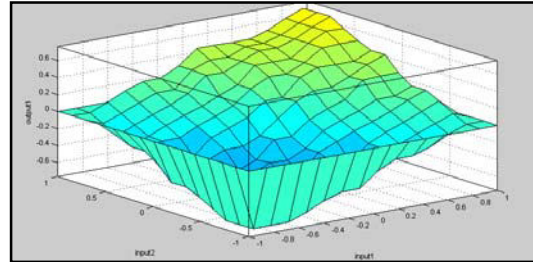


Fig. 6 : Control surface of FLC with triangular membership function.

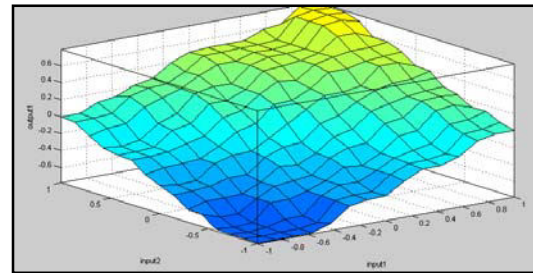


Fig.7 : Control surface of FLC with Gaussian membership function.

IV. SIMULATION RESULTS

The simulation of DC servo motor position control system is done in Matlab/Simulink toolbox. Mamdani type fuzzy logic controller is used for the implementation of this work. The simulated response of fuzzy logic controller with triangular membership function is shown in fig.7 and with Gaussian membership function is shown in fig.8.

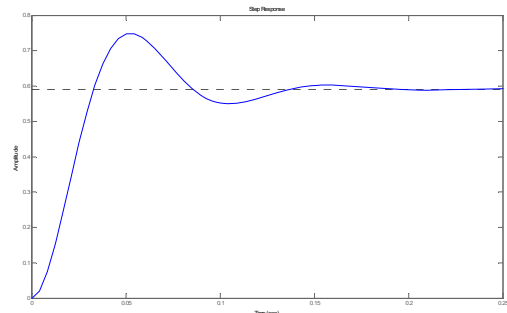


Fig. 7 : Time response of the system with fuzzy-logic controller having triangular membership function.

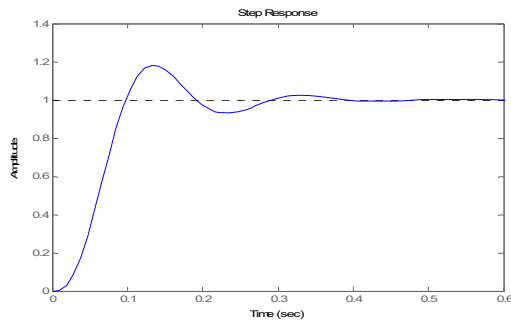


Fig. 8 : Time response of the system with fuzzy-logic controller having Gaussian membership function

The performance comparison of Fuzzy logic controller with triangular membership functions and with Gaussian membership function is presented in table 2.

Table 2 : Simulation Results

Sl. No.	Parameters	Response with triangular membership function	Response with Gaussian membership function
1.	Overhoot(%)	22%	18%
2.	Rise-time	0.1 sec	0.09sec
3.	Settling-time	0.38 sec	0.38 sec
4.	Steady-state error	0.002	0.0035

The table shows that in case of Gaussian membership function overshoot is reduced but steady state error increased. However settling time remains same for both FLCs.

During the simulation of this work it is also observed that that system response is highly affected by the variations in the spread of membership functions. With the increase in spread oscillations reduced but settling time increases.

V. CONCLUSION

This paper presents a simple approach to design FL based controllers using MATLAB/Simulink environment. Matlab based Fuzzy inference system (FIS) is used for the implementation of this work. In this work performance of FLC with Gaussian type membership function is compared with FLC having triangular membership function. Simulation results of both FLCs are also presented. After the implementation of this of this work it is concluded that system behaviour is highly depends upon the following factors:

- i. Total number of input and output variables
- ii. Number of fuzzy sets which are used to define the particular variable
- iii. Overlapping between the fuzzy sets and
- iv. Type of membership function.

REFERENCES

- [1] I.H. Altas and A.M. Sharaf, “A Generalized Direct Approach for Designing Fuzzy Logic Controllers in Matlab/Simulink GUI Environment”, International Journal of Information Technology and Intelligent Computing, Int. J. IT&IC no.4 vol.1, 2007.
- [2] Ch. Satyananda Reddy and KSVSN Raju, “An Improved Fuzzy Approach for COCOMO’s Effort Estimation using Gaussian Membership Function” JOURNAL OF SOFTWARE, VOL. 4, NO. 5, JULY 2009
- [3] J. Gayathri Monicka Dr. N.O.Guna Sekhar & K. Ramesh Kumar, “Performance Evaluation of Membership Functions on Fuzzy Logic Controlled AC Voltage Controller for Speed Control of Induction Motor Drive”, International Journal of Computer Applications (0975 – 8887,)Volume 13– No.5, January 2011
- [4] Neeraj Gupta and Sanjay K. Jain, “Comparative Analysis of Fuzzy Power System Stabilizer Using Different Membership Functions”, International Journal of Computer and Electrical Engineering, Vol. 2, No. 2, April, 2010
- [5] Krishna Moorthy JAR, Marthe Rajeev and Babu Hari, “Fuzzy Controller For Line-of-Sight Stabilization”, Journal of optical engineering, Vol. 43, pp 1394-1400, November, 2004
- [6] Salang Musikasuwan and Jonathan M. Garibaldi, “On Relationships between Primary Membership Functions and Output Uncertainties in Interval Type-2 and Non-Stationary Fuzzy Sets” , 2006 IEEE International Conference on Fuzzy Systems Sheraton Vancouver Wall Centre Hotel, Vancouver, BC, Canada, July 16-21, 2006



Implementation of Addressable ROM

Kanchana M. Pawar

REVA ITM Bangalore, India

Abstract - Active-HDL allows building the ROM and access data from memory by using address location of memory .memory of any bit length can be designed to store data which can be read. ROM implementation is carried out and verified using Hardware description language, verilog code. And software used Xilinx 9.1ISE and modelsim. Active HDL allows you to build the ROM. An embedded system designer is often faced with the situation of needing a particular-sized memory (ROM or RAM), but having readily available memories of a different size. For example, the designer may need a 2k x 8 ROM, but may have 4k x 16 ROMs readily available. Alternatively, the designer may need a 4k x 16 ROM, but may have 2k x 8 ROMs available for use.

I. INTRODUCTION

Any Embedded System's functionality consists of three aspects: processing, storage and communication. Processing is the transformation of data, storage is the retention of data for later use, and communication is the transfer of data. Each of these aspects must be implemented. We use processors to implement processing, memories to implement storage, and buses to implement communication. The earlier chapters described common processor types: general-purpose processors, standard single-purpose processors, and custom single-purpose processors. This chapter describes memories. A memory stores large numbers of bits. These bits exist as m words of n bits each, for a total of $m \times n$ bits. We refer to a memory as an $m \times n$ ("m-by-n") memory. $\log_2(m)$ address input signals are necessary to identify a particular word. Stated another way, if a memory has k address inputs, it can have up to 2^k words. n signals are necessary to output (and possibly input) a selected word. To read a memory means to retrieve the word of a particular address, while to write a memory means to store a word in particular address. Some memories can only be read from (ROM), while others can be both read from and written to (RAM). There isn't much demand for a memory that can only be written to (what purpose would such a memory serve?). Most Memories have an enable input; when this enable is low, the address is ignored, and no data is written to or read from the memory

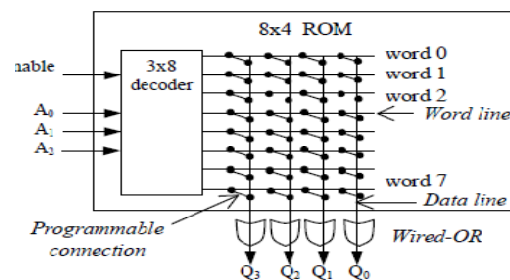


Fig 1.1 : 8x4 ROM internal

1.1 Historical background:

The simplest type of solid state ROM is as old as semiconductor technology itself. Combinational logic gates can be joined manually to map n -bit address input onto arbitrary values of m -bit data output (a look-up table). With the invention of the integrated circuit came mask ROM. Mask ROM consists of a grid of word lines (the address input) and bit lines (the data output), selectively joined together with transistor switches, and can represent an arbitrary look-up table with a regular physical layout and predictable propagation delay.

In mask ROM, the data is physically encoded in the circuit, so it can only be programmed during fabrication. This leads to a number of serious disadvantages:

1. It is only economical to buy mask ROM in large quantities, since users must contract with a foundry to produce a custom design.
2. The turnaround time between completing the design for a mask ROM and receiving the finished product is long, for the same reason.
3. Mask ROM is impractical for R&D work since designers frequently need to modify the contents of memory as they refine a design.

- If a product is shipped with faulty mask ROM, the only way to fix it is to recall the product and physically replace the ROM.

Subsequent developments have addressed these shortcomings. PROM, invented in 1956, allowed users to program its contents exactly once by physically altering its structure with the application of high-voltage pulses. This addressed problems 1 and 2 above, since a company can simply order a large batch of fresh PROM chips and program them with the desired contents at its designers' convenience. The 1971 invention of EPROM essentially solved problem 3, since EPROM (unlike PROM) can be repeatedly reset to its unprogrammed state by exposure to strong ultraviolet light. EEPROM, invented in 1983, went a long way to solving problem 4, since an EEPROM can be programmed in-place if the containing device provides a means to receive the program contents from an external source (e.g. a personal computer via a serial cable). Flash memory, invented at Toshiba in the mid-1980s, and commercialized in the early 1990s, is a form of EEPROM that makes very efficient use of chip area and can be erased and reprogrammed thousands of times without damage.

All of these technologies improved the flexibility of ROM, but at a significant cost-per-chip, so that in large quantities mask ROM would remain an economical choice for many years. (Decreasing cost of reprogrammable devices had almost eliminated the market for mask ROM by the year 2000.) Furthermore, despite the fact that newer technologies were increasingly less "read-only," most were envisioned only as replacements for the traditional use of mask ROM.

The most recent development is NAND flash, also invented by Toshiba. Its designers explicitly broke from past practice, stating plainly that "the aim of NAND Flash is to replace hard disks,"^[1] rather than the traditional use of ROM as a form of non-volatile primary storage. As of 2007, NAND has partially achieved this goal by offering throughput comparable to hard disks, higher tolerance of physical shock, extreme miniaturization (in the form of USB flash drives and tiny microSD memory cards, for example), and much lower power consumption. ROM, or read-only memory, is a memory that can be read from, but not typically written to, during execution of an embedded system. Of course, there must be a mechanism for setting the bits in the memory (otherwise, of what use would the read data serve?), but we call this "programming," not writing. Such programming is usually done off-line, i.e., when the memory is not actively serving as a memory in an embedded system. We usually program a ROM before

inserting it into the embedded system. We can use ROM for various purposes..

Another common use is to implement a combinational circuit. We can implement any combinational function of k variables by using a $2^k \times 1$ ROM, and we can implement n functions of the same k variables using a $2^k \times n$ ROM.

1.2 Scope of Project:

Active-HDL allows you to build the ROM and access data from memory by using address location of memory .memory of any bit length can be designed to store data which can be read.

An embedded system designer is often faced with the situation of needing a particular-sized memory (ROM or RAM), but having readily available memories of a different size. For example, the designer may need a $2k \times 8$ ROM, but may have $4k \times 16$ ROMs readily available. Alternatively, the designer may need a $4k \times 16$ ROM, but may have $2k \times 8$ ROMs available for use. The case where the available memory is larger than needed is easy to deal with. We simply use the needed lower words in the memory, thus ignoring unneeded higher words and their high-order address bits, and we use the lower data input/output lines, thus ignoring unneeded higher data lines. (Of course, we could use the higher data lines and ignore the lower lines instead).

The case where the available memory is smaller than needed requires more design effort. In this case, we must compose several smaller memories to behave as the larger memory we need. Suppose the available memories have the correct number of words, but each word is not wide enough. In this case, we can simply connect the available memories side-by-side. We connect three ROMs side-by-side sharing the same address and enable lines among them, and concatenating the data lines to form the desired word width.

II. DESIGN AND IMPLEMENTATION

2.1 Design of ROM:

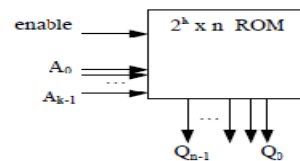


Fig. 2.1 : $2^k \times n$ ROM

Of course, there must be a mechanism for setting the bits in the memory (otherwise, of what use would the read data serve?), but we call this "programming," not writing. Such programming is usually done off-line, i.e., when the memory is not actively serving as a

memory in an embedded system. We usually program a ROM before inserting it into the embedded system. Figure provides a block diagram of a ROM. We can use ROM for various purposes. One use is to store a software program for a general-purpose processor. We may write each program instruction to one ROM word. For some processors, we write each instruction to several ROM words. For other processors, we may pack several instructions into a single ROM word. A related use is to store constant data, like large lookup tables of strings or numbers.

Another common use is to implement a combinational circuit. We can implement any combinational function of k variables by using a $2^k \times 1$ ROM, and we can implement n functions of the same k variables using a $2^k \times n$ ROM

2.2 Simulated waveform:

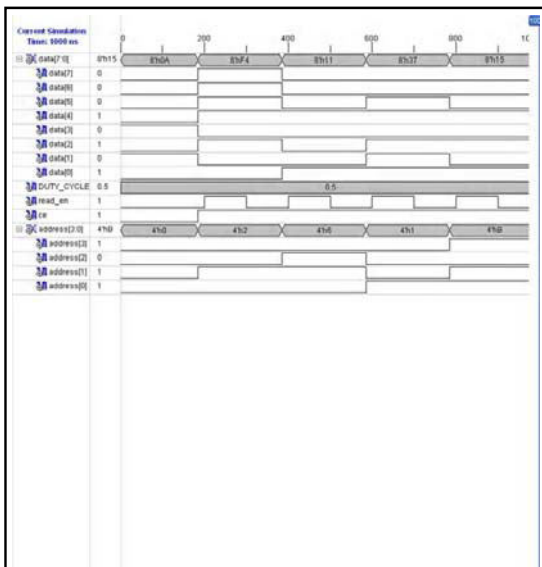


Fig. 2.2: Simulated waveform

3. ADVANTAGES AND APPLICATIONS

3.1 Advantages:

1. ROM could be implemented at a lower cost-per-bit than RAM for many years.
2. In modern PCs, "ROM" (or Flash) is used to store the basic bootstrapping firmware for the main processor, as well as the various firmware needed to internally control self contained devices such as graphic cards, hard disks, DVD drives, TFT screens
3. ROM is also useful for binary storage of cryptographic data, as it makes them difficult to replace, which may be desirable in order to enhance information security.

4. For large volumes of parts (thousands of pieces or more), mask-programmed ROMs are the lowest cost devices to produce.

3.2 Applications:

1. Industrial robots
2. Home appliances and consumer electronics (MP3 players, set-top boxes, etc)
3. Like EPROM chips, such microcontrollers came in windowed (expensive) versions that were useful for debugging and program development
4. Flash memory can be used High speed application

IV. RESULTS AND DISCUSSION

In project, I have used to write the code a Hardware description language, verilog code. And software used Xilinx 9.1 ISE and modelsim.

Plotted waveforms using code and testbench to verify the project. We can use ROM for various purposes. One use is to store a software program for a general-purpose processor. We may write each program instruction to one ROM word. For some processors, we write each instruction to several ROM words. For other processors, we may pack several instructions into a single ROM word. A related use is to store constant data, like large lookup tables of strings or numbers.

Another common use is to implement a combinational circuit. We can implement any combinational function of k variables by using a $2^k \times 1$ ROM, and we can implement n functions of the same k variables using a $2^k \times n$ ROM

V. CONCLUSION AND FUTURE SCOPE

5.1 Conclusion:

ROM implementation is carried out and verified using Hardware description language, verilog code. And software used Xilinx 9.1 ISE and modelsim. Active HDL allows you to build the ROM.

5.2 Future Scope :

An embedded system designer is often faced with the situation of needing a particular-sized memory (ROM or RAM), but having readily available memories of a different size. For example, the designer may need a $2k \times 8$ ROM, but may have $4k \times 16$ ROMs readily available. Alternatively, the designer may need a $4k \times 16$ ROM, but may have $2k \times 8$ ROMs available for use.

The case where the available memory is larger than needed is easy to deal with. We simply use the needed lower words in the memory, thus ignoring unneeded higher words and their high-order address bits, and we

use the lower data input/output lines, thus ignoring unneeded higher data lines. (Of course, we could use the higher data lines and ignore the lower lines instead).

The case where the available memory is smaller than needed requires more design effort. In this case, we must compose several smaller memories to behave as the larger memory we need. Suppose the available memories have the correct number of words, but each word is not wide enough. In this case, we can simply connect the available memories side-by-side. We connect three ROMs side-by-side sharing the same address and enable lines among them, and concatenating the data lines to form the desired word width.

REFERENCES:

- [1] See page 6 of Toshiba's 1993 NAND Flash Applications Design Guide
- [2] See chapters on "Combinatorial Digital Circuits" and "Sequential Digital Circuits" in Millman & Grable, Microelectronics, 2nd ed.
- [3] From Wikipedia, the free encyclopedia
- [4] The Free Online Dictionary of Computing (<http://www.instantweb.com/~foldoc/contents.html>) includes definitions of a variety of computer-related terms. These include definitions of various ROM and RAM variations beyond those discussed in the chapter, such as Extended Data Output (EDO) RAM.



Robot Localization by Particle Filter using Visual Database

Nagaraj N Bhat & Tarun Vashisth

Department of Electrical and Electronics Engineering, Birla Institute of Technology, Mesra, Ranchi, India

Abstract - One of the major problems in robotics is to recognize the robots position with respect to a given environment. More recently researchers have begun to exploit the structural properties of robotic domains that have led to great success. A general solution for such problem is the implementation of particle filters. The particle filter is more efficient than any other tracking algorithm because this mechanism follows Bayesian estimation rule of conditional probability propagation. In this paper we would like to present an approach to improvise the particle filter algorithm using SIFT pattern recognition technique and image database processing to obtain unimodal uncertainty for effective position tracking.

Keywords - Particle Filter, SIFT, Monte Carlo, Fast SLAM.

I. INTRODUCTION

One of the key developments in robotics is the development of probabilistic techniques for global localization. Most of the research focused on planning and control in a fully deterministic environment. Brooks proposed a method of control directly based on the sensor behavior [1]. Since the robot localization was never certain this method was typical. Later most of the models started making use of imperfect models and statistical distribution of sensor data to solve the problem. Traced back to 1960 probabilistic laws and Bayesian networks were used to integrate imperfect models and imperfect sensors. Many recently related field employ probabilistic techniques for perception and decision making [2, 3, 4].

A general solution of such probabilistic decision model was Particle Filter algorithm. They comprise a broad family of Monte Carlo algorithms for approximate inference in partially observable Markov Chains. Early successes of Particle Filter implementation can be seen in [5]. Particle filter mainly solved 2 main problems, global localization [6] and kidnapped robot, in which the robot has to recover its pose under global uncertainty. A sincere approach was made by Sebastian Thrun for Particle Filter implementation in robotics [7].

However the application of particle filters to robotics is not without caveats. Some factors arise from the fact that however detailed the probabilistic model may be, it shall still be wrong. Hence to overcome these problems much high probabilistic based decisions has to be made. One such way would be the use of pattern recognition and image data analysis of map scenes. In this paper our main motive is to provide an efficient method to improve robot localization problem by the

use of SIFT pattern recognition implemented through particle filters. We would see that such method would lead to much quicker and efficient unimodal solution for robot localization. This would lead to more accurate solution of the position of the robot in a given environment by rejecting the uncertainties in particle filter. The organization of the paper is as follows: Section 2 deals with the Particle filter algorithm. SIFT pattern recognition is explained in Section 3. Various database and map models and their analysis are dealt in Section 4. Overall algorithm is discussed in Section 5. Finally Section 6 deals with the Conclusion and Future work. A block diagram of the entire algorithm is shown below.

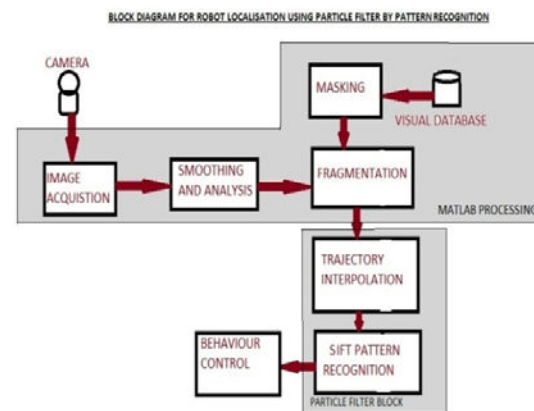


Fig. 1 : Block Diagram of robot localization by Implementation of Pattern Recognition in Particle Filter.

II. PARTICLE FILTER ALGORITHM

One of the major problems with the robot in real time system is the robot localization problem. Localization is the ability of the robot to locate itself in space. Efforts have been made throughout the years to solve the localization problem rather than using GPS devices in robot where margin of error is high (of orders of 10 meters). Objective of implementing successful localization demands the need to reduce the margin of error up to two to three centimeters. To every point or state space there is an associated probability. Posterior probability function is the best representation of robots current belief. This has led to increase in robustness of mobile robot and localization problem with a given map to be solved. [7]

Fast SLAM, a particle filter algorithm has been used, because of its capability to solve the high dimension localization problem in real time. Particle filters are approximate technique for calculating the posteriors in partially observable controllable Markov chains with discrete time.

The most basic version of particle filter is given by the following algorithm.

- Initialization: At time $t=0$, N particles are drawn according to $p(x_0)$, which is the probability distribution of initial state x_0 as shown in.
- Recursion: At time $t>0$, generate the particle x_t according to probabilistic law $p(x_t|u_t, x_{t-1})$ (also referred to as actuation model) where u_t is the control asserted in the interval $(t-1, t)$. The state in Markov chain is not observable. So one can measure z_t which is the stochastic projection of true state x_t generated from the probabilistic law $p(z_t|x_t)$ (also referred to as measurement model).

Bayes filters [9] provide the solution to recover posterior distribution over the state x_t at any time t .

In the context of localization Particle filters are commonly known as Monte Carlo localization (MCL). MCL is basically inspired by condensation algorithm, a particle filter that gained popularity in computer vision [10].

Fig 2 describes the working of Monte Carlo Localization. In Fig 2(a) robots position along with global uncertainty state or state of maximum confusion is shown. In Fig 2 (b) after condensation of particles an intermediate state is shown. Fig 2 (c) shows the final state where robot has successfully localized itself eliminating confusion. MCL has also been made temporarily more persistent by clustering particles and using different sampling rate for different clusters.

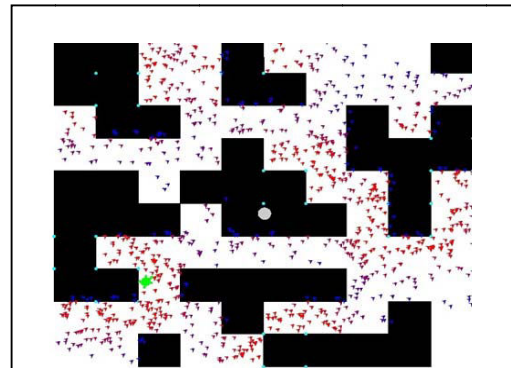


Fig. 2(a) : Initial State

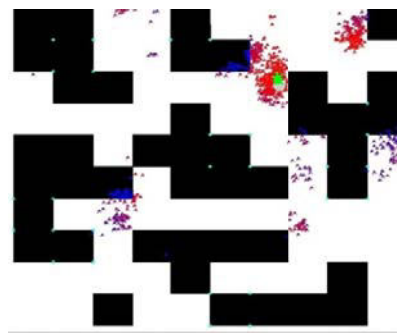


Fig. 2(b) : Intermediate state

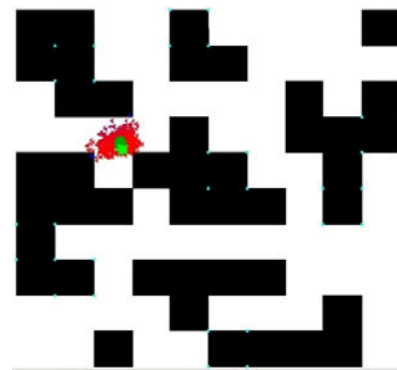


Fig. 2(c) : Final State.

One of the main problems encountered in particle filters is the poor performance in higher dimension spaces because the number of particles needed to populate a state space increases exponentially with dimension of state space. As this article deals with localization in higher dimension space, the problems concerning the higher dimension space needs to be considered. The localization error can occur because of errors in the environmental features of the map and data association problem of determining whether two

environment features, observed at different points in time, correspond to the same physical feature in the environment. Also all applications require real time processing [7].

The resulting estimation is described as a problem of jointly estimating a time-variant robot pose x_t and time invariant location of N features denoted, y_1 to y_n :

$$\begin{aligned} p(x_t, y_1, \dots, y_N | z^t, u^t) \\ = \text{const.} \cdot p(z_t | x_t) \int p(x_t | u_t, x_{t-1}) \\ p(x_{t-1}, y_1, \dots, y_N | z^{t-1}, u^{t-1}) dx_{t-1} \end{aligned} \quad (1)$$

This integration involves only the robot pose x_t and not the variables $y_1 \dots y_n$.

A particle filter algorithm, Fast SLAM, is used as it overcomes the problems associated with high dimensional space. Also it exploits the fact that robot may only observe a finite number of features at any point of time. The use of particle filter opens the door to solution of data association problem. Fast SLAM makes it possible to sample over data associations rather than simply assuming that the most likely association is correct. FastSLAM can also incorporate negative information that is, not seeing a feature that the robot expects to see. This is achieved by modifying the importance factors of individual particles accordingly.[7]

III. SIFT

Since robot localization requires accurate pattern matching results, SIFT algorithm was chosen for this purpose. Scale Invariant Feature Transform (SIFT)[8] algorithm developed by David Lowe is proven as efficient method in Object recognition leading to very satisfying results due to invariance to translation, rotation, partial illumination changes and affine or 3D projection. The SIFT features share a number of properties in common with the responses of neurons in Inferior Temporal cortex in primate vision [1].

The SIFT approach firstly identifies the key locations in scale space by locating local maxima or minima of Difference of Gaussian function. These points are used to generate the feature vectors describing image region sampled relative to its scale space coordinates. These features are invariant to local variations by blurring image gradient locations. A 2D Gaussian function (1) is used for blurring the image.

$$g(x) = (1/\sqrt{2\pi\sigma}) \cdot \exp(-x^2/(\sigma^2)) \quad (2)$$

Where σ is the standard deviation of the Gaussian distribution.

The feature vectors are called SIFT key points. These key points are used in indexing to identify candidate object models. The keys which match are identified through hash table. When at least 3 to 4 keys agree, there is a strong evidence of a match. Fig 3 depicts the key points identified by SIFT algorithm. The red markings are the key points found by SIFT in the image.

There are variety of benefits of using SIFT algorithm over other methods.

- SIFT performs an accurate pattern match due to large number of features under consideration.
- The algorithm is Scale, Rotation, Illumination and View point invariant.
- Due to requirement of less number of key points for recognition purpose, the solution is highly redundant and can sustain substantial occlusion.

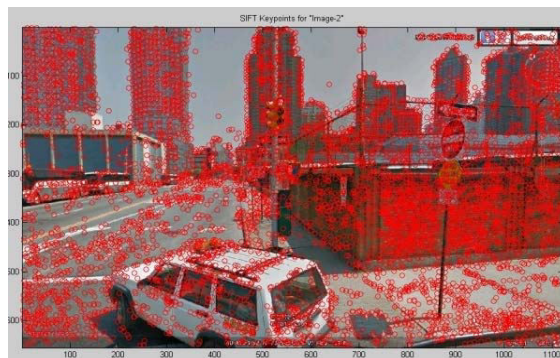


Fig. 3. (a) : Key points of input image 1

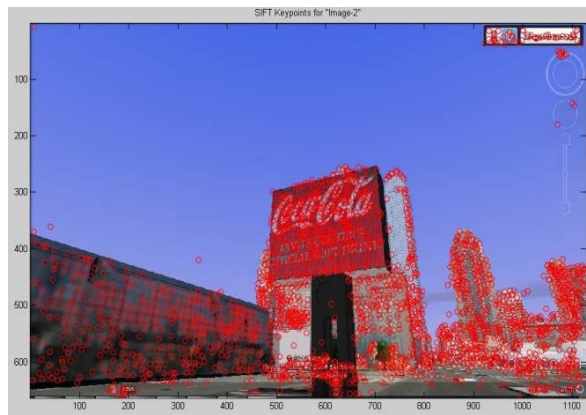


Fig. 3 (b) : Key points of input image 2.

Fig 4 shows the matched key points of input images 1 and 2. These key points are marked green for reference. A probability analysis is carried out based on the number of matched points with the database (explained in section 3). The result of the matching technique is shown in Fig 5. Also a table describing the stability of SIFT algorithm is shown in Table 1.

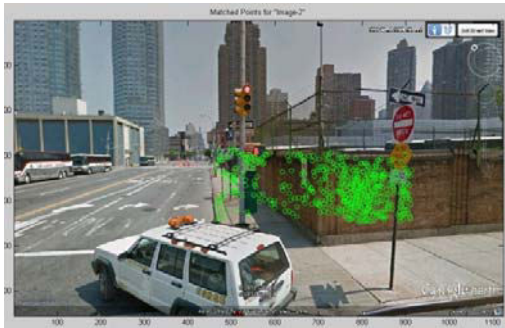


Fig. 4. (a) : Matched Key points of input image 1



Fig. 4. (b) : Matched key points of input image 2.



Fig. 5. (a) : Matched Database image1 vs. input image1.



Fig. 5.(b) : Matched Database image2 vs. input image2.

TABLE I. Table describing the stability of SIFT transform

Sl. No.	Key Stability to image Transformations		
	Image transformation	Match %	Ori %
A	Increase Contrast by 1.3	89.0	86.6
B	Decrease Intensity by 0.3	88.5	85.9
C	Scale by 0.7	85.1	80.3
D	Stretch by 1.3	83.5	76.1
E	Add 10% pixel noise	90.3	88.4

IV. SELECTION OF MAP MODEL AND DATABASE IMAGES

The very first task of the project is to provide a model of robot environment generally referred to as Map Model for robot to locate itself. The robot locates or knows its position with respect to this map. Also database images has to be supplied for SIFT recognition and Particle Filter analysis. Now the main challenge is to select specific database images for recognition purpose in a given Map. The following subtopics deal with the Map model and selection of database images in a given Map.

A. Map Model:

For global localization of a robot in its given environment a Map of the environment is provided which is the reference for the robot to localize itself. Initially if the robot is left in this environment in a random point, it shall have no clue about its position. Certain points are marked which confirms the position of the robot to its given environment. A map of a street area in New York is shown in Fig 6. The numbers marked in red boxes corresponds to the respective database images in those positions. In this case 1 corresponds to database image1 and 2 for Database image2 respectively (shown in Fig7).



Fig. 6 : Map Model describing the position of Database Images.

B. Database Model:

The selection of database images is a tricky task as images have to be chosen such that they are less repetitive or unique in the environment. Map model of Fig 6 shows 5 varied locations of different database images. These database images are shown in Fig 7. Marking "1" in Fig 6 corresponds to Database image 1 in Fig 7 (a). Similarly "2" for Database image 2 and so on. These images are stored in the memory for matching purpose. Every time the robot views an image it compares that image with these predefined database images. Once the comparison is matched, the location can then be tracked with respect to the position of that image placed in the map. Hence the database images selected should be static images/scenes/figures etc. It should be noted that presence of same object in more than one place shall lead to slight uncertainty but still maintaining its efficiency.



Fig. 7 (a) : Database Image



Fig.7(b) : Database image 2

V. ALGORITHM DESCRIPTION

Initially suppose the robot is left in a random position in the given environment, the main task is to search for the images in the surroundings which are similar to database images. But at the same time robot

has to continue its locomotion in a particular direction according to particle filter algorithm with equal probability distribution at every point. The following processes are carried out:

A. Image Acquisition and processing:

The initial stage of the algorithm is the acquisition of the input images through the camera. Once these images are acquired they are then smoothed using a Gaussian function to reduce the noise in the images as real time images are more subject to noise. It is then filtered using a median mask. Once these processes are completed the image is ready for further pattern matching algorithm.

B. Object Recognition and Probability Analysis:

Once the image is smoothed it is then tested for key points matching through SIFT algorithm as described in Section 3. Suppose if the input image is recognized with the database image the probability distribution of the entire map is drastically changed as the robot recognizes its position in the given environment. A second case would be if there are similar images in the Map model, the particle probability would be concentrated more in those areas where these images are present. For example consider the database image of trees. In Fig 6 it can be seen that trees are mostly present at the right most side of the map and in few other places. Hence this would give a probability distribution such that more particles are present near the tree part either in the rightmost side or in other places with much probability at the right side. Further the position can be determined only after observing upcoming images.

Fig 8 depicts the process of the algorithm as the robot moves initially in a random location in the given environment. In Fig 8(a) the robot is left in a initial unknown position. It can be seen that the probability distribution in this case is over the entire map as the probability of robot being in every place is same. Now as the robot moves forward the particle probabilities starts getting concentrated at only some particular positions. This is shown in Fig 8(b). Further in Fig 8(c) it can be seen that once the robot is closer to the image points where the object is recognized with the database image there is a drastic change in the probability distribution according to the posterior function. It can be seen that the particles are more concentrated at one position after the robot comes nearer to the data base points in the map. Like this the robot gets to know its present position in the environment. Now it shall be able to achieve its destination according the user requirement.



Fig. 8 (a) : Initial position of the robot and its particle distribution.



Fig. 8 (b) : Particle distribution as the robot moves ahead.

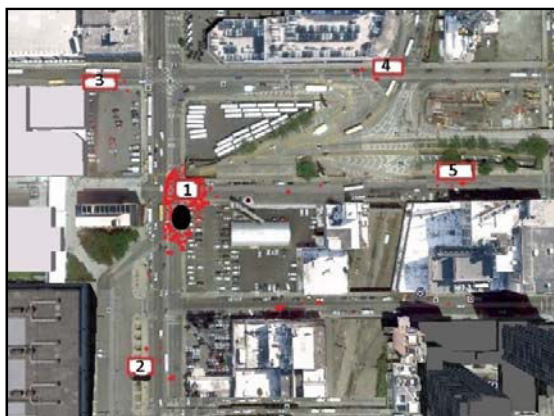


Fig. 8(c) : Particle distribution as the robot recognizes the object.

VI. CONCLUSION

In this paper we have presented a Fast SLAM particle filter approach with visual database recognition for enhancement of robot localization techniques.

Particle filters have always been applied for localization on small scale. Recently, advancement variants of particle filters have provided new solutions to challenging higher dimension problems. These approaches use representations expressed by conditional independence.

The main idea was to develop a mechanism for robot localization in an unknown environment. This technique is more valid in real time environment but the only disadvantage would be in the matter of computation time when a large number of database images have to be matched. However this could be overcome by using certain AI techniques for image classifiers. In future we would like to enhance this technique by investigating 3 D models using stereo vision analysis.

ACKNOWLEDGMENT

We would like to thank our Departments and all our colleagues and well wishers for their support in completion of the paper.

REFERENCES

- [1] R. A. Brooks. A robot that walks; emergent behaviors from a carefully evolved network. *Neural Computation*, 1(2):25, 1989.
- [2] H. F. Durrant-Whyte. Autonomous guided vehicle for cargo handling applications. *International journal of Robotics Research*.
- [3] S. Williams, G. Dissanayake, and H. F. Durrant-Whyte. Towards terrain aided navigation for underwater robotics. *Advanced Robotics*, 15(5), 2001.
- [4] C. Thrope and H. Durrant-Whyte. *Field Robotics*. In *ISRR-01*.
- [5] S. Thrun, D. Fox, W. Burgard and F. Dellaert, Robust monte carlo localization for mobile robots. *Artificial Intelligence*, 128(1-2), 2000.
- [6] J. Borrenstein, B. Everett and I. Feng. *Navigating Mobile Robots: Systems and Techniques*. A. K. Peters 1996.
- [7] Sebastian Thrun. *Particle Filters in Robotics*. *Proceedings of Uncertainty in AI 2002*.
- [8] *Journal of WSCG*, Vol.12, NO 1-3, ISSN 1213-6972.
- [9] A. M. Jazwinsky. *Stochastic Processes and Filtering Theory*. Academic Press,1970. Article in a conference proceedings:
- [10] Yang Weon Lee, development of Practical particle filter for Human Gesture Recognition.

Reconstruction of Corrupted Image From Salt And Pepper Noise From Median Filter

Vishal Gautam & TarunVarma

Department of Electronics and communication Engineering, M.N.I.T, Jaipur, India

Abstract - In this paper, we propose an improved median filtering algorithm. Here, we introduced salt and pepper noise for the image corruption and reconstruct original image using different filters i.e. mean, median and improved median filter. The performance of improved median filter is good at lower noise density levels. The mean filter suppresses little noise and gets the worst results. The experimental results show that our improved median filter is better than previous median filter for lower noise density (upto 60%). It removes most of the noises effectively while preserving image details very well.

Keywords - Median filter, noise detection, PSNR salt and pepper noise

I. INTRODUCTION

Salt and pepper noise is produced at the processes of collection and transmission of digital image. It represents itself as randomly occurring white and black pixels. An effective noise detection method for this type of noise involves the usage of a median filter. Shot and spike noise terms are also used to refer salt and pepper noise. Noise impulses can be negative or positive. Negative impulses appear as black (pepper) points in an image. For the same reason, positive impulses appear white (salt) noise. For an 8-bit image this means that $a = 0$ (black) and $b = 255$ (white). The different types of filters are referred by many authors. In [1-3], different algorithm schemes are proposed to remove salt and pepper noise while preserving its image information. Researches in median filters are continued and came to existence a new median filter is called optimal weighted median filter, is given in [4]. In [5], it is claimed that improved median filter performs better than previous weighted median filter for high quality image restoration. In [6], a new method, called boundary discriminative noise detection (BDND), is proposed from the switching median filter. It is seen that the all proposed algorithm are satisfied if and only if the original image is blurred with salt and pepper noise upto a certain limit. In [7], the technique to remove a different noise; impulsive noise, is proposed when this noise is present in a huge amount.

Our paper is organized as follows, in section I, the research level related to, technique to remove the salt and pepper noise in the image from the median filter, switching median filter and improved median filter and preliminaries of mean filter, median filter are discussed.

In section II, our technique is proposed in algorithm form. In section III, simulation results corresponds to the proposed technique are shown and compared it with the mean and median filter performance. Finally, section IV concludes the paper.

Mean Filter:

The arithmetic mean filtering process computes the average value of the corrupted image $g(x,y)$ in the area defined by S_{xy} . The value of the restored image f at any point (x,y) is simply the arithmetic mean computed using the pixels in the region defined by S_{xy} . In other words

$$\hat{f}(x,y) = \frac{1}{m * n} \sum_{(s,t) \in S_{xy}} g(s,t)$$

This operation can be implemented using a convolution mask in which all coefficients have value $1/mn$. A mean filter simply smoothes local variations in an image.

Median Filter:

The best known order-statistics filter is the median filter, which replaces the value of a pixel by the median of the gray levels in the neighborhood of that pixel-

$$\hat{f}(x,y) = \frac{1}{mn} \sum_{(s,t) \in S_{xy}} g(s,t)$$

The original value of the pixel is included in the computation of the median. Median filters are quite popular because, for certain types of random noise, they provide excellent noise reduction capabilities, with

considerably less blurring than linear smoothing filters of similar size.

II. PROPOSED ALGORITHM

In this proposed technique, salt and pepper noise from the corrupted image is removed, the algorithm are presented as below:

Table:1 PSNR Values for Different Filters

Filter	Noise Density								
	10(%)	20(%)	30(%)	40(%)	50(%)	60(%)	70(%)	80(%)	90(%)
Mean	23.59	19.81	17.52	15.75	14.28	13.11	12.01	10.99	10.21
Median	37.20	35.60	32.68	29.41	25.00	20.89	16.48	11.86	8.22
Improved median	27.93	27.73	27.65	26.73	23.74	18.73	13.78	9.67	6.37

Step 2: Sort pixels from the selected window according to the ascending order and find out the median pixel value (denoted by P_{med}), maximum pixel value P_{max} and minimum pixel value P_{min} of the sorted vector V_0 . Now the minimum, maximum and median pixels are of the vector V_0 is P_{min} , P_{max} and P_{med} respectively.

Step 3: Now, the axiom is considered that if the processed pixel follows this condition $P_{min} < p(x, y) < P_{max}$, and $P_{min} > 0$ and $P_{max} < 255$, then it is assumed that the pixel is uncorrupted and it is kept the same value as before. If above condition is not satisfied, then pixel is treated as corrupted pixel and have to correct that pixel from noisy pixel.

Step 4: If $p(x, y)$ is corrupted pixel, then we have the following two cases:

Case 1: If pixels are satisfied this condition $P_{min} < P_{med} < P_{max}$ and $0 < P_{med} < 255$, then corrupted pixel $p(x, y)$ is replaced with P_{med} .

Case 2: If case 1 is not satisfied, then it is considered that the median pixel P_{med} is corrupted with noise. Then the differences between each pixels pair of adjacent pixels across the sorted vector V_0 is performed and obtain the difference vector V_D .

Then find out maximum value in the difference vector V_D and considered this pixel as processes pixel and follow the further step.

Step 5: Steps 1 to steps 4 are repeated until the complete process of removing the salt and peppers noise from the noisy image is done for the entire image.

III. RESULTS AND ANALYSIS

Here, the proposed technique is verified and demonstrated on MATLAB Platform. In this simulation result, 'girl.jpg' image of size 256 x 256 is selected as a original image as shown in the figure 2.a and noise density of 60 % of salt and peppers mixed in the

Step 1: Window size of 3x3 is selected from the noisy image and focused all pixels around the processed pixel $p(x, y)$ in the corrupted image.

original image which produced noisy image as shown in the figure 2.b. Figure 2.c shows the image which is filter with the mean filter and figure 2.d is corresponding the median filter. From the produced images from mean and median filter it can be seen that median filter has better performance than mean filter. the convention median filter and figure 2.d shows the image which is produced with our proposed technique improve median filter.

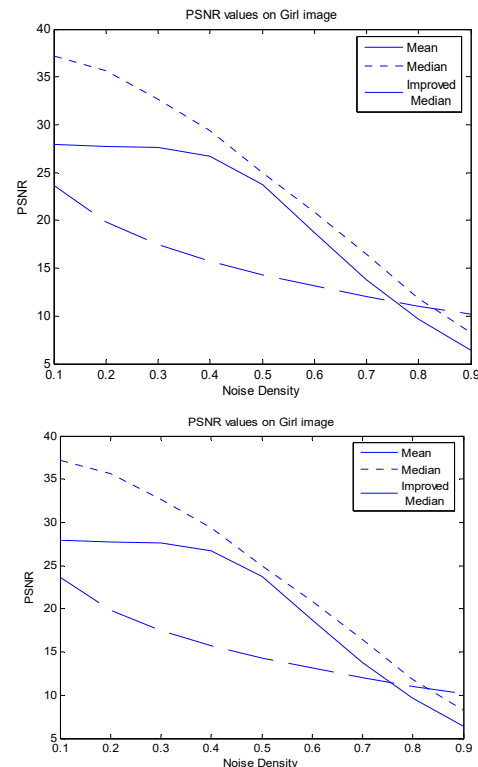


Fig 1: Plot for PSNR values of Girl image

Moreover, Figure 1 shows the PSNR performance of different filters. Also from the figure, it can be

concluded that the performance of mean filter is worst and improved median filter has better performance. For the lower noise density, PSNR values of improved median filter is good but it fall down abruptly and generate a worse result when the noise ratio is high. As the performance of our improved proposed median filter is better than other filters when the noise ratio considered lower than 60 %.

IV. CONCLUSION

The performance of these filters are tested on the well-known standard image (Girl Image) corrupted by salt and pepper noise with equal probabilities. Improved median filter preserves the integrity of edge and detailed information and remove impulse noise effectively, and provide more satisfying visual quality. This proposed improved median filter is used for practical application for removing such types of noise which is present on images.

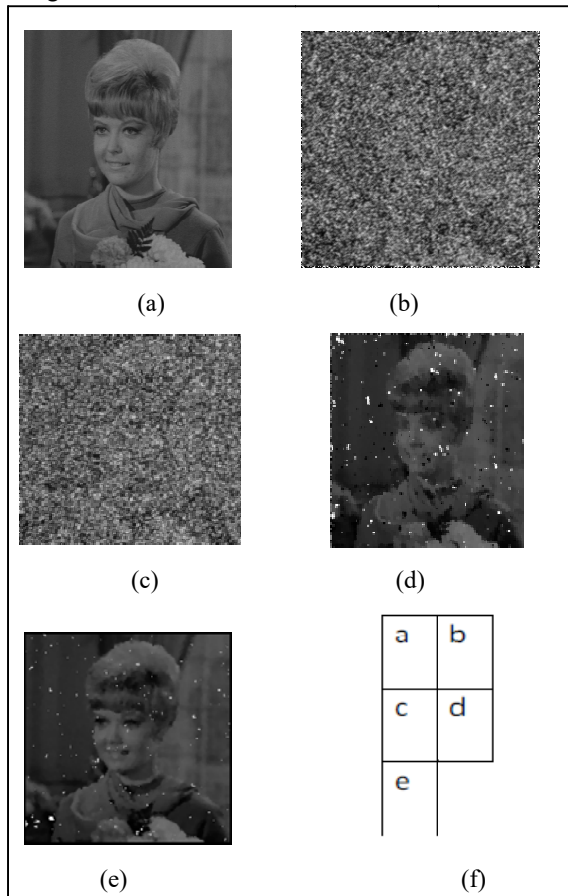


Fig2: (a)original image (b) corrupted with 60% noise (c)output from mean filter (d)output from median filter (e)output from improved median Filter

REFERENCES

- [1] Yu Jiang, Guohongwei, Li chao, Guohongwei and Li chao, (2010), “A Filtering Algorithm for Removing Salt and Pepper Noise and Preserving Details of Images”, *wireless communication networking and mobile computing (WiCOM),6th international conference*, pp.1-4.
- [2] T. Song, M. Gabbouj, and Y. Neuvo, (1994), “Center Weighted Median Filters: Some Properties and Applications in Image Processing,” *Signal Processing*, Vol. 35, No. 3, pp. 213-229.
- [3] K. S. Srinivasan and D. Ebenezer, (March 2007), “A New Fast and Efficient Decision-Based Algorithm for Removal of High-Density Impulse Noises,” *IEEE Signal Processing Letters*, Vol. 14, No. 3.
- [4] R. Yang, L. Lin, M. Gabbouj, J. Astola, and Y. Neuvo, (Mar 1995), “Optimal Weighted Median Filters Under Structural Constraints,” *IEEE Trans. Signal Processing*, Vol. 43, pp. 591-604.
- [5] JafarRamadhanMohammed,(May 2008), “An Improved Median Filter Based on Efficient Noise Detection for High Quality Image Restoration,”*IEEE Int. Conf*, pp. 327 – 331.
- [6] Pei-Eng Ng and Kai-Kuang Ma, (June 2006), “A Switching Median Filter with BDND for Extremely Corrupted Images”, *IEEE Trans ImageProcessing*, Vol. 15, No. 6, pp. 1506-1516.
- [7] S. Indo and C. Ramesh, (March 2007), “A Noise Fading Technique forImage Highly Corrupted with Impulse Noise,” *International Conference on Computing: Theory and Applications*, pp. 627-632,.

□□□